Florida State University Libraries

2011

Surface Heating and Restratification of the Ocean after a Tropical Cyclone

Robert Deal

THE FLORIDA STATE UNIVERSITY

COLLEGE OF ARTS AND SCIENCES

SURFACE HEATING AND RESTRATIFICATION OF THE OCEAN AFTER A

TROPICAL CYCLONE

By

ROBERT DEAL

A Thesis submitted to the
Department of Earth, Ocean, and Atmospheric Sciences
in partial fulfillment of the
requirements for the degree of
Master of Science

Degree Awarded:
Spring Semester, 2011

The members of the committee approve the thesis of Robert Deal defended on April 30, 2011.

Carol Anne Clayson
Professor Directing Thesis

Robert Hart
Committee Member

Paul Ruscher
Committee Member

The Graduate School has verified and approved the above-named committee members.

I dedicate this to those of you who always help push me onwards, you know who you are. Without all the creative encouragement, love, support and most of all patience, this work would not have been possible. This is for you Mom Mom, I wish you could have seen this happen.

ACKNOWLEDGMENTS

TABLE OF CONTENTS

LIST OF TABLES

LIST OF FIGURES

ABSTRACT

Ocean transport of heat is a substantial component of the climate system but its characteristics and dynamic causes are still somewhat unknown. Prior research has shown that global observations from the ocean and atmosphere indicate that the ocean and atmosphere transport about 6 PW of energy from the equatorial regions towards the poles. Studies have shown that approximately 2 PW of that transport are carried by the ocean. It has been proposed that global tropical cyclone activity could account for a large amount of the mixing needed to explain the thermohaline circulation driving this transport. However, there remain insufficient observations to conclusively prove this hypothesis.

After a tropical cyclone moves across the ocean it leaves behind a wake of colder temperatures in the upper ocean. The cold wake is primarily caused by mixing, upwelling and an enthalpy flux into the atmosphere. This study makes use of the JASON-1, and TOPEX/POSEIDON satellite altimeters to investigate the amount of heating of the ocean required to re-stratify the ocean to pre storm conditions. Argo floats are also used to validate results found from the sea surface height anomalies from satellite.

In order to attain the necessary spatial and temporal resolution, the Climate System Forecast Reanalysis (CFSR) model is used. Given that CFSR is a coupled atmospheric and ocean model, it enabled this study to compare the modeled storms and then the impact of storms on the ocean. After the storm passed through the area, surface heating fluxes could be determined over the duration of the storm thus providing a direct comparison of heat loss and net heat gain over the entire duration of the storm. It was found that during the time period of the cold wake, the surface heating imbalance was high enough to account for all of the rewarming of the cold wake. Therefore it is possible that global cyclone activity could

account for the large amount of mixing required to explain the thermohaline circulation.

CHAPTER 1

INTRODUCTION

1.1 Motivation

Ocean transport of heat is a substantial component of the climate system but its characteristics and dynamic causes are still incompletely understood (Ferrari and Ferreira, 2011). The ocean heating budget has long been studied, and global observations indicate that the ocean and atmosphere together transport about 6×10^{15} W from the equatorial regions towards the poles. Studies have shown that approximately 2×10^{15} W of that transport is carried by the ocean (Wentz et al., 2000). Emanuel (2001) proposed that global tropical cyclone activity could account for a large amount of the mixing needed to explain the thermohaline circulation. The reasoning behind this argument was that the reheating of cold wakes from surface fluxes must be balanced by oceanic heat transport out of the cold wake regions.

As a hurricane passes over the ocean, it leaves behind a wake of colder sea surface temperatures. The cold sea surface temperatures (SSTs) in the ocean result from a combination of surface flux loss, mixing and Ekman transport (Price, 1981). The strong winds induce vertical mixing that brings the colder deeper water to the surface and leave behind an area of colder SSTs. This entrainment also deepens the mixed layer. Ekman transport can cause upwelling of the colder water to the surface. Heat flux loss at the surface can cool the ocean by both the loss of heat and the resultant convection as the cooled water sinks. This volume of colder temperature is known as the cold wake.

In comparisons with the studies focusing on the formation of the cold wakes, relatively little has been written about the re-stratification effects. The extent to which re-stratification occurs due to surface heating versus other dynamical processes such as baroclinically driven mesoscale eddies along the edges of the wakes remains a very open question. The goals of this research are to look at the effects of hurricane-induced mixing on the upper ocean, with a special focus on the re-stratification time- and length-scales of the upper ocean column and how this is expressed in ARGO buoy observations, sea surface altimetry measurements, and a coupled atmosphere-ocean reanalysis model.

1.2   Literature Review

1.2.1   Observational Approaches

One of the initial studies describing the response of the ocean to a hurricane was Leipper (1966). That study used observations from hurricane Hilda (1964) in the Gulf of Mexico to describe the response of the Gulf to the mechanical forcing from Hilda (1964). This study predated the use of satellites and reliable buoy observations so the data used for the study was collected via observations from merchant vessels and noted the marked pattern of cooler SSTs after the passage of Hilda (1964)

The upper ocean was observed to cool by 5^oC down to at least $50 - 60$ m depth, with the coolest temperatures to the left of the storm track (disagreeing with the earlier estimates of Jordan (1964) which were based on considerations due to the strongest winds location on the right side of the storm track). Leipper (1966) also estimated the varying importance of the effects of cooling by heat loss to the atmosphere, cooling of the SST through mixing, and changes in SST due to horizontal and vertical advection.

Dickey et al. (1998) also studied direct observations of the ocean response. In this study, the authors analyzed the observations from hurricane Felix (1995) as it passed directly over the Bermuda testbed mooring. Unique to this case is that the moorings were over open ocean whereas many of the earlier studies were over relatively shallow water. The shallow

water caused understanding the oceans response to be more complicated due to topographic and boundary effects (Dickey et al., 1998). The SSTs from the AVHRR dataset were roughly $3.5\text{-}4.0^oC$ cooler in the wake, which spanned roughly 400km, than in the surrounding waters. The center of the hurricane's wake was located 200km to the right of the storm track (Dickey et al., 1998).

Prior to the passage of Felix (1995) the conditions at the observation site had shown signs of strong heating during the summer and into August and stratification consistent with minimal cloud cover (Dickey et al., 1998). As Felix (1995) passed the testbed mooring inertial currents were generated within the upper mixed layer. Before the storm had crossed over the testbed moorings, the depth of the mixed layer was near 15 m. Then within 3 days of the passage of Felix (1995), the mixed layer depth had deepened to 45 m as measured through both CTD profiles and moored buoys. The temperature at 25 meters had decreased by about $3.5^o-4.0^o$C while the temperature at a depth of 45m had increased by roughly 2.0^oC.

An early study using SSTs to look at the impact of a hurricane was Stramma et al. (1986). The authors used AVHRR satellite data to look at the characteristics of 13 hurricanes as they passed over the ocean. Using the AVHRR satellite data, they were able to generate SST maps using composites of multiple SST scans creating a single image where the extent of the wake is easily distinguishable. The reason for the need of the composites is due to limitations of the AVHRR satellite. AVHRR is a 5 optical channel satellite with 1 channel in the visible spectrum, 1 in the near infrared (IR) and 3 in the IR spectrum. It is particularly useful because the 3 IR channels are particularly sensitive to blackbody emissions and enable a good estimate for the SST. The major limitation in using an IR satellite is the inability to retrieve SSTs through clouds. Time composite images are used to show a complete SST field because the oceanic features change on a much slower time scale then the cloud features. By combining multiple images, the clouds are eliminated providing one SST map. Using these composite images, Stramma et al. (1986) were able to make distinct conclusions about the size, duration and magnitude of the SST response. One of the ex-

amples shown in Stramma et al. (1986) was hurricane Harvey (1981). Hurricane Harvey showed a distinct cooling of SST towards the right of the storm track. As shown in the paper, the maximum area of cooling, cooled by about 3.5^oC and occurred approximately 80 to 100 km to the right of the storm track. From the AVHRR composites they were able to conclude that the SST cooling persisted for approximately 16 days before no longer being noticeable. Through the study it was noted that the storms with slower translational speeds seemed to have the largest impact along the track path as opposed to the right of the path. The explanation for this was that because the storm was moving much slower upwelling was initiated and played a role in the cooling at the surface as opposed to solely one-dimensional effects as in Price (1981).

A later study that also utilized the AVHRR satellite SST was Monaldo et al. (1997). That study used 3 day composites to show the impact of hurricane Edouard (1996). Once again composites were necessary to alleviate the cloud limitations. This study was able to demonstrate that the effects of the SST cooling were not an artifact of the cloud limitation but rather the true impact of the wind mixing the ocean to leave behind a cooler wake of temperatures. In order to dismiss the possibility of the artifact of cloud limitation, the study noted that the ocean's SST was much warmer then the cloud tops in the same area. Thus, the satellite was retrieving the temperature of the ocean and not the cloud tops. Also, more definitively, there were multiple scans in which the initial field with clouds showed cooling of SST's in locations where the storm had just passed through. They also concluded that the temperature of the ocean has an impact on the intensity of the storm. This is based on the fact that when Edouard (1996) moved across the Gulf Stream into colder waters the intensity of the storm dropped rapidly. This study was consistent with Stramma et al. (1986) that satellite SST's were a valuable resource in determining the impact of the storm on the ocean and showed that the results from the AVHRR were consistent with modeled and in-situ observations of the SSTs in the region of the cold wake.

One of the next studies to show the value in SST from satellite was Wentz et al. (2000). In that particular study, the authors used microwave satellite radiometers in order to solve

the cloud problem from the IR satellites. The study noted that frequencies below 12 Ghz are immune to the effects of aerosols, and that the microwaves are able to penetrate the cloud layers with little attenuation enabling accurate measurements of SST in regions of clouds (but not in heavy precipitation regimes). Using a well-calibrated Tropical Rainfall Measuring Mission (TRMM) Microwave Imager (TMI) radiometer, Wentz et al. (2000) were able to show a direct improvement over the AVHRR with the respect to the cold wake in terms of more complete retrievals, decreasing the need to smooth over multiple days. Wentz et al. (2000) went on to state that microwave SST products have the potential to improve the forecasts of tropical storms given that microwave retrieval is possible ahead of the storm. This enables forecasters to have more quality information about the current thermal structure ahead of the storm. At the time of publication of Wentz et al. (2000) the only available microwave satellite capable of retrieving SST in all weather conditions was the TMI satellite, but that the Advanced Microwave Scanning Radiometer (AMSRE) was in preparation for deployment, which will be made use of in a blended TMI/AMSRE SST product.

Shay et al. (2000) studied the impact of using SSH to determine pre-storm oceanic features for hurricane Opal (1995). The authors showed that while the pre-storm SST from both microwave radiometers and IR satellite retrievals showed no indication of a warm core ring in the Gulf of Mexico. Topography from the TOPEX SSH indicated the possibility of warm core ring, which post storm SST from AVHRR confirmed, and that hurricane Opal (1995) had crossed over the warm core ring during its period of rapid intensification. Using SSH, Shay et al. (2000) showed that after Opal (1995) moved through the area of the warm core ring the SSH dropped by 20cm. Given that it had already been shown in previous research that the cold wake is a function of mixing, upwelling, and enthalpy loss into the atmosphere, the authors concluded that the drop in SSH was likely the result of a heat flux to the atmosphere. Further evidence from National Data Buoy Center buoy 42001, located at 25º55'N, 89º39'W on the left side of the storm track, combined with SSH decrease suggested that the ocean lost a significant amount of energy as the storm passed

by Shay et al. (2000). In summary, the study showed the improved capabilities of using SSH anomalies in determining information about the thermal structure of the upper ocean.

D'Asaro (2003) wrote about the first use of neutrally buoyant air deployed floats to observe the mixing directly beneath hurricane Dennis (1999). Three floats were air deployed ahead of the hurricane designed to accurately measure three dimensional trajectories, pressure and temperature. Even with the problems faced from one of the floats being buoyant, the study was able to show that on the right (left) side of the storm the temperatures decreased 2.8^o C (0.75^o C). The floats were able to determine that a significant amount of the cooling actually occurred prior to the passage of the eye indicating that the cooling could contribute a large factor in the hurricane's thermodynamics (D'Asaro, 2003). Using the temperature measurements, surface heat fluxes were estimated and within the ocean boundary layer the heat fluxes were estimated to be several thousand $Wm^{-}2$ but with large error bars. Errors in estimates prevented any meaningful conclusions on the importance of sea-spray fluxes. Finally using the profiles, D'Asaro (2003) was able to show that the cooling was maximized on the right side of the storm track. This was also reflected in the entrainment heat fluxes, where the fluxes on the right side of the storm were double the size of the left.

Argo floats provide the first continuous set of global observations of temperature, salinity, and velocity of the upper ocean as a part of the Global Ocean Data Assimilation Experiment (GODAE)(Gould et al., 2004). The Argo project involves dropping large numbers of autonomous floats into the ocean. Each float can collect high quality temperature and salinity profiles at it sinks to a floating depth and then surfaces ten days later. The floats fill an external bladder creating negative buoyancy causing the floater to sink until it reaches a certain predetermined depth. The floater then remains buoyant at that depth moving with the currents and then on the 10th day rises taking high quality measurements over a time period of approximately six hours (Gould et al., 2004). The target array called for at least one buoy within a 3x3^o square of latitude and longitude. Given the target array size, mesoscale variability was not one of the functions that the Argo project could resolve.

However, with the increased amount of upper ocean information, Argo floats represent an enormous increase in the sub-surface of the ocean (Gould et al., 2004). Despite the limitation of not resolving mesoscale variability, the Argo floats were able to take observations beneath hurricanes and show a decrease in temperature on both the left and right side of the track. From initial results, salinity did not prove to have quite as distinct results in determining the upper ocean response to a hurricane (Gould et al., 2004). One of the goals of this work is to determine whether the Argo floats provide enough accurate determination of the cold wake formation and re-stratification

In a later study, D'Asaro et al. (2007) used an array of air-deployed floats and surface drifters to measure the three dimensional response of hurricane Frances (2004). The in-situ observations showed a cooling of the SST on the right side of the storm, displaced some 60-85 km from the center of the storm. The wake was determined to be approximately 50km in width and cooled 2.2^oC from pre-storm conditions. They showed that the heat content, and specifically the hurricane heat content decreased in the wake of the storm similar to the SST drop. The decrease in hurricane heat content was primarily a function of upwelling while mixing only provided a small contribution to the heat loss. D'Asaro et al. (2007) also show that there was only a weak impact on the left side of the track and in the region of the core of the storm with corresponding drops in temperature of 0.8^oC and 0.4^oC, respectively.

1.2.2 Numerical Modeling Approaches

Chang and Anthes (1978) later followed up on the work of Leipper (1966) and Jordan (1964) using a numerical model to describe the ocean's baroclinic response to a moving hurricane. An important advance from that study was the use of an asymmetric nonlinear ocean model to accurately model the stresses induced by the moving hurricane. Previous theoretical and analytic studies had all considered axisymmetric hurricanes. The reasons for using an asymmetric model as opposed to an axisymmetric model are that first, the stress exerted by a moving hurricane is symmetric to the relative coordinate system. The stresses are moving with the center of the hurricane but not symmetric with respect to

7

the ocean. Second, as a hurricane approaches a given area, the ocean will begin to be accelerated by the wind stresses of increasing magnitude and direction. Chang and Anthes (1978) noted that on the right (left) of the storm track the stresses veer (back) with time. An axisymmetric model could not properly simulate the stressed exerted by the moving storm or the acceleration of the ocean as described previously (Chang and Anthes, 1978). The results from the numerical simulations of the control experiment showed a maximum in the oceanic current on the order of 1.7 m/s. The region where the current is the strongest is on the right side of the storm track. Chang and Anthes (1978) state that the reason for the asymmetry in the current field is due to variations in the movements of water parcels relative to the symmetric stress as the storm moves. The authors show that the maximum in ocean current, as well as the upwelling/downwelling patterns, all move with the storm. The authors also show that the ocean response is rightward biased relative to the storm track and that for faster moving storms the inertial gravity waves also increase. While the thermocline depth is sensitive to the translation speed, the maximum currents are not. Chang and Anthes (1978) determined that the maximum cooling of the SSTs varied from 2^oC to 8^oC but that this was dependent on the translation speed of the storm. The smaller translational speeds correspond to areas with larger maximum cooling.

Price (1981) was also one of the early studies to use a model to predict the upper ocean response to a moving hurricane. Price (1981) identified four specific questions with regards to the ocean's response to a hurricane (1) What physical mechanism(s) dominates the SST response and what causes the rightward bias in the SST response; (2) How does the response depend on translation speed, hurricane size, intensity, and ocean initial conditions; (3) What are the roles of upwelling, horizontal advection and pressure gradients on the upper ocean response; and (4) Is there any evidence that air-sea transfer coefficients increase significantly under hurricane conditions?

By the time Price (1981) was published, there was general agreement that unlike in Leipper (1966), the most pronounced area of cooling was on the right side of the storm track. Similarly to Chang and Anthes (1978), Price (1981) noted that from previous studies it

was apparent that for decreasing hurricane translation speed and increased hurricane intensity, the response increases (larger ΔSST). Price (1981) states that the reason the Leipper (1966) observations show a leftward bias in the SST field is due to the small translation speed. Price (1981) also contends that in Leipper (1966) the right side of the storm track represents the most extensive cooling while not a maximum of cooling.

Price's (1981) goal was to use the model to accurately describe the upper ocean response from a three dimensional perspective. In order to capture the resolution of the hurricane wind field the model had to have 20km horizontal resolution and cover a width of 500km. While 20km is a much smaller resolution then previous work, it is still not small enough to capture the full resolution of the hurricane eye and eyewall. The model was run for a period of 3 days after the hurricane passage in order to include the majority of the SST response.

The specific case studied by Price (1981) was hurricane Eloise (1975). Since Eloise (1975) passed directly over a moored buoy (EB-04 and EB-10) this allowed Price to gain valuable information for a comparison of the ocean model. From the model results of hurricane Eloise, the ocean response has an expected strongly rightward bias in the mixed layer current. It was shown that there is also a corresponding rightward bias in the SST field for all inertial periods and the maximum in ΔSST is approximately 60km from the center of the storm. Price also demonstrated that the rightward bias in the SST response is primarily a result of the asymmetry in the turning direction of the wind-stress vector turning clockwise (counter-clockwise) on the right (left) side of the storm and not based on the asymmetric wind field where winds are strong in the right front quadrant. He also determined that the SST response was a function of hurricane strength and translation speed along with the initial mixed layer depth and upper thermocline gradient. It was determined that hurricane size and the latitude via the coriolis force have some impact but only a weak impact.

Price et al. (1994) next examined the cold wake relaxation stage. The authors described the ocean response as two fold: a "forced stage", and a "relaxation stage". The study described here focused on the latter stage. The primary goal was to simulate storm-driven

currents for design purposes. Using an advanced version of the ocean model in Price (1981), the authors were able to simulate the upper ocean transport and realistic SST responses for hurricane Gloria (1985) as shown by Stramma et al. (1986). A rightward bias in the efficiency of the coupling between the transport and the SST responses was observed. On the left side the coupling was less efficient due to the counter-clockwise rotation of the wind stress vectors and the opposite is true for the right side of the coupling. The model showed that in the cooling there was a marked asymmetry with 4 times more cooling on the right side of the storm track. Price et al. (1994) also noted that in the test case for hurricane Norbert (1984), there was upwelling of nearly 25m with thermocline-depth currents of 0.3m/s beneath the rear half of the hurricane.

1.2.3   Re-stratification of cold wake

In Emanuel (2001), Figure 5 shows that while the surface manifestation of the cold wake is erased within days, there is still a cold pool at depth that has to be heated in some manner in order to fully restore the ocean to pre-storm conditions. The cold pool is shown in the sea surface height anomalies as a proxy for the vertically integrated heat content. In this case, a pronounced maximum in SSH is seen developing after the crossing of hurricane Edouard (1996) on the right of the storm track. Emanuel (2001) assumes that this is due to the reheating of the cold wake. This feature is seen developing over several weeks and is evident for more than 40 days.

Using MPI anomalies, Hart et al. (2007) showed that the "memory, or length of statistically significant anomalies compared to an evolving climatology, for the tropical atmosphere was on the order of one week. The corresponding oceanic memory is approximately 1-2 months depending on the storm intensity, lifespan and location of the storm. This is consistent with the Emanuel (2001) study. Hart et al. (2007) state that the removal of oceanic memory is done via temporary heat fluxes from the atmosphere to the ocean and enhanced isolation resulting from a stable post storm temperature profile. It also states that in some areas the oceanic memory could be accelerated through low salinity rainfall

accumulation. This is because the accumulation of rainfall in areas with low salinity would act to suppress entrainment and accelerate SST warming through surface heat fluxes.

Emanuel (2001) continued the study of the cold wake of hurricanes as it pertains to the meridional transport of heat. The study hypothesized that as the ocean starts to re-stratify and restore normal conditions by entrainment and surface fluxes there is large amount of heating that must occur. Emanuel (2001) uses the example of hurricane Edouard (1996) to explain the amount of heating required to restore the ocean to pre-storm SST. A wake whose average negative temperature anomaly of 3^oC extends downward to 50 m with a width of approximately 400 kilometers and a track length of 2000 kilometers would require nearly 5×10^{20} J of surface heating to restore to the pre-storm conditions. Such amounts of heating are important to the energy budget. Emanuel (2001) estimates that the approximate annual heating induced by tropical cyclones is $1.4\pm0.7\times10^{15}$W. Given that the total amount of energy transported by the ocean and atmosphere is approximately 6×10^{15} W, the annual heating induced by tropical cyclones is significant in the energy budget. However, this assumes that all warming of the cold wake is due to surface heating, an assumption that this work will address.

The organization of the paper is as follows. The second chapter identifies the methods used in the research and a description of the data used in the work. The third chapter presents and discusses the results from the satellite altimetry and the ARGOS floats. The fourth chapter presents and discusses the results from the CFSR model. The final chapter is a review of the work with conclusions and ideas for future work.

CHAPTER 2

DATA AND METHODOLOGY

2.1 Data

The goals of this study are to estimate the amount of upper ocean heating needed to re-stratify a cold wake, and to determine the extent to which surface heating is responsible for this change. There will be three different storms presented and tested through a number of different techniques in order to find an estimate for the amount of upper ocean heat loss and the corresponding amount of energy needed to re-stratify the ocean. Each of the three storms, Hurricane Felix (2001), Hurricane Isabel (2003) and Hurricane Bill (2009) is described in more detail in the case study section of this chapter.

2.1.1 Satellite sea surface height fields

As noted in Emanuel (2001), an evaluation of sea surface height anomaly from TOPEX/ POSEIDON in 1996 demonstrated a response of the sea surface height to the existence of the cold wake on the order of 10 cm, which was visible for several weeks during the recovery of the cold wake. SSH anomaly data from TOPEX/ POSEIDON, JASON-1, and the GFO altimeters were available for Hurricane Felix (2001). TOPEX/ POSEIDON and JASON-1 were available for studying Isabel (2003) and the Bill (2009). These data are available from the Physical Oceanography Distributed Active Archive Center for the Jet Propulsion Laboratory[1]. The specific data set used is the Product 133 data. These data are along-track

---

[1]Data Available http://podaac.jpl.nasa.gov/PRODUCTS/p133.html

gridded sea surface anomaly data. Nominal reported accuracies are 2 cm. The repeat cycle on the TOPEX/ POSEIDON and Jason-1 altimeters is 10 days. The GFO altimeter had a 17 day repeat cycle.

2.1.2   Satellite SST Measurements

Microwave SSTs were used by Wentz et al. (2000) to demonstrate the feasibility of observing cold wakes by satellite SSTs, as microwave imagers are able to determine an SST through clouds (but not heavy rain). The SST dataset used for the initial search for storms that showed a clear change in SST was the OI TMI and AMSR-E data produced by Remote Sensing Systems©.[2] The optimally interpolated SST product uses the SST fields from TMI and when available the AMSRE. The TMI satellite was the first well-calibrated microwave radiometer capable of the accurate through-cloud SST retrieval. The Advanced Microwave Scanning Radiometer for EOS (AMSR-E) from NASA's AQUA satellite which was the first microwave radiometer capable of accurate global through-cloud SSTs (Wentz et al., 2001). The data from the two radiometers is daily Optimally Interpolated (OI) at quarter degree resolution and represents a significant improvement of the weekly, 1 degree NCEP OI (Reynolds) SST product (Reynolds et al., 2002).

2.1.3   Argo Float Data

An Argo float is a battery powered autonomous float that drifts along the currents of the ocean at a given buoyancy depth and surfaces every 10 days. The purpose of the Argo floaters is to measure temperature and salinity profiles for the upper 2km of the ocean at high resolution (Gould et al., 2004). The Argo float sinks to a depth known as the parking depth where the float is stabilized through attaining a density equal to that of the ambient pressure of the ocean at a certain depth. Then, because the floater is less compressible than sea-water, the floater is able to remain at a constant depth. The Argo float drifts along in the current for approximately 10 days then pumps fluid into an external bladder in order to

---

[2]Data Available ftp://ftp.discover-earth.org/sst/daily/tmi_amsre/

surface in a controlled manner. As it surfaces, the Argo float takes temperature and salinity measurements on the way up to create temperature and salinity profiles for its location. The Argo floater then transmits the data to a satellite and then repeats the process of sinking to the parking depth and drifting for another ten days. Given the transitory nature of the floats, and the relative sparseness of the array, few cases were found in which comparisons could be made of in situ profiles before, during, and after the development of a cold wake. These data were collected as a part of the Global Ocean Observing System and made freely available by the International Argo Program as well as national programs, such as NODC[3], that contribute to it (http://www.argo.ucsd.edu, http://argo.jcommops.org).

2.1.4 CFSR Model Analyses

The CFSR data is from the NCEP Climate Forecast Systems Reanalysis dataset[4]. The model configuration consists of a coupled atmospheric model with an oceanic model. The atmospheric model was on a T382 horizontal resolution (38km) and consisted of 64 sigma-pressure hybrid vertical levels. The atmosphere model used the simplified Arakawa and Schubert (1974) convection scheme with momentum mixing scheme and incorporated the Tiedtke (1983) shallow convection scheme. The atmospheric model was a data assimilation model and incorporated radiances from satellite.

The atmospheric model was coupled to the GFDL MOM version 4p0d and a two-layer sea ice model (Griffies et al., 2004). The MOM version 4 is a finite differencing model of the ocean primitive equations under the Boussinesq and hydrostatic approximations. The horizontal resolution is based on the tripolar grid developed by Murray (1996). The zonal resolution is 0.5^o. The meridional resolution is 0.25^o between 10° S and 10° N, increasing to 0.5^o poleward of 30° both north and south. The ocean has 40 layers vertically, but most of the layers are near the surface with 27 of the layers in the upper 400m. The bottom depth of the model is approximately 4500m. The resolution in the top 240m is at 10m intervals. Vertical mixing follows nonlocal K-profile parameterization of Large et al. (1994)

---

[3]Available at ftp://ftp.nodc.noaa.gov/pub/data.nodc/argo/data
[4]Data Available http://dss.ucar.edu/pub/cfsr.html

and horizontal mixing uses the nonlinear scheme of Smagorinsky (Saha et al., 2010). The ocean model assimilated Argo profiles but not satellite altimetry. Therefore the model should provide a good basis for comparison versus in-situ observations.

2.2 Methodology

The overall analysis follows this outline: first, a hydrostatic height anomaly is either estimated or calculated from observations. The formation of the cold wake may not cause a depression in sea surface height, particularly if the change in temperature in the upper ocean is solely a function of mixing (e.g. Emanuel 2001). However, once the cold wake is formed and reheating of the upper ocean commences, the sea surface height is anticipated to increase due to the expansion of the formerly cold water. This sea surface height anomaly is estimated by Emanuel (2001) to be related to the temperature anomaly as in

$$h' = \int_0^\infty \beta T' dz \qquad (2.1)$$

where h is the SSH anomaly, T is the temperature anomaly, and β' is the coefficient of thermal expansion of seawater. This height anomaly is then related to the total heat anomaly of upper ocean content by:

$$Q' = \int_{-\infty}^\infty \frac{1}{\beta} \rho_0 C_l h' dW \qquad (2.2)$$

where ρ_0 and C_l are the density and heat capacity of seawater and W is the cross-track distance. The total heat anomaly is calculated more directly from the CFSR reanalysis data, as described below. These values are then compared for consistency. Lastly, the total incoming surface flux during the recovery time period is based on a temperature gradient calculation along a vertical cross section of the ocean. After the storm crosses through the ocean there is a temperature gradient where the waters in the upper ocean have cooled. Once the gradients return to defined pre-storm threshold the storm is to be considered

recovered. If the heat anomaly is roughly consistent with the total incoming surface flux, then the hypotheses of Emanuel (2001) could be correct. Thus, an argument can be made that tropical cyclones are an important driver of lateral heat flux away from the tropics. However, if there are other important processes occurring to re-stratify the upper ocean (one example being mesoscale eddies), then the magnitude of the effects of tropical cyclones on oceanic meridional heat transport is reduced.

2.2.1 Estimating height anomalies

Since one goal of this research was to evaluate the extent to which observations can provide information on upper ocean heat content changes, altimeter and Argo floats were evaluated for all hurricanes in the Atlantic Basin between 2000 and 2009. The first step was to find storms with visible cold wakes using TMI/AMSRE SST data. The first step in identifying cases for the study was to use the SST data to identified storms that have a noticeable cold wake. Once the storms were shown to have a clear cold wake in the SST, each was evaluated using the satellite altimetry to determine if there was good satellite altimeter coverage of the area affected by the storm. Further filtering of the storms was done using Argo float availability as described below.

The swaths chosen for this study need to cross the storm's track in a perpendicular path to show both the affected area of the ocean and the non-affected area. Each swath also needed to cross over the area that showed the greatest decrease in SST. For this study a scan from before or as the storm moves through the area is taken to be a pre-storm condition that becomes the basis for comparison. Then a difference between each repeat orbit scan is taken and shown in a similar fashion to Emanuel (2001) such that an increase in SSH represents an increase in the total amount of heating over the area. This comparison gives information as to the size and strength of the impact of the hurricane on the ocean. Lastly, a value of the total anomaly of upper ocean heat content is calculated from Equation 2.2 along each available altimeter track.

The next step in the process is to identify if the signal (if found) corresponds to in situ

data. The data used for this step in the process are Argo floats. In this case the floats were specified to provide useful information if we were able to find two observations within a 1° by 1° box and within 3 degrees of the actual storm track. The size of the box was chosen to be sufficiently large enough to have two buoys within the box yet small enough to hopefully capture the same body of water. The first observation had to be no more than 25 days before the storm passed through the area to capture as close as possible the pre-storm conditions needed for comparison. For the second observation, there needed to be an Argo float within the same box as the first observation and be no more than 5 days after the storm had passed so that it was possible to observe the exact impacts of the storm.

Given these strict conditions many storms either had relatively few or no usable Argo data points. While many storms have many Argo floaters near the storm track, only a select few actually met the basic criteria for having data that was within the time constraints. Furthermore, when those storms were investigated further for data quality control only 6 storms from the decade actually had usable data. The 6 storms were investigated for quality signal in microwave SST, number of available Argo floats in the area, and finally a clear cold wake that was not in the same area of a previous storm. The final three storms used as case studies in this research are described in more detail in section 2.3, and are Hurricanes Felix (2001), Isabel (2003), and Bill (2009). Hurricane Isabel (2003) did cross over the cold wake of Hurricane Fabian (2003); however, there was a very clear signal in the microwave SST in the area that was unaffected by Fabian (2003). Unfortunately, these three storms also presented their own troubles with the Argo float data and will be discussed later.

For each of the three storms, a hydrostatic height anomaly is calculated using the Argo float profiles. For this calculation, both Argo float profiles were linearly interpolated at 10 m increments from 5m to a depth of 105 meters. The interpolated temperature differences from before the storm has passed to after the storm had passed are calculated and integrated using Equation 2.1. The height anomalies are then compared to the satellite altimeter height anomalies from TOPEX/POSEIDON and JASON-2 for each storm.

17

2.2.2 Along-track and total cold wake re-stratification estimates

Given the very small amount of available data from concurrent Argo floats and altimeter tracks, the study also included more spatially-complete reanalysis model results. The Climate Forecast Systems Reanalysis (CFSR) model was used due to the fact it was a coupled atmosphere and ocean model. Thus, the cold wake recovery in the model is most likely related to the modeled surface heat fluxes, data assimilation, and other atmospheric and oceanic dynamics provided the modeled physics match reality. With data at every one-half degree in the ocean at every six hours the CFSR model provided ample data coverage both spatially and temporarily. It was important to give some validation to use the model so each of the previous methods for identifying the existence of a cold wake was performed.

As the first step of a reality check, the CFSR data was examined to see if a storm existed at the correct location as in the best track data and that there is distinguishable wind pattern similar to a hurricane in that location. The magnitude of the winds in the CFSR should not be comparable to the winds from the best track because at a resolution of 0.5^o the wind and pressure gradients would be much weaker then the best track. Furthermore the best track winds are not actually observed winds and so even with a very high resolution the model would not be expected to replicate the actual intensity Walsh et al. (2007). The model showed the formation and intensification of the hurricanes. The modeled winds were much less then the observed peak wind speeds, but as described before at a zonal grid resolution of 0.5^o and a meridional resolution increasing from 0.25^o to 0.5^o in the tropics, the sampling of averaged wind speeds is still too large to account for the mesoscale features such as the eye and eyewall Walsh et al. (2007). For Felix (2001), the maximum intensity of Hurricane Felix was 100 kts on September 14, 2001 (Stewart, 2001); and during the corresponding time in the CFSR the storm had winds of just 33kts at 1000hpa. The modeled winds represent an area averaged wind field and so general shape and structure is a good indication that the model is resolving the existence of a tropical cyclone. For each case the model did show evidence of a tropical cyclone forming during the correct period of time and moving along the right track as shown in the best track dataset (Landsea et al., 2004). As a further check,

SSTs were compared from a pre-storm date to a couple of days after the date of maximum sustained winds to check for a surface manifestation of a cold wake. Each of the three case studies showed a pronounced surface cold wake in the CFSR data. Detailed results of these analyses are shown in Chapter 4.

In order to determine the depth to which the cold wake formed, vertical slices of the CFSR temperature were plotted to see the impact of the mixing. The slice taken for each storm was selected to be the area where the maximum cooling had occurred in the SST and was taken to intersect the storm track perpendicularly. For both Hurricane Isabel (2003) and Bill (2009) the cross section was zonally oriented. For Hurricane Felix (2001) the cross section was meridionally oriented. In each case there was a clear signal at depth in the CFSR data. After it was shown that the storm existed in the CFSR and that the storm produced an oceanic response, the next step involves comparisons of the model with in situ data. It is difficult to to directly compare the SSH signal from the model with the SSH anomaly fields from the satellite, as the anomaly fields from the altimeter data are calculated based on differences from climatology whereas the modeled differences are from the days leading up to the storm to the days immediate following the storm. However, some comparisons are possible with respect to changes in SSH fields from before, during, and after cold wake formation, and these comparisons are shown in Chapter 4.

The CFSR data are also used to determine the cold wake extent and duration, the amount of warming needed to recover from the cold wake, and finally the actual surface warming that occurred during re-stratification. The extent of the cold wake was determined from the SST values. First, a base day was chosen to be the pre-storm condition. Then the SST for each successive day was subtracted from the original SST. The latitude and longitude for each grid point with at least a 1^oC decrease was recorded so that as each successive day passed new grid points were added to the previous grid points. Using this technique, a polygon is created that shows the movement of the storm and is an objective way of defining the area the storm impacted.

Once the area of the ocean was determined, then the upper ocean heat loss was calcu-

lated. This was done by integrating from the bottom of the upper ocean (chosen to be 105m to capture the top 100m of heat change) to the surface (5m) using the following equation;

$$\Delta q = \int_z^0 \rho C p \Delta T \mathrm{d}z \tag{2.3}$$

where Δq is the heat loss, ρ is the density of water, Cp is the specific heat of water (at 0° C), ΔT is the change in temperature at depth z as z increases from the the bottom to the surface, and $\mathrm{d}z$ is interval between depths which was 10m. This equation provides the mean heat loss of a grid cell centered at a given latitude and longitude. The heat loss was calculated for each day for which there is a best track observation and was calculated at each grid point in the polygon. The reference profile for each grid was the profile from two days prior to the date in the best track and profile used as the after storm was from two days after the day of best track given a range of 4 days for each time period. The maximum heat loss was recorded for each grid point in the polygon and was determined to be the heat loss due to the passage of the tropical cyclone.

The final step of the analysis requires an estimate of the total amount of surface heating that the ocean actually receives before cold wake recovery is complete. However, before this could be calculated an objective method to identify how long the cold wake exists needed to be created. A thermal gradient perpendicular to the track of the storm was calculated. To calculate this gradient, the temperature at one grid point was subtracted from a grid point 0.5^o apart along a line intersecting the path of the storm. The absolute value of each of the differences was added together to get a total gradient. The reason the absolute value is used is because as the difference approaches (moves away from) the center of the path, the temperatures should be decreasing (increasing). For example, in the case of hurricane Felix (2001), the maximum ΔSST was about 2° C. So as a difference is calculated moving perpendicular to the track path, each temperature closer to the center of maximum ΔSST would be smaller thus creating a positive difference. As the temperatures move away from the center of the ΔSST, each temperature would be larger then the previous temperature

creating a negative difference. By taking the absolute value of the differences, it is possible to isolate the change in the temperature gradient along a constant depth. This was calculated at 5 different depths: 35m, 45m, 55m, 65m and 75m. Depths less then 35m were excluded to negate transient warming effects such as diurnal variability effects and 75m was chosen to be the maximum depth because in the cross sections it was the deepest depth that showed change in the upper ocean due to hurricane passage in the three cases from the CFSR data.

To create an objective determination of how long the cold wake lasted in the thermal gradient, the pre-storm thermal gradient was compared to the post storm thermal gradient. The level that the post-storm thermal gradient needed to decrease to was defined as the average of the thermal gradient of the 5 depths plus two times the standard deviation allowing for error in the initial mean. Since each depth returned to the pre-storm level at different times, the duration of the cold wake was taken to be the average time it took to return to the pre-storm condition. Examples of these calculations for each storm are shown in Chapter 4. Further discussion about the impacts of the choice of two standard deviations occurs when results are shown in Chapter 4 as well.

Once the area affected and the duration of the cold wake was determined it was then possible to make the energy budget calculations. In order to compare how much heating was performed by the ocean and how much was due to incoming solar radiation, the total incoming flux from CFSR was summed over the duration of the cold wake at each of the same points for which a heat loss maximum was calculated. This enabled a direct comparison of the amount of heat loss to the amount of heat gained from the atmosphere during the duration of the cold wake. The difference between these values would presumably indicate additional re-stratification of the cold wake by dynamic oceanic processes. It should be noted that the importance of hurricanes to meridional heat transport as hypothesized by Emanuel (2001) was predicated upon the assumption that all cold wake heat loss would be restored by surface warming; these quantitative results will test that assumption.

2.3 Hurricane Case Studies

2.3.1 Hurricane Felix 2001

The methods described previously were performed on three different case studies. The first of these case studies is hurricane Felix (2001). The following is a summary of the National Hurricane Centers (NHC) report on hurricane Felix (2001) (Stewart, 2001). Felix formed as a tropical wave as a surface low crossed over the African coast on the 5 September 2001. The next day the system moved westward into the Atlantic Ocean and started to develop some initial circulation. As the storm continued to track westward, convection continued to increase and weak banding features began to develop around the center of the storm. On the 7 September 2001, convection became more centered and the banding features continued to increase in intensity and lead to being designated Tropical Depression (TD) Seven. At this point TD Seven was located roughly 360 nautical miles to the southwest of the Cape Verde Islands.

As TD Seven continued to track across the ocean it ran into an unfavorable shearing environment and quickly became disorganized. During the next three days the storm passed through unfavorable shearing areas and reorganized into the storm that would be named Tropical Storm Felix. Tropical Depression Seven was named Felix on 11 September 2001 around 1200 UTC after maintaining intensity near 30kts for a period of 24 hours then intensifying to an estimated tropical storm force with banding consistent with tropical storm features. After being named the storm curved to the north and reached hurricane intensity on 13 September near 0000 UTC. Upon strengthening to hurricane status the storm then underwent rapid intensification and increased intensity by 30kts over an 18 hour period. NHC estimates that hurricane Felix (2001) reached its maximum intensity of 100kts around 0000 UTC on 14 September 2001 at an estimated 1400 miles southwest of the Azores. Felix continued to recurve back towards the northeast and followed a weakening pattern as in moved. By the 17 September 2001, Felix (2001) had weakened to a tropical storm and continued to move towards the northeast into colder waters. Hurricane Felix (2001) did

not make landfall as a tropical system. The following table is the best track locations and intensity for hurricane Felix (2001)[5]:

Table 2.1: **Best track data for hurricane Felix (2001).**

ADV	LAT	LON	TIME	WIND	PR	STAT
1	13.90	-28.40	09/07/18Z	30	1008	TROPICAL DEPRESSION
2	14.40	-29.50	09/08/00Z	30	1007	TROPICAL DEPRESSION
3	14.80	-31.00	09/08/06Z	30	1007	TROPICAL DEPRESSION
4	15.00	-33.00	09/08/12Z	30	1008	TROPICAL DEPRESSION
5	15.00	-35.10	09/08/18Z	25	1009	TROPICAL WAVE
6	15.00	-37.00	09/09/00Z	25	1009	TROPICAL WAVE
7	15.00	-38.70	09/09/06Z	25	1009	TROPICAL WAVE
8	15.00	-40.20	09/09/12Z	25	1009	TROPICAL WAVE
9	15.00	-41.70	09/09/18Z	25	1009	TROPICAL WAVE
10	15.20	-43.10	09/10/00Z	25	1009	TROPICAL WAVE
11	16.00	-43.70	09/10/06Z	30	1008	TROPICAL DEPRESSION
12	16.50	-44.80	09/10/12Z	30	1008	TROPICAL DEPRESSION
13	16.90	-45.80	09/10/18Z	30	1007	TROPICAL DEPRESSION
14	17.30	-46.80	09/11/00Z	30	1006	TROPICAL DEPRESSION
15	17.80	-47.40	09/11/06Z	30	1004	TROPICAL DEPRESSION
16	18.60	-47.70	09/11/12Z	35	1003	TROPICAL STORM
17	19.40	-48.00	09/11/18Z	35	1003	TROPICAL STORM
18	20.20	-48.40	09/12/00Z	40	1000	TROPICAL STORM
19	21.00	-48.80	09/12/06Z	45	998	TROPICAL STORM
20	22.00	-48.90	09/12/12Z	55	994	TROPICAL STORM
21	22.90	-49.00	09/12/18Z	60	993	TROPICAL STORM
22	23.90	-48.90	09/13/00Z	65	987	HURRICANE-1
23	24.80	-48.60	09/13/06Z	75	979	HURRICANE-1
24	25.90	-48.40	09/13/12Z	85	972	HURRICANE-2
25	27.10	-48.00	09/13/18Z	95	966	HURRICANE-2
26	28.20	-47.20	09/14/00Z	100	962	HURRICANE-3
27	29.30	-46.60	09/14/06Z	100	962	HURRICANE-3
28	30.10	-45.50	09/14/12Z	95	966	HURRICANE-2
29	30.90	-44.30	09/14/18Z	90	970	HURRICANE-2
30	31.20	-42.80	09/15/00Z	90	970	HURRICANE-2
31	31.50	-41.40	09/15/06Z	90	970	HURRICANE-2
32	31.70	-39.50	09/15/12Z	90	970	HURRICANE-2
33	32.10	-37.60	09/15/18Z	85	975	HURRICANE-2
34	32.10	-36.00	09/16/00Z	85	975	HURRICANE-2
35	32.60	-34.80	09/16/06Z	80	976	HURRICANE-1
36	33.40	-33.30	09/16/12Z	75	977	HURRICANE-1
37	34.30	-32.40	09/16/18Z	70	979	HURRICANE-1
38	35.10	-32.00	09/17/00Z	70	981	HURRICANE-1
39	35.40	-31.70	09/17/06Z	65	983	HURRICANE-1

Continued on Next Page...

---

[5]Available from Unisys Weather at http://weather.unisys.com/hurricane/atlantic/2001/FELIX/track.dat

Table 2.1 – Continued. Best Track Data for Hurricane Felix (2001)

ADV	LAT	LON	TIME	WIND	PR	STAT
40	35.30	-31.50	09/17/12Z	60	985	TROPICAL STORM
41	35.20	-31.80	09/17/18Z	55	990	TROPICAL STORM
42	35.00	-32.00	09/18/00Z	45	995	TROPICAL STORM
43	34.80	-32.00	09/18/06Z	40	998	TROPICAL STORM
44	34.70	-31.90	09/18/12Z	35	1001	TROPICAL STORM
45	34.70	-31.70	09/18/18Z	30	1002	TROPICAL DEPRESSION
46	34.60	-31.60	09/19/00Z	25	1002	TROPICAL DEPRESSION

2.3.2 Hurricane Isabel 2003

The second storm profiled is Hurricane Isabel (2003). Isabel was a Cape Verde Hurricane and moved across the Atlantic and eventually made landfall on the east coast of the United States. Once again the following is a summary of NHC's tropical cyclone report (Beven and Cobb, 2004). Similar to Hurricane Felix, Isabel formed as a tropical wave moved off the coast of Africa on 1 September 2003. The wave moved westward and slowly became organized. Isabel was first classified as a tropical depression on 6 September 0000 UTC and only 6 hours later was named a tropical storm. The next day Isabel turned to the west-northwest and strengthened to a hurricane. This strengthening continued over the next 2 days. The storm turned westward again and tracked to the south of the Azores-Bermuda high pressure system. During this time Isabel (2003) reached a peak intensity of a category 5 at an estimated 145kt one minute sustained wind speed on 11 September 2003. Isabel moved towards the Azores Bermuda high pressure system and once again turned from west-northwest to north-northwest on 16 September where it would continue for the rest of the duration of the storm's existence.

As the storm moved closer to landfall increased vertical shear weakened Isabel. The storm weakened to below major hurricane strength on the 16 September 2003. For the next two days Isabel would continue on a path tracking right into the Outer Banks of North Carolina. The storm made landfall as a Category 2 storm with winds of 85-90 kts near Drum

Inlet, NC late in the date of 18 September 2003. The storm continued in the same direction and weakened to tropical storm strength over Virginia. As Isabel moved into western Pennsylvania it underwent extratropical transition and continued as an extratropical storm into Canada where it was absorbed into a baroclinic system moving eastward across Canada on the 20 September 2003. The following table is the best track locations and intensity for hurricane Isabel (2003)[6]:

Table 2.2: **Best track data for hurricane Isabel (2003).**

ADV	LAT	LON	TIME	WIND	PR	STAT
1	13.80	-31.40	09/06/00Z	30	1009	TROPICAL DEPRESSION
2	13.90	-32.70	09/06/06Z	35	1005	TROPICAL STORM
3	13.60	-33.90	09/06/12Z	40	1003	TROPICAL STORM
4	13.40	-34.90	09/06/18Z	45	1000	TROPICAL STORM
5	13.50	-35.80	09/07/00Z	55	994	TROPICAL STORM
6	13.90	-36.50	09/07/06Z	60	991	TROPICAL STORM
7	14.40	-37.30	09/07/12Z	65	987	HURRICANE-1
8	15.20	-38.50	09/07/18Z	70	984	HURRICANE-1
9	15.80	-39.70	09/08/00Z	80	976	HURRICANE-1
10	16.50	-40.90	09/08/06Z	95	966	HURRICANE-2
11	17.10	-42.00	09/08/12Z	110	952	HURRICANE-3
12	17.60	-43.10	09/08/18Z	110	952	HURRICANE-3
13	18.20	-44.10	09/09/00Z	115	948	HURRICANE-4
14	18.90	-45.20	09/09/06Z	115	948	HURRICANE-4
15	19.40	-46.30	09/09/12Z	115	948	HURRICANE-4
16	20.00	-47.30	09/09/18Z	115	948	HURRICANE-4
17	20.50	-48.30	09/10/00Z	110	952	HURRICANE-3
18	20.90	-49.40	09/10/06Z	110	952	HURRICANE-3
19	21.10	-50.40	09/10/12Z	115	948	HURRICANE-4
20	21.10	-51.40	09/10/18Z	120	942	HURRICANE-4
21	21.20	-52.30	09/11/00Z	125	935	HURRICANE-4
22	21.30	-53.20	09/11/06Z	125	935	HURRICANE-4
23	21.40	-54.00	09/11/12Z	135	925	HURRICANE-4
24	21.50	-54.80	09/11/18Z	145	915	HURRICANE-5
25	21.60	-55.70	09/12/00Z	140	920	HURRICANE-5
26	21.70	-56.60	09/12/06Z	140	920	HURRICANE-5
27	21.60	-57.40	09/12/12Z	140	920	HURRICANE-5
28	21.70	-58.20	09/12/18Z	140	920	HURRICANE-5
29	21.80	-59.10	09/13/00Z	135	925	HURRICANE-4
30	21.90	-60.10	09/13/06Z	130	935	HURRICANE-4
31	22.10	-61.00	09/13/12Z	135	935	HURRICANE-4

Continued on Next Page...

---

[6]Available from Unisys Weather at http://weather.unisys.com/hurricane/atlantic/2003/ISABEL/track.dat

Table 2.2 – Continued. Best Track Data for Hurricane Isabel (2003)

ADV	LAT	LON	TIME	WIND	PR	STAT
32	22.50	-62.10	09/13/18Z	140	932	HURRICANE-5
33	22.90	-63.30	09/14/00Z	135	935	HURRICANE-4
34	23.20	-64.60	09/14/06Z	135	939	HURRICANE-4
35	23.50	-65.80	09/14/12Z	135	935	HURRICANE-4
36	23.90	-67.00	09/14/18Z	140	933	HURRICANE-5
37	24.30	-67.90	09/15/00Z	130	937	HURRICANE-4
38	24.50	-68.80	09/15/06Z	125	940	HURRICANE-4
39	24.80	-69.40	09/15/12Z	120	946	HURRICANE-4
40	25.30	-69.80	09/15/18Z	115	949	HURRICANE-4
41	25.70	-70.20	09/16/00Z	105	952	HURRICANE-3
42	26.30	-70.50	09/16/06Z	100	955	HURRICANE-3
43	26.80	-70.90	09/16/12Z	95	959	HURRICANE-2
44	27.40	-71.20	09/16/18Z	95	959	HURRICANE-2
45	28.10	-71.50	09/17/00Z	95	957	HURRICANE-2
46	28.90	-71.90	09/17/06Z	95	957	HURRICANE-2
47	29.70	-72.50	09/17/12Z	90	957	HURRICANE-2
48	30.60	-73.00	09/17/18Z	90	955	HURRICANE-2
49	31.50	-73.50	09/18/00Z	90	953	HURRICANE-2
50	32.50	-74.30	09/18/06Z	90	956	HURRICANE-2
51	33.70	-75.20	09/18/12Z	90	956	HURRICANE-2
52	35.10	-76.40	09/18/18Z	85	958	HURRICANE-2
53	36.70	-77.70	09/19/00Z	65	969	HURRICANE-1
54	38.60	-78.90	09/19/06Z	50	988	TROPICAL STORM
55	40.90	-80.30	09/19/12Z	35	997	EXTRATROPICAL STORM
56	43.90	-80.90	09/19/18Z	30	1000	EXTRATROPICAL DEPRESSION
57	48.00	-81.00	09/20/00Z	25	1000	EXTRATROPICAL DEPRESSION

2.3.3   Hurricane Bill 2009

The final storm used as a case study was Hurricane Bill (2009). Bill was also a Cape Verde hurricane and skirted by Bermuda and Nova Scotia without making direct landfall as a hurricane. Per NHC's synoptic history (Avila, 2009), Bill's genesis was the result of a vigorous tropical wave with an associated broad low pressure system that moved off of the coast of western Africa on 12 August 2009. This system moved westward to the south of the Cape Verde Islands on the 13 August 2009 and two days later was named a tropical depression located about 330 n mi to the west-southwest of the Cape Verde Islands.

Aided by a region of relatively light vertical shear of the east-central tropical Atlantic,

the system continued to strengthen. On 15 August 2009, approximately 12 hours after being named a tropical depression, the system had strengthened to tropical storm intensity and became a hurricane 36 hours later. The storm continued to move westward and intensify reaching an estimated peak intensity of 115 kt at 0600 UTC on the 19 August 2009 was centered approximately 300 n mi east northeast of the northern Leeward Islands.

As Bill neared the southwestern edge of a subtropical ridge, the storm started to recurve toward the north in between a large trough on the east coast of the United States and the subtropical ridge that had been the driving force across the Atlantic. Bill moved north in between Bermuda and the United States and missed a direct hit by about 150 miles to the west on 22 August 2009. As Bill moved northward it gradually began to weaken as it moved into a stronger shearing environment. The storm picked up speed and continued to recurve just off of the coast and then clipped the southern coast of Nova Scotia and eventually made landfall in Newfoundland as a weakened tropical storm on 24 August 2009. The best track and locations are shown in Table 2.3[7]: .

Table 2.3: **Best track data for hurricane Bill (2009).**

ADV	LAT	LON	TIME	WIND	PR	STAT
1	11.50	-34.00	08/15/15Z	30	1006	TROPICAL DEPRESSION
2	11.30	-35.20	08/15/21Z	35	1004	TROPICAL STORM
3	11.30	-36.60	08/16/03Z	35	1004	TROPICAL STORM
4	11.40	-37.20	08/16/09Z	40	1002	TROPICAL STORM
5	12.10	-38.40	08/16/15Z	50	997	TROPICAL STORM
6	12.80	-40.00	08/16/21Z	55	994	TROPICAL STORM
7	13.40	-41.70	08/17/03Z	60	990	TROPICAL STORM
8	13.80	-44.00	08/17/09Z	65	987	HURRICANE-1
9	14.10	-45.20	08/17/15Z	80	977	HURRICANE-1
10	14.60	-46.70	08/17/21Z	80	969	HURRICANE-1
11	15.00	-48.30	08/18/03Z	85	967	HURRICANE-2
12	15.50	-49.70	08/18/09Z	85	967	HURRICANE-2
13	15.90	-51.20	08/18/15Z	90	963	HURRICANE-2
14	16.60	-52.20	08/18/21Z	95	962	HURRICANE-2
15	17.20	-53.40	08/19/03Z	110	952	HURRICANE-3
16	18.00	-54.90	08/19/09Z	115	948	HURRICANE-4

Continued on Next Page. . .

[7]Available from Unisys Weather at http://weather.unisys.com/hurricane/atlantic/2009/BILL/track.dat

Table 2.3 – Continued

ADV	LAT	LON	TIME	WIND	PR	STAT
17	18.70	-56.30	08/19/15Z	115	950	HURRICANE-4
18	19.80	-57.60	08/19/21Z	115	947	HURRICANE-4
19	20.70	-58.90	08/20/03Z	115	945	HURRICANE-4
20	21.60	-60.30	08/20/09Z	110	949	HURRICANE-3
21	22.60	-61.70	08/20/15Z	105	951	HURRICANE-3
21A	23.20	-62.60	08/20/18Z	105	951	HURRICANE-3
22	23.80	-63.20	08/20/21Z	110	948	HURRICANE-3
22A	24.40	-63.90	08/21/00Z	110	948	HURRICANE-3
23	24.90	-64.30	08/21/03Z	110	943	HURRICANE-3
23A	25.50	-64.90	08/21/06Z	105	951	HURRICANE-3
24	26.20	-65.40	08/21/09Z	105	951	HURRICANE-3
24A	26.80	-65.80	08/21/12Z	100	958	HURRICANE-3
25	27.60	-66.30	08/21/15Z	100	958	HURRICANE-3
25A	28.50	-66.80	08/21/18Z	95	957	HURRICANE-2
26	29.40	-66.90	08/21/21Z	90	954	HURRICANE-2
26A	30.20	-67.00	08/22/00Z	90	954	HURRICANE-2
27	31.00	-67.50	08/22/03Z	90	957	HURRICANE-2
27A	32.20	-68.20	08/22/06Z	90	959	HURRICANE-2
28	33.00	-68.50	08/22/09Z	90	960	HURRICANE-2
28A	34.00	-68.40	08/22/12Z	90	960	HURRICANE-2
29	35.10	-68.60	08/22/15Z	85	964	HURRICANE-2
29A	36.00	-68.80	08/22/18Z	85	964	HURRICANE-2
30	37.10	-68.80	08/22/21Z	75	961	HURRICANE-1
30A	37.80	-68.30	08/23/00Z	75	961	HURRICANE-1
31	39.10	-67.80	08/23/03Z	75	961	HURRICANE-1
31A	40.10	-67.40	08/23/06Z	75	962	HURRICANE-1
32	41.20	-66.50	08/23/09Z	75	961	HURRICANE-1
32A	42.40	-65.40	08/23/12Z	75	965	HURRICANE-1
33	43.30	-64.00	08/23/15Z	75	967	HURRICANE-1
33A	44.40	-62.50	08/23/18Z	70	970	HURRICANE-1
34	45.10	-60.80	08/23/21Z	65	970	HURRICANE-1
34A	46.20	-57.90	08/24/00Z	65	970	HURRICANE-1
35	47.10	-55.50	08/24/03Z	65	975	HURRICANE-1
35A	47.90	-53.60	08/24/06Z	65	980	HURRICANE-1
36	48.60	-50.20	08/24/09Z	60	980	TROPICAL STORM

These three storms form the basis for both the in situ analysis described in the Chapter 3 as well as the CFSR analysis in Chapter 4.

CHAPTER 3

OBSERVATIONAL RESULTS

This chapter outlines an analysis of the estimated total heat anomaly through the use of satellite altimetry. Where possible for each of the three cases, the assumption that the height anomaly can be closely tied to the temperature anomaly induced by the hurricane, is investigated through the ARGO floats.

3.1 Hurricane Felix (2001)

The satellite SST field shows a distinct cold wake that formed to the right of the best track of hurricane Felix of roughly 2 to 3° C (Figure 3.1). There are only two satellite passes that have a swath that crosses the best track at roughly right angles over the area associated with the largest impacted SSTs. These are passes 215 and 226 and are depicted in cyan and magenta, respectively, in Figure 3.1 from the TOPEX/POSEIDON satellite. The other black lines show other passes that were not chosen due to either not crossing the largest impacted area or not crossing close enough to perpendicular. A time series of the SSH anomalies recorded along the track before and after for passes 215 and 226 the cold wake formation is shown in Figure 3.2 and 3.3. Each time series represents a repeat orbit of 10 days after the original orbit. For Figure 3.2, Hurricane Felix (2001) passed over the location on the 17 September. The first time period shown is 16 September, just before the passage of Felix, thus this orbit contains the cold wake-induced changes to the SSH (if any). The following orbits are shown as differences from this orbit. The vertical dashed

line depicts the best track location. The right of the figure corresponds to the right of the storm

Given that the cause of a cold wake is predominantly mixing (Price, 1981), not enthalpy flux into the atmosphere, there should be minimal changes in the overall volume of heat surrounding the track of the storm. The heat is redistributed both away from and deeper from the track. Therefore the heating of the cold wake should show up in post-storm SSH time series as an increase in height and thus an increase in the total amount of volume-integrated heat. There is an apparent height rise just to the right of the storm's center. In Figure 3.2, the height rise is on the order of magnitude of about a 10 cm rise over a width of 30 km and persists for a month after the storm passed. In Figure 3.3, there is a height rise of about 15 cm over a distance of about 50 km and that signal lasts for a full 2 months after the storm has passed. Using the h' from the SSH and Equation 2.2 shown below, the estimated amount of heating occurring for hurricane Felix is 1.5439×10^{14} Jm^{-1} for pass 226 and 6.1755×10^{13} Jm^{-1} for pass 215. These estimates are of similar magnitude to the estimated Q' from Emanuel (2001).

$$Q' = \int_{-\infty}^{\infty} \frac{1}{\beta} \rho_0 C_l h' dW$$

$$\rho_0 = 1025 \frac{kg}{m^3} \quad C_l = 4217.4 \frac{J}{kgK} \quad \beta = 2.1 \times 10^{-4} \frac{1}{K}$$

Pass 226

$$h' = 15cm = 0.15m, dW = 50km = 50000m$$

$$Q' = \left(\frac{1}{2.1 \times 10^{-4}} K \right) \left(1025 \frac{kg}{m^3} \right) \left(4217.4 \frac{J}{kgK} \right) (0.15m)(50,000m)$$

$$Q' = (\cancel{K}) \left(\frac{kg}{\cancel{m^3}} \right) \left(\frac{m^{\cancel{2}}}{s^2 \cancel{K}} \right) (\cancel{m})(\cancel{m})$$

$$Q' = 1.5439 \times 10^{14} \frac{kg\, m}{s^2} = Jm^{-1}$$

Pass 215

$$h' = 10cm = 0.1m, dW = 30km = 30000m$$

$$Q' = \left(\frac{1}{2.1 \times 10^{-4}}K\right)\left(1025\frac{kg}{m^3}\right)\left(4217.4\frac{J}{kgK}\right)(0.10m)(30,000m)$$

$$Q' = 6.1755 \times 10^{13}\frac{J}{m}$$

The change in SSH associated with the cooling of the upper ocean is next determined from an analysis of the ARGO float data. Figure 3.5 shows the locations of the buoys for hurricane Felix that met the criteria for being either a before storm observation or an after storm observation. Comparing the number of post-storm quality control buoys, Figure 3.5, to the location of all of the buoys simply meeting location constraints, Figure 3.4, demonstrates the severe restriction of these time and location constraints on possible buoys measurements. Figure 3.6 is the calculated SSH anomaly from Equation 2.1 for the ARGO float profiles.

The expected values of SSH anomaly in Figure 3.6 should be larger on the right of the storm track and smaller on the left to be consistent with the SSH anomalies. This is because warmer water is less dense at constant salinity and thus has more total volume and the increased heating is expected to be on the right side of the storm. Figure 3.6 does not give expected results. The burgundy and olive colors on the left of the storm are greater than that of the one observation on the right of the storm track. Recalling Figure 3.1 to look at the location of the most pronounced colder waters, the location of the three observations also do not fall in the area where the strongest part of the cold wake was located.

Upon closer inspection of the actual profiles in Figures 3.7 through 3.11, there does not seem to be any pair of buoys that shows the expected profile of a cold wake. The profile best located with respect to the maximum cooling of the cold wake is shown in Figure 3.10 and it shows the temperature at the surface to be warmer than the pre-storm near surface temperature. This is counter to what is observed in the SST so either the profiles are not measuring the same body of water, or enough time had passed that the surface had begun to reheat before the Argo profile surfaced again. It is clear that in Figure 3.9, the two

profiles are not measuring the same body of water because there is a difference of almost 2 degrees at a depth of 200m.

Unfortunately this is an extremely small sample size and not collocated with the crossing of the satellite, so the results are at best inconclusive from the hurricane Felix case. While, the SSH shows a signal of heating to the right of the storm track that signal can not be validated using the actual Argos profiles. The main reason for this is the small sample size of Argo floats in the available area. Therefore, the calculated ARGO height anomaly cannot be completely trusted due to the possibility of measuring different water masses.

3.2   Hurricane Isabel (2003)

For hurricane Isabel (2003), the SST show a large area of cooler temperatures to the right of the track shown in Figure 3.12. The satellite passes of importance for hurricane Isabel are pass 217 and pass 65 shown in cyan and magenta. There is between a 2° and 6° drop in temperature relative to SSTs near the cold wake. Figure 3.13 shows the SSH for pass 217. There is an increase in magnitude of SSH on the right side of the storm albeit it is a much broader signal. There is an increase of between 15cm and 20cm over about 250km and persists until the end of the data record meaning that the increase in SSH lasts for at least 2 months. There is a missing cycle in the data and that was due to bad or missing JASON-1 data. Estimating the amount of heating in Figure 3.13 on 20 October 2003 gives the result of 1.029×10^{15} Jm^-1. This is an order of magnitude larger than Emanuel (2001) predicted and that may be because Isabel was a stronger storm then hurricane Edouard (1996).

<div align="center">Pass 217</div>

$$h' = 20cm = 0.2m, dW = 250km = 250,000m$$

$$Q' = \left(\frac{1}{2.1 \times 10^{-4}} K \right) \left(1025 \frac{kg}{m^3} \right) \left(4217.4 \frac{J}{kgK} \right) (0.20m)(250,000m)$$

$$Q' = 1.029 \times 10^{15} \frac{J}{m}$$

Looking at the SSH for pass 65 in Figure 3.14, there is a very large increase in SSH, however, it is not to the left of the storm. Instead, the largest increase in SSH occurs directly over the center of where the storm moved through the area. An estimation of the heating from Figure 3.14 on 24 October 2003 shows Q' to be 1.69×10^{15}Jm^{-1}. This is consistent with the amount of Q' from pass 217. Similarly to pass 217, the signal in the data lasts for the entire duration of the time period which is more than 2 months.

$$\text{Pass } 65$$

$$h' = 50cm = 0.5m, dW = 165km = 165000m$$

$$Q' = \left(\frac{1}{2.1 \times 10^{-4}}K\right)\left(1025\frac{kg}{m^3}\right)\left(4217.4\frac{J}{kgK}\right)(0.50m)(165,000m)$$

$$Q' = 1.69 \times 10^{15}\frac{J}{m}$$

Continuing into case number 2 from the Argo approach, once again there is a limiting factor in the number of available Argo floats to calculate a true anomaly field. As mentioned before, although there were a larger number of before and after buoys that met the criteria as shown in Figure 3.15, only one location provided a set that could be calculated into an anomaly. Each of the other buoy observations either did not have a before time or an after time that matched the location. Without multiple matching profiles, a figure similar to Figure 3.6 provides little information. Instead, the single location with matching Argo floats is shown in Figure 3.16 with the corresponding SST for the day when the profile was taken. From the figure, it is evident that the storm had passed over the location and that the second observation was directly in the path of the storm. Comparing the before and after profiles shows almost no change. This is most likely due to issues in data quality control; however with no other available observations that match the criteria it is difficult to tell whether or not the Argo profile actually felt the effects of the passing storm.

33

3.3   Hurricane Bill (2009)

An analysis of the SSH tracks for hurricane Bill show that there are many different passes that cross the cold wake of the storm. In Figure 3.17, all of the crossing satellite passes are shown with the passes that were chosen for the study in a different color. The three passes used are pass 39 (cyan), pass 202 (magenta) and pass 115 (green). Each of these passes cross the cold wake closest to 90° and cross at its strongest impacted area. Similar to hurricane Felix (2001) the cold wake temperatures are lower than the surrounding waters by 3° to 5^oC. In this case there are two passes, pass 39 and 115, that move from southwest to the northeast that intersect the cold wake once. There are is one along track passes where the pass moves from east to west and northward. This pass, pass 202, actually intersects the track twice.

The first pass is pass 39, shown in cyan in Figure 3.17. Figure 3.18 shows the time series of successive SSH scans across the impacted area. There does not appear to be any distinguishable signal in the data and so Q' will not be calculated from this SSH field.

The second pass, pass 202 shown in magenta, is the pass that crosses the track twice. The first crossing was in the area where the storm was at near peak intensity as a category 4 storm with winds at 130 mph and moving at 18 mph. At this time, the storm was located approximately due east of Puerto Rico shown in Figure 3.17. The SSH for the first crossing is shown on the left of Figure 3.19. There is a clear increase in SSH on the right side of the storm track on the order of about 35cm on 14 October 2009. Given that the area affected is on the order of about 150km, the Q' for that location is approximately 1.08×10^{15} Jm^{-1}. The second time that pass 202 crosses the path of the cold wake is to the southeast of Nantucket Island. That crossing is show on the right side of Figure 3.19 with the right side of the storm appearing on the left side of the red dashed line. At that location, the hurricane was weakening and was a category 1 storm with wind speeds of approximately 60kt as it progressed towards the northwest into colder waters. It is unsurprising that the

SSH effects are hard to distinguish given the close proximity to the Gulf Stream current.

<div align="center">Pass 202</div>

$$h' = 35cm = 0.35m, dW = 150km = 150000m$$

$$Q' = \left(\frac{1}{2.1 \times 10^{-4}}K\right)\left(1025\frac{kg}{m^3}\right)\left(4217.4\frac{J}{kgK}\right)(0.35m)(150,000m)$$

$$Q' = 1.69 \times 10^{15}\frac{J}{m}$$

The final pass, pass 115, is shown in green in Figure 3.17. It is similar to the second crossing of pass 202 and pass 39 in that there is a lack of a distinguishable signal to the right side of the storm. On the left side there does appear to be an increase in SSH of about 20cm over about 160km. This is on the opposite side of where the expected induced heating is. It is not obvious as to why the ocean is receiving an estimated 6.59×10^{14} Jm^{-1} on the left side of the storm.

<div align="center">Pass 65</div>

$$h' = 20cm = 0.2m, dW = 160km = 160000m$$

$$Q' = \left(\frac{1}{2.1 \times 10^{-4}}K\right)\left(1025\frac{kg}{m^3}\right)\left(4217.4\frac{J}{kgK}\right)(0.20m)(160,000m)$$

$$Q' = 1.69 \times 10^{15}\frac{J}{m}$$

Evaluating the Argo float data for case 3, there are a substantial number of Argo float profiles that exist near the best track for hurricane Bill (Figure 3.29). The matches occur on both sides of the storm track and multiple locations along the track. This allows for an adequate representation of calculated ARGO height anomaly. Figure 3.30 shows all of the calculated anomalies based on the Argo floats. Recall from Figure 3.17 that the most pronounced area of colder temperature is in the eastern most part of the hurricane track where the storm is traveling in a track that is nearly parallel track to the East Coast. However, just as before with hurricane Felix (2001) (Figure 3.6) , the data do not show a

clear succinct signal of warmer, reheated, values on the right side of the storm track.

In the developing phase of the hurricane there are larger values on the right side of the storm, however, there is nothing for comparison to on the left side of the storm track. At the peak intensity of the storm there is one larger value at about 24^oN, 66^oW on the left of the storm track, but there are no values on the right that would give a clear signal. The larger cluster of data points in the region with the most pronounced colder temperatures does not seem to have a distinct signal. The larger values are on the right side of the storm track making it possible that the storm has started to recover at that point. However there are a large number of discrepancies from this figure because the largest values actually occur as singular points on the left side of the storm track.

The sets of profiles are shown in Figures 3.21- 3.27 with the corresponding satellite SSTs for each location and time of observation. For simplicity, of the seventeen pairs of ARGO floats, only the ARGO floats that had the after storm observation clearly located in the cold wake will be shown and described. The first profile is the one located at 19^oN 54° W and is shown in Figure 3.21. In the before storm observation, the SST field shows a weak temperature gradient with warmer temperatures in the west and becoming colder towards the east. The SST in the after observation shows that the storm has passed through the area in a northwesterly direction and has left a clear wake of temperatures colder then the surroundings by about 2^oC. The profiles in this case show that the was at the surface and down to approximately 50 m is colder after the storm had past by about 1^oC so this gives an indication that the second profile is actually in the wake of the hurricane.

In Figure 3.22 the set of profiles lies just outside of the apparent cold wake as shown in the SST field. From the structure of the profiles each seems to be very similar down to 100m at which the point the after storm observation cools slightly more so then the before storm observation. The next set of profiles that has a location within the cold wake is shown in Figure 3.23. This set of profiles raises some questions about the validity of the observations because the two profiles are clearly not sampling the same body of water. The difference in ΔT is greater then 7° C at 200m indicated completely different source regions.

The same is true in Figure 3.24. The upper 40 meters show the expected results but with a difference of greater than 4^oC, the two profiles are not measuring the same body water. This is especially frustrating due to the location of the profile just to the left of the track given the need for comparison to satellite altimeter pass 115 which showed an increase in heating on the left side of the storm.

The next set of profiles all have very similar characteristics. In Figures 3.25, 3.26, and 3.28, the first observations all show a shallow surface mixed layer with a relatively strong near surface thermal gradient. The second observation is located in the cold wake and shows a much stronger near surface mixed layer and then a sharp temperature gradient so that the after storm temperature neared the value of the before storm temperature at depth. This change in type of profile is exactly the expected result. The winds of the storm entrain deeper colder waters towards the surface leaving a deeper colder mixed layer while leaving the deeper water, greater then 120 meters, relatively undisturbed. The fact that so many sets of profiles had produced the expected profile results was extremely positive. What was concerning thought, is that recalling Figure 3.30, the height anomalies calculations do not show an apparent trend in increasing h' values on the right side of the storm track. At this point in the research it was clear that data issues were going to prevent using in-situ observations as the sole metric for describing the longevity and impact of the hurricane on the ocean. In the following chapter, the CFSR model results will be discussed and calculations of the hurricanes impact will be shown.
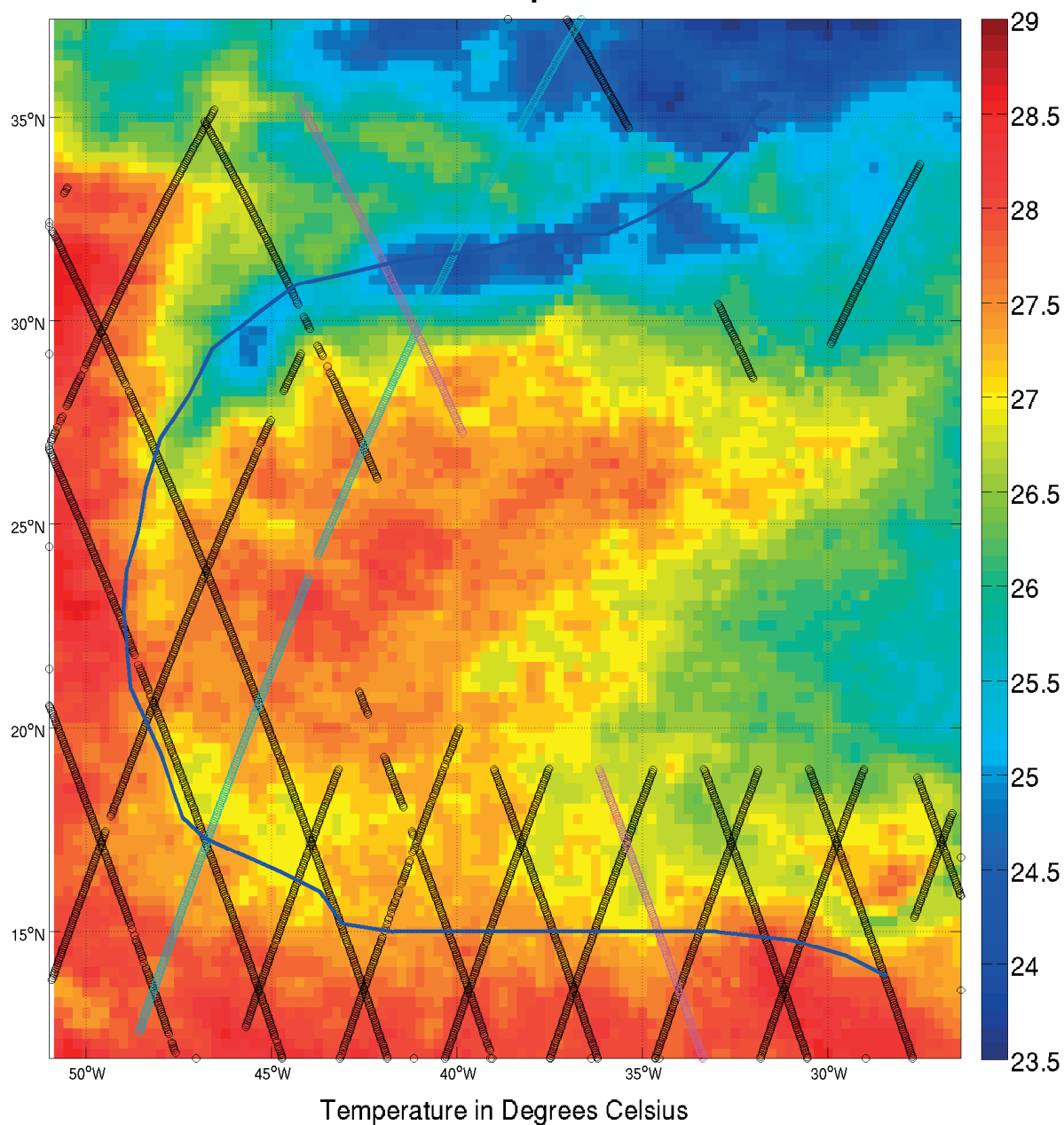
Figure 3.1: OI TMI Sea surface temperature field on 17 September 2001. Overlaid is the best track of hurricane Felix (2001) as a blue line and the path of the satellite altimetry observations from TOPEX/POSEIDON as black lines. The cyan colored line is pass 215 and the magenta colored line is pass 226.
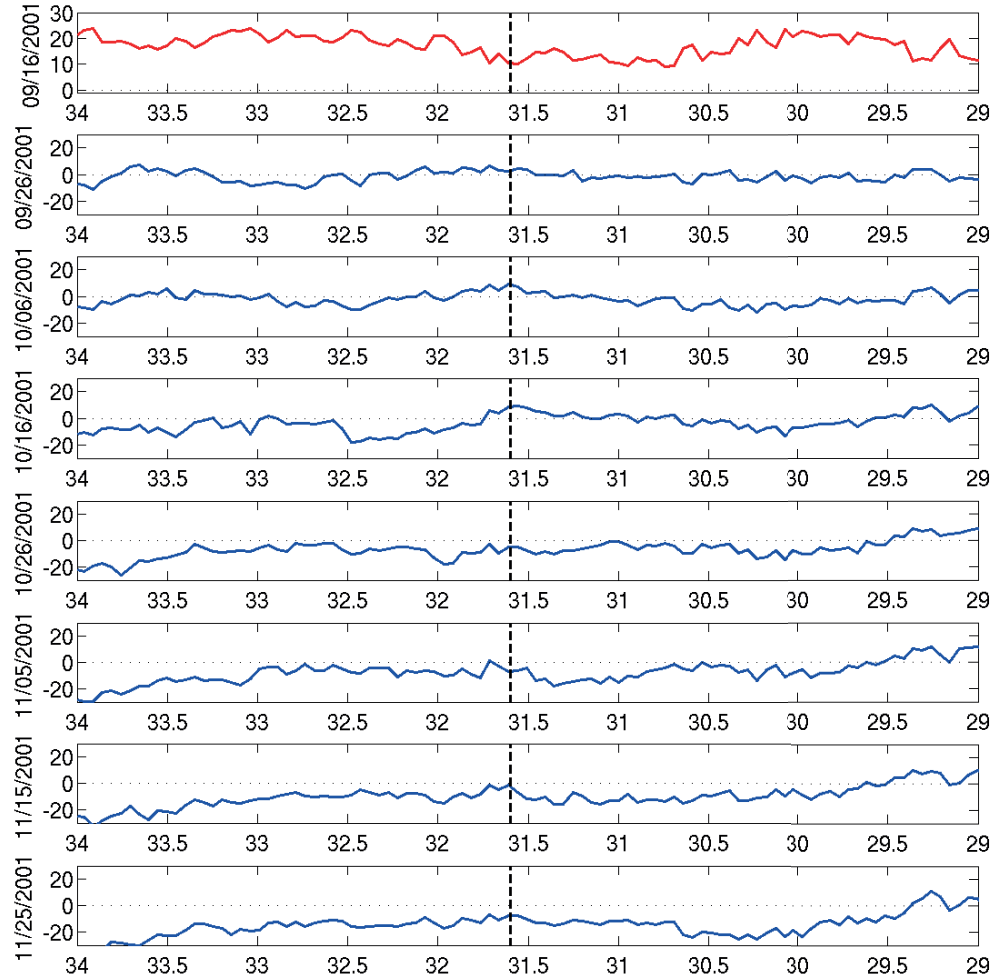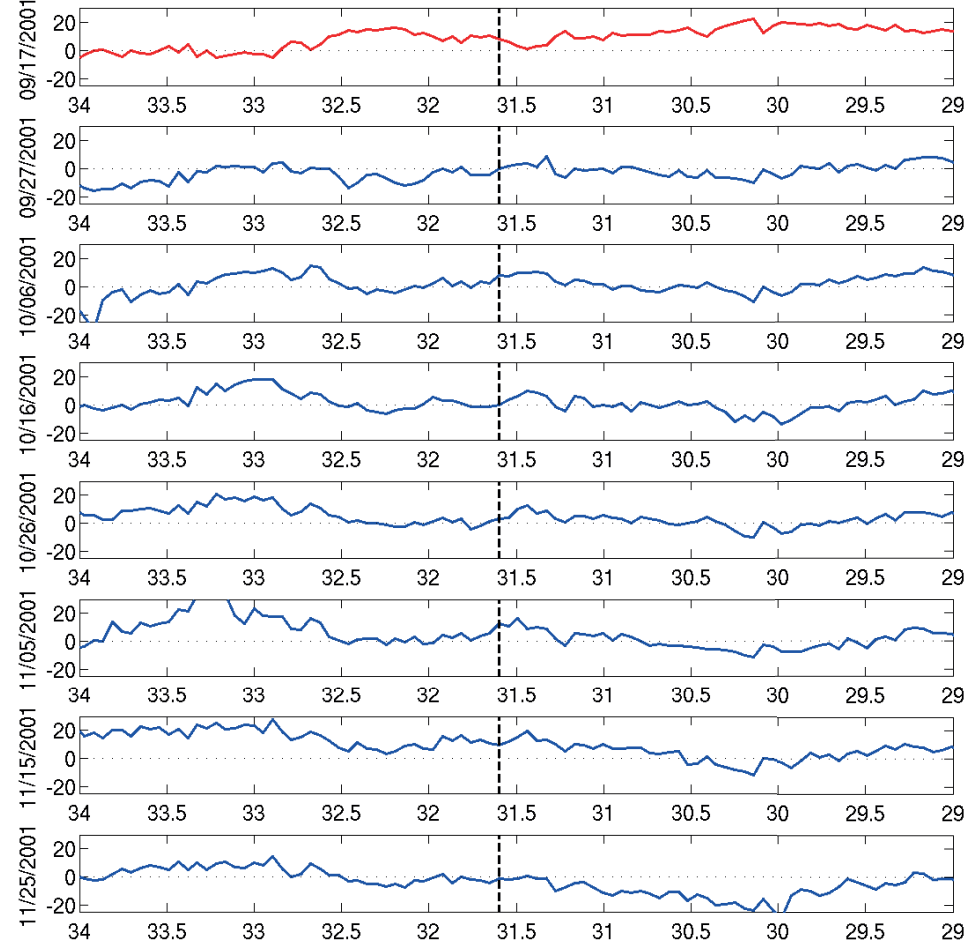
Figure 3.2: Sea surface height anomalies (cm) as calculated from the TOPEX/POSEIDON Altimeter for pass 215 during hurricane Felix (2001). Each time series represents the difference from the original date at the bottom to the date listed on the y-axis.

Figure 3.3: Sea surface height anomalies (cm) as calculated from the TOPEX/ POSEIDON Altimeter for pass 226 during hurricane Felix (2001). Each time series represents the difference from the original date at the bottom to the date listed on the y-axis.
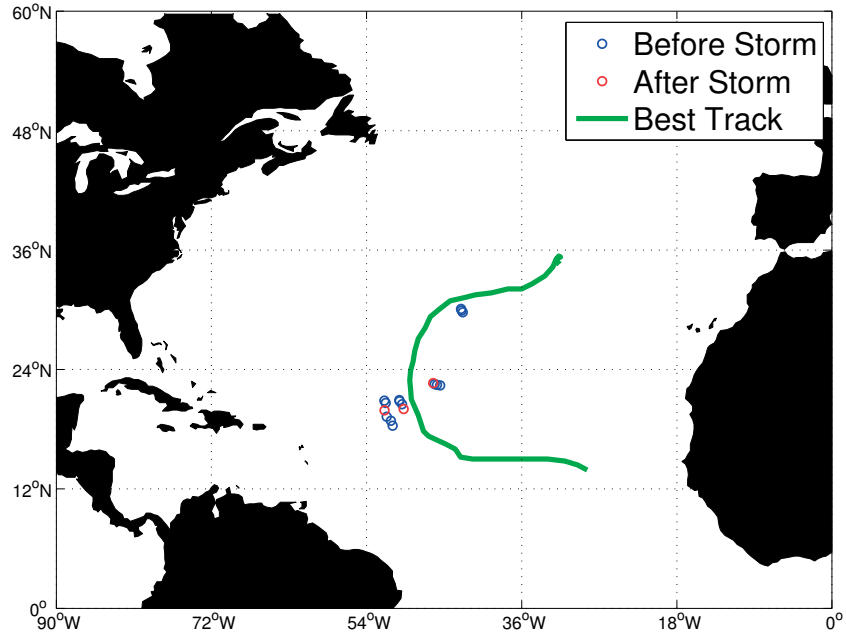
Figure 3.4: Location of Argo floats from before and after storm that met the criteria for timing with the passing of the hurricane. The blue circles represent the before storm observations and the red circles represent the after storm observations. The green line represents the best track for the storm.
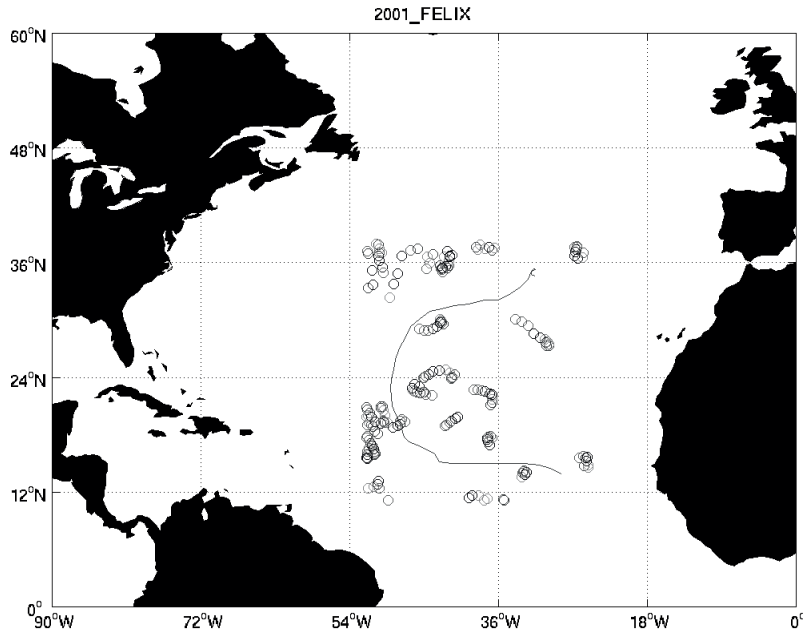
Figure 3.5: Location of Argo floats from before and after storm that met the criteria for timing with the passing of hurricane Felix (2001). The circles represent all of the available buoys within a box over the hurricane track. These buoys were from the two months before and two months after the passage of the storm.

41
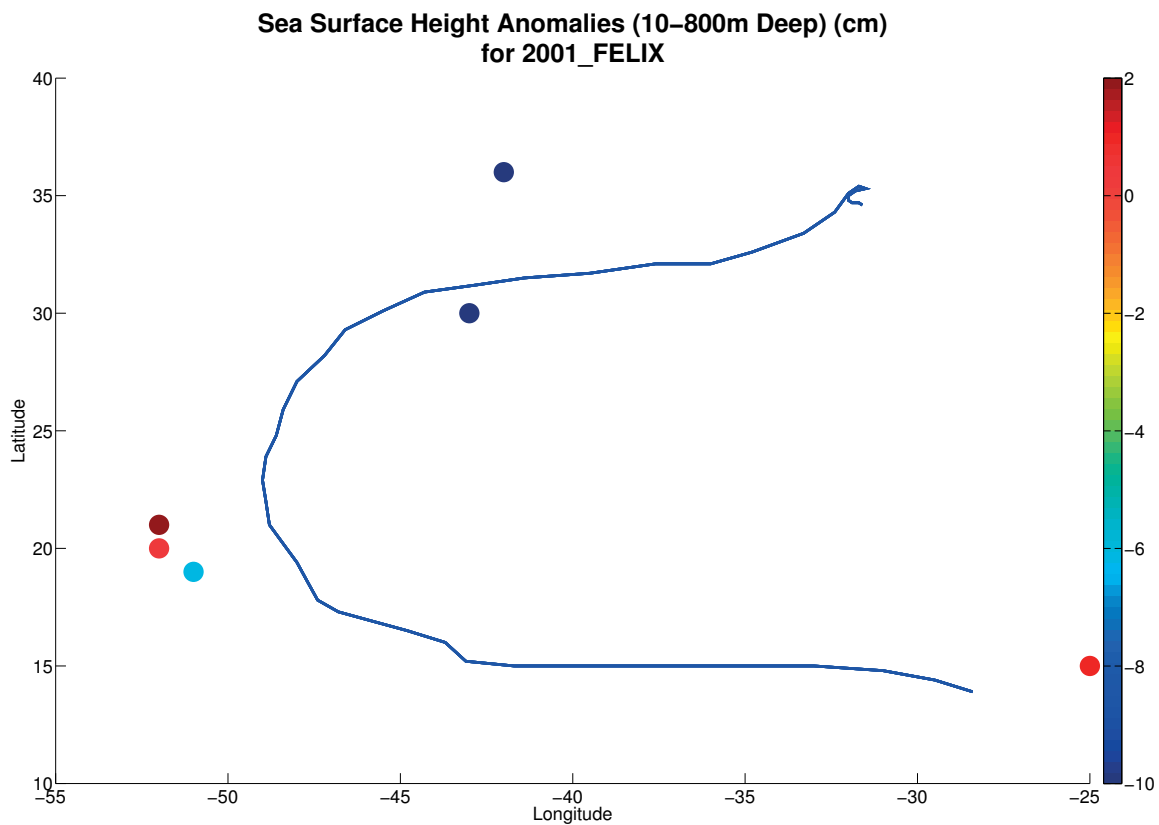
Figure 3.6: Argo calculated height anomaly (cm) via Emanuel 2001 for hurricane Felix in (2001). The blue line represents the track of the hurricane from the Best Track and the dots are the location where the anomaly is calculated.
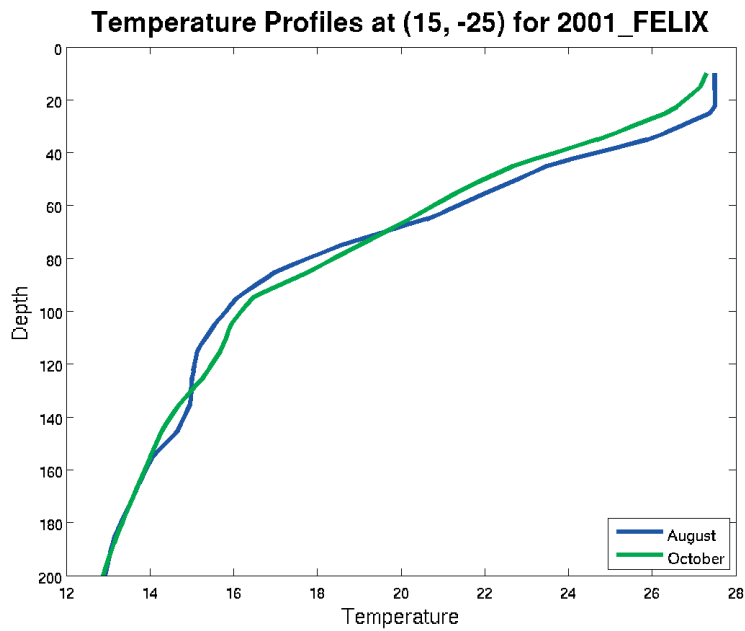
Figure 3.7: Argo profile for hurricane Felix (2001) located within a 1° x 1° box centered at 15^oN 25^oW. The blue profile is before the storm and the green profile is after the storm.
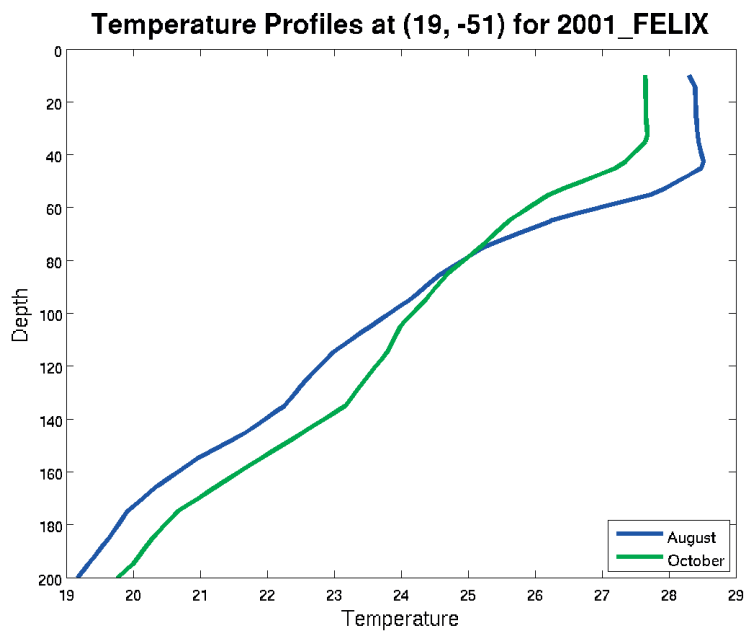
Figure 3.8: Argo profile for hurricane Felix (2001) located within a 1° x 1° box centered at 19^oN 51^oW. The blue profile is before the storm and the green profile is after the storm.
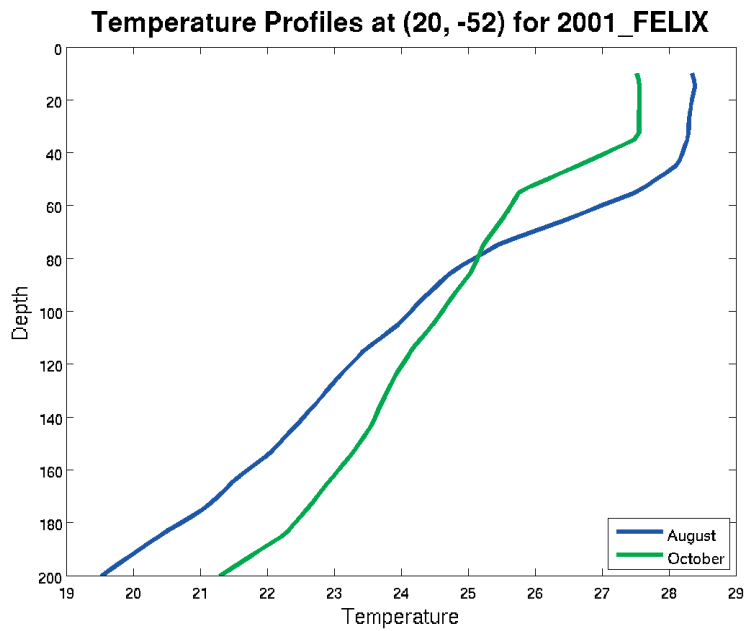
Figure 3.9: Argo profile for hurricane Felix (2001) located within a 1° x 1° box centered at 20°N 52°W. The blue profile is before the storm and the green profile is after the storm.
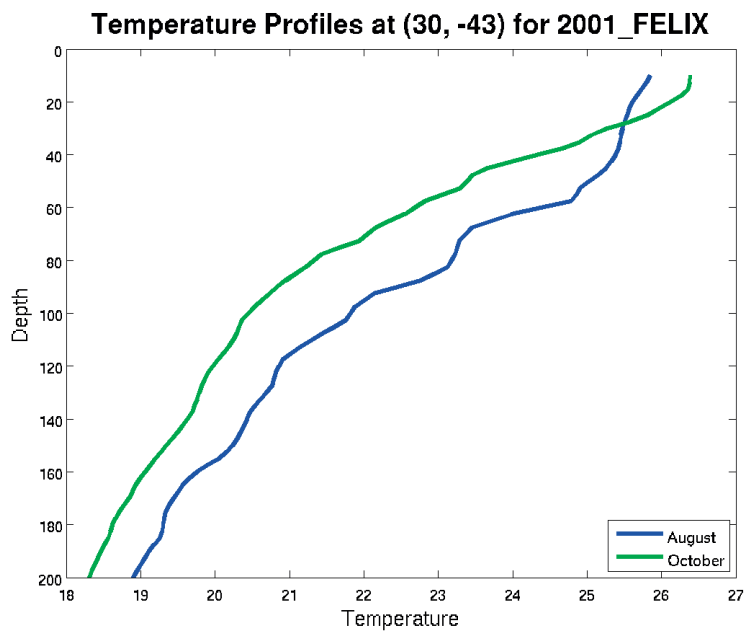
Figure 3.10: Argo profile for hurricane Felix (2001) located within a 1° x 1° box centered at 30°N 43°W. The blue profile is before the storm and the green profile is after the storm.

Temperature Profiles at (36, -42) for 2001_FELIX
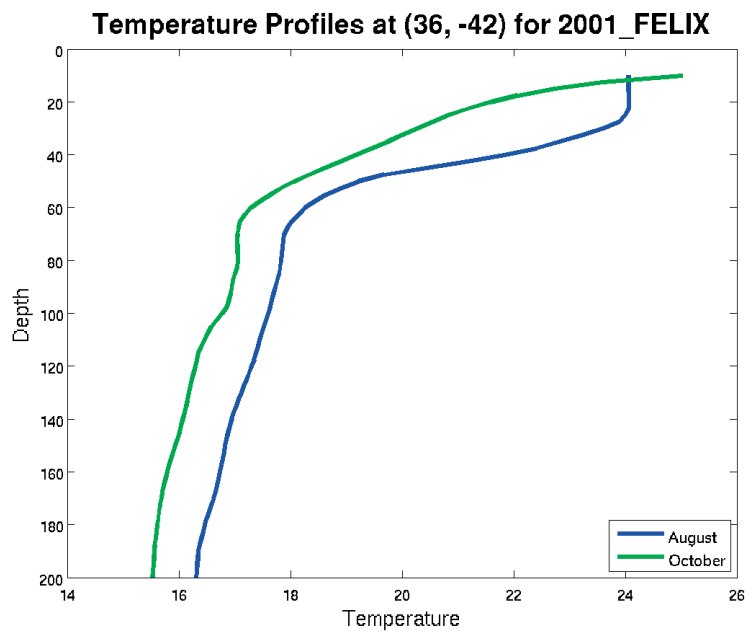
Figure 3.11: Argo profile for hurricane Felix (2001) located within a 1° x 1° box centered at 36^oN 42^oW. The blue profile is before the storm and the green profile is after the storm.
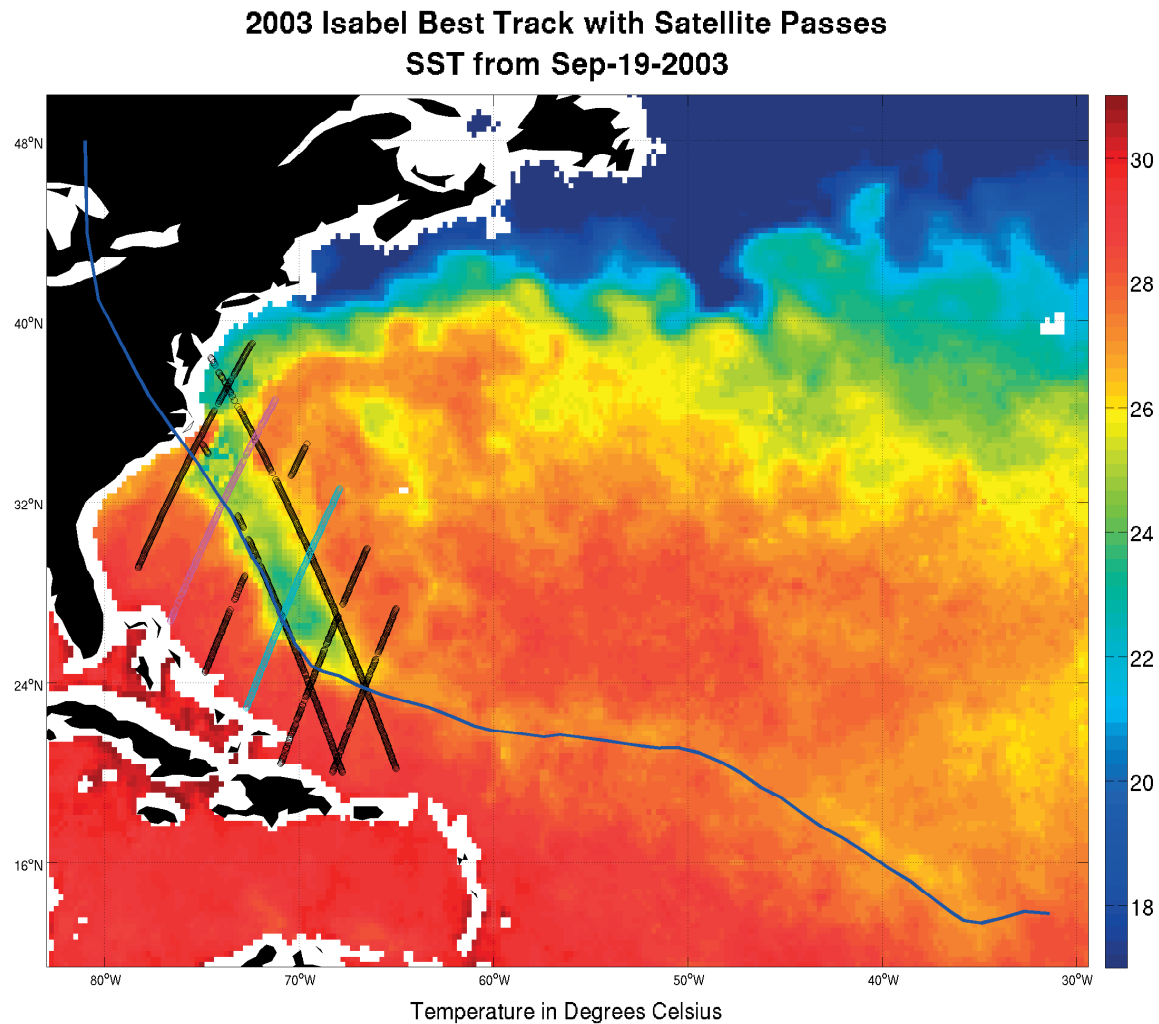
Figure 3.12: OI TMI/AMSRE Sea Surface Temperatures (^{o}C) on 19 September 2003. Overlaid is the best track of hurricane Isabel (2003) as a blue line and the path of the satellite altimetry observations from JASON-1 as black lines. The cyan colored line is pass 217, and the magenta colored line is pass 65.
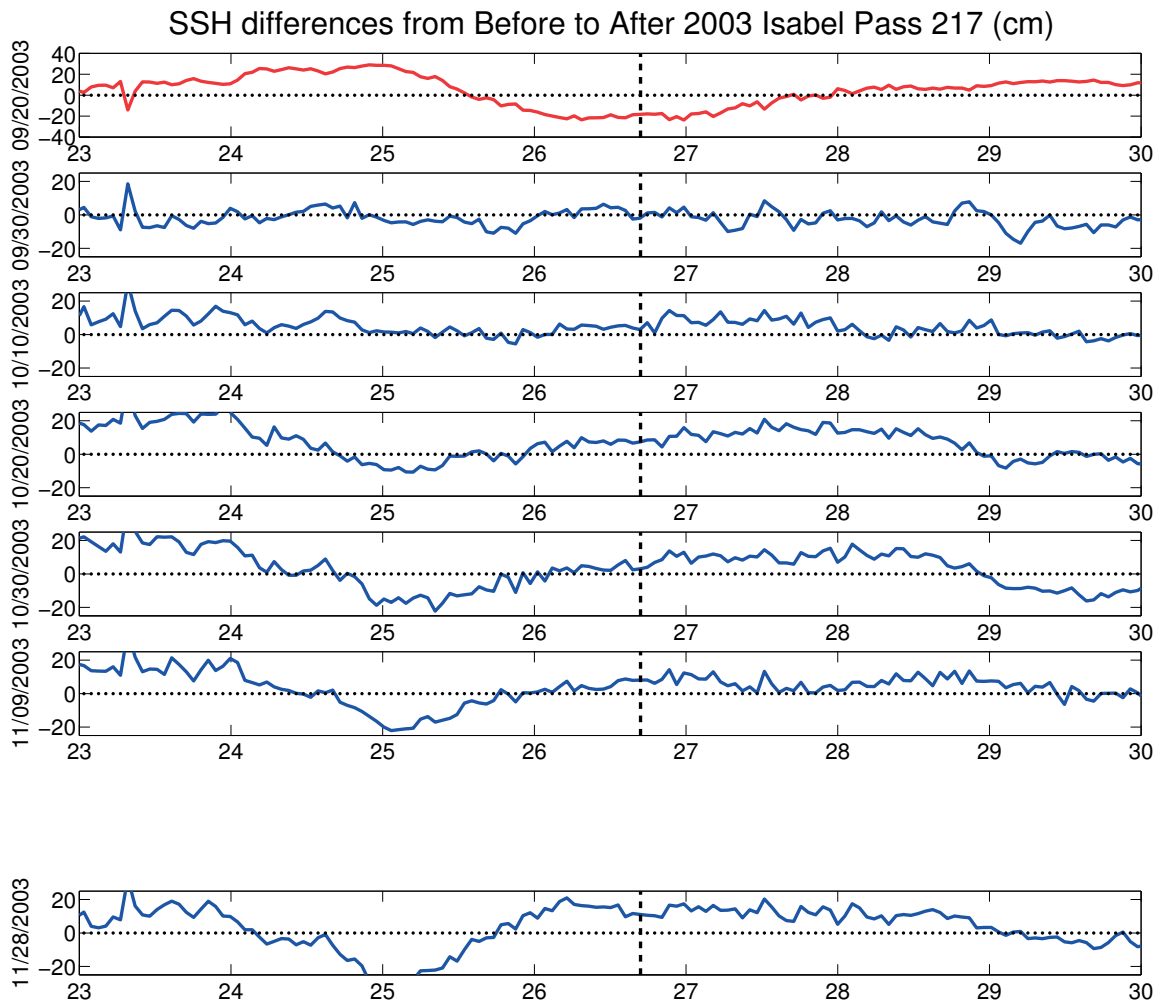
Figure 3.13: Sea surface height anomalies as calculated from the JASON-1 Altimeter for pass 217 during hurricane Isabel (2003). Each time series represents the difference from the original date at the bottom to the date listed on the y-axis.
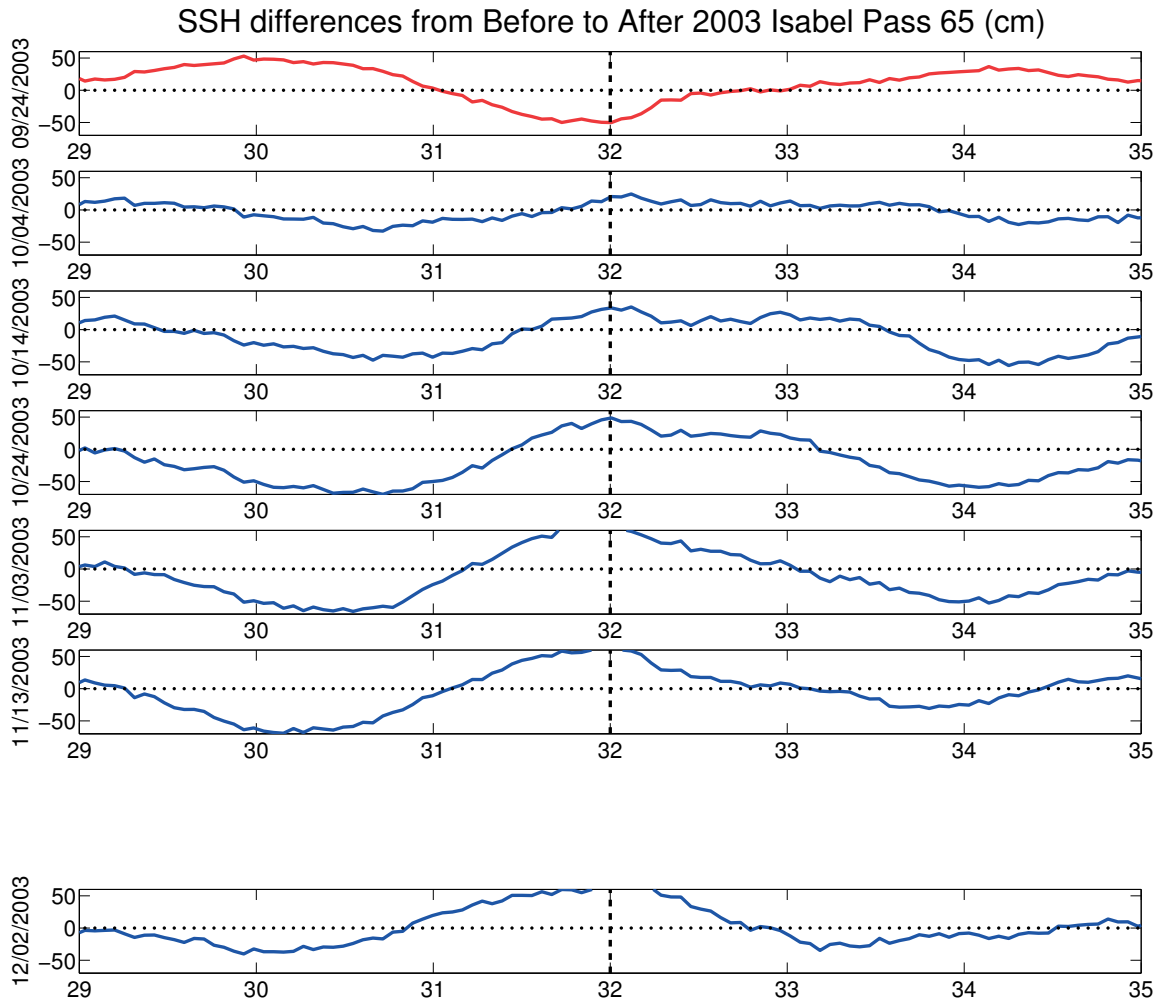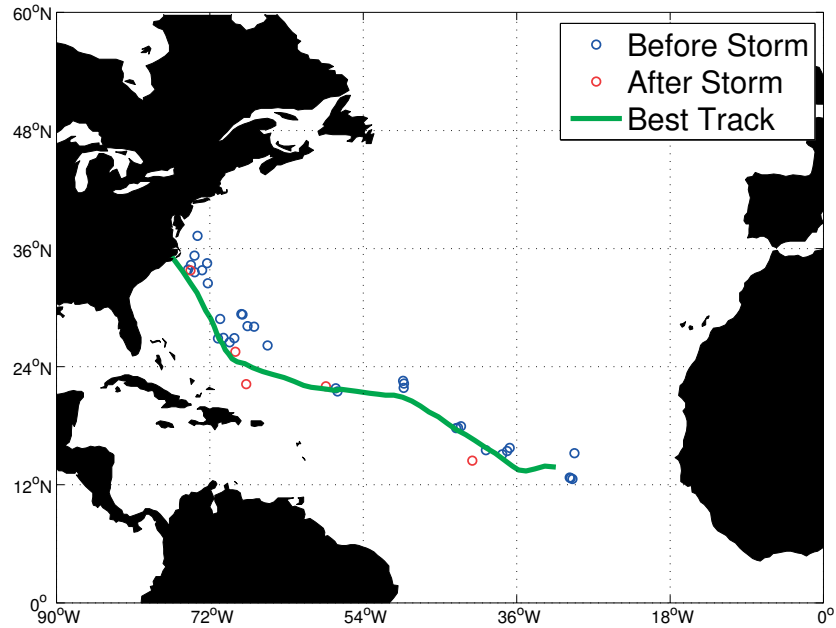
Figure 3.14: Sea surface height anomalies as calculated from the JASON-1 Altimeter for pass 65 during hurricane Isabel (2003). Each time series represents the difference from the original date at the bottom to the date listed on the y-axis.

Figure 3.15: Location of Argo floats from before and after storm that met the criteria for timing with the passing of the hurricane. The blue circles represent the before storm observations and the red circles represent the after storm observations. The green line represents the best track for the storm.
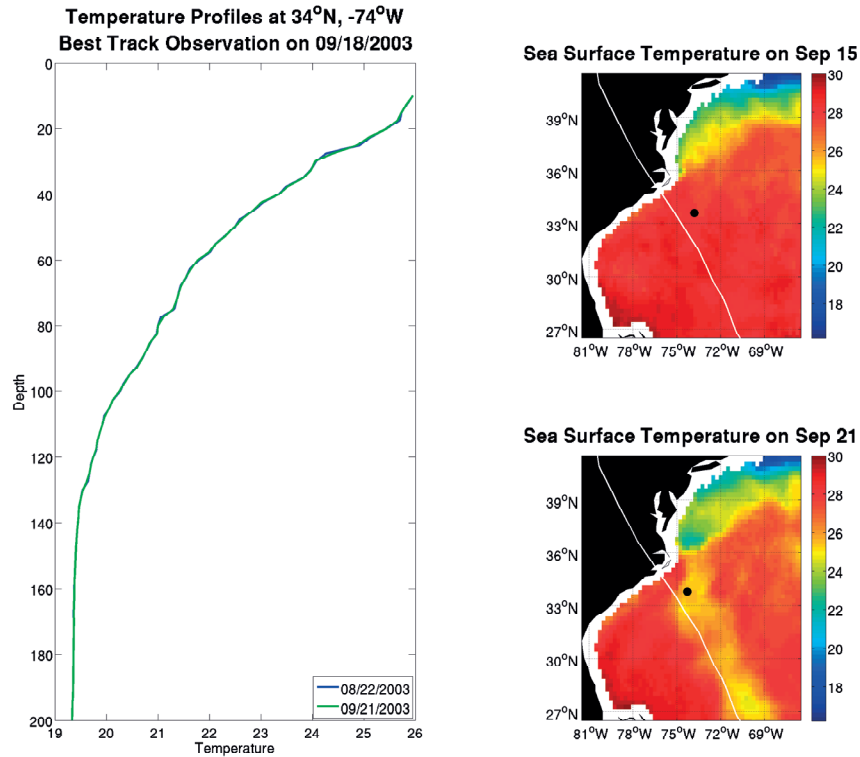
Figure 3.16: Argo profile for hurricane Isabel (2003). The temperature profile (^{o}C) is shown on the left and the SST (^{o}C) fields on the right represent the SST during the date of the observation of the temperature profile.
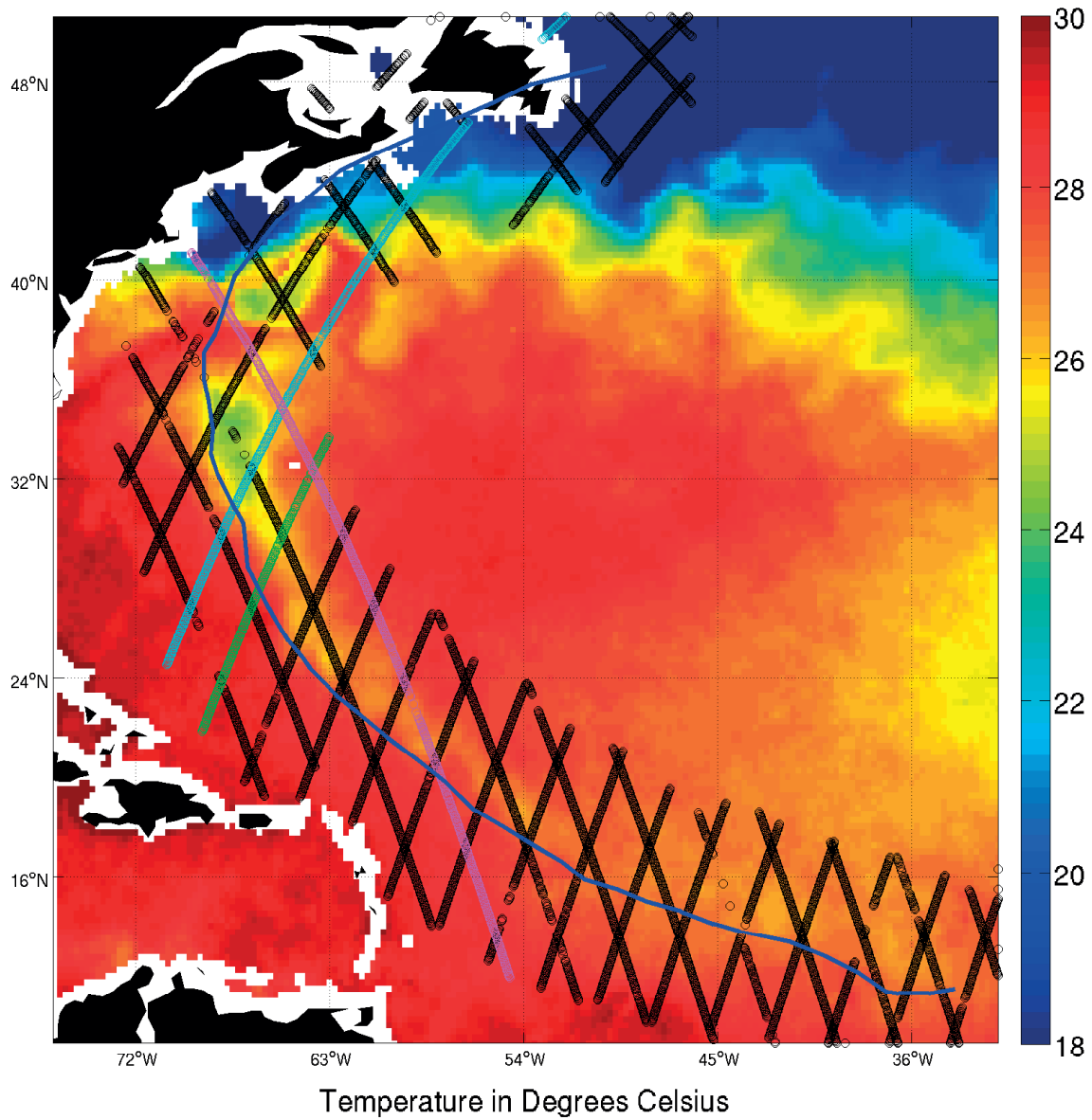
Figure 3.17: OI TMI/AMSRE Sea surface temperatures (^{o}C) on 24 August 2009 during hurricane Bill (2009) as a blue line and the path of the satellite altimetry observations from JASON-1 as black lines. The cyan colored line is pass 39, the magenta colored line is pass 202, and the green colored line is pass 115.
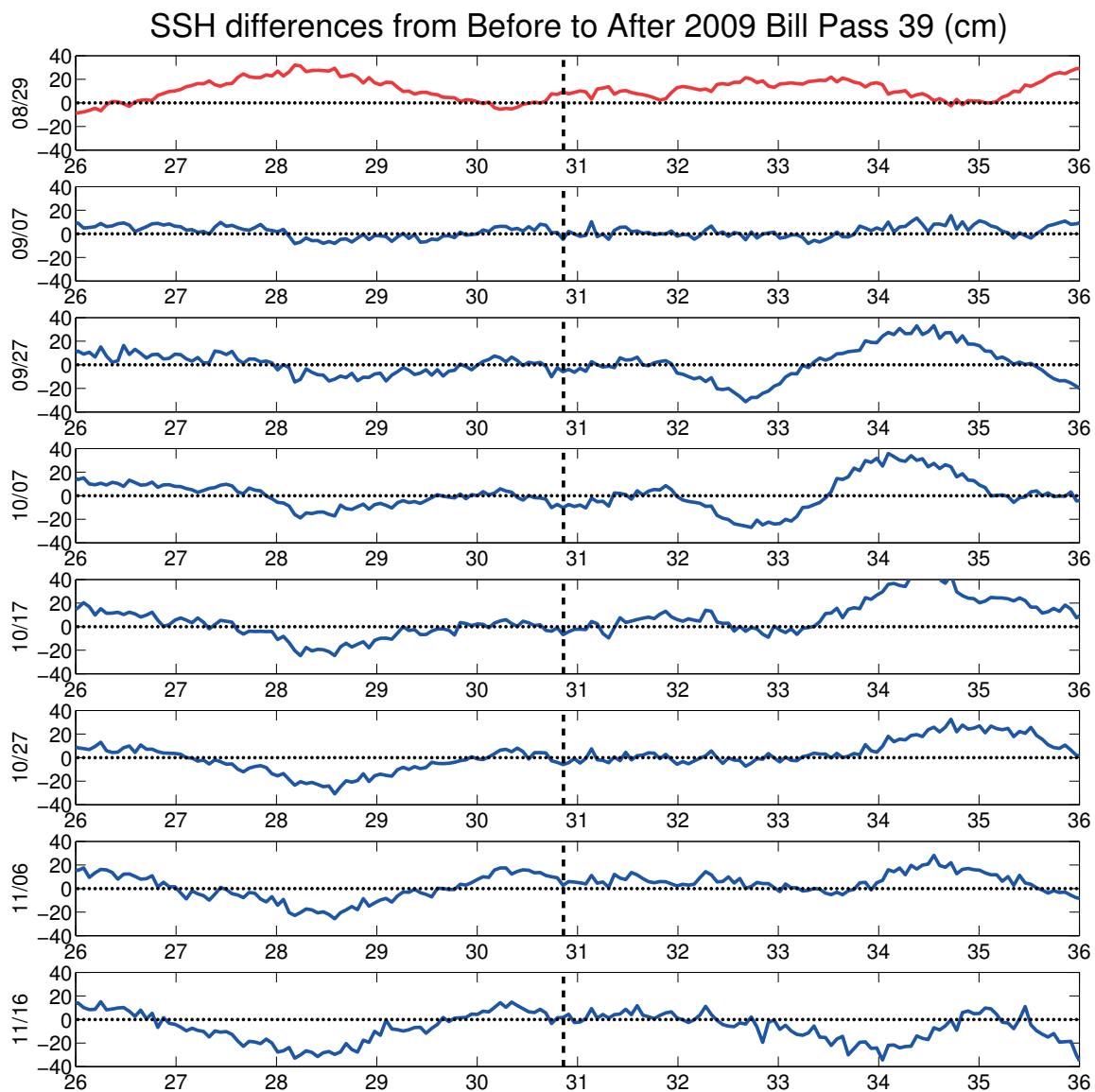
Figure 3.18: Sea surface height anomalies (cm) as calculated from the JASON-1 Altimeter for pass 39 during hurricane Bill (2009). Each time series represents the difference from the original date at the bottom to the date listed on the y-axis.
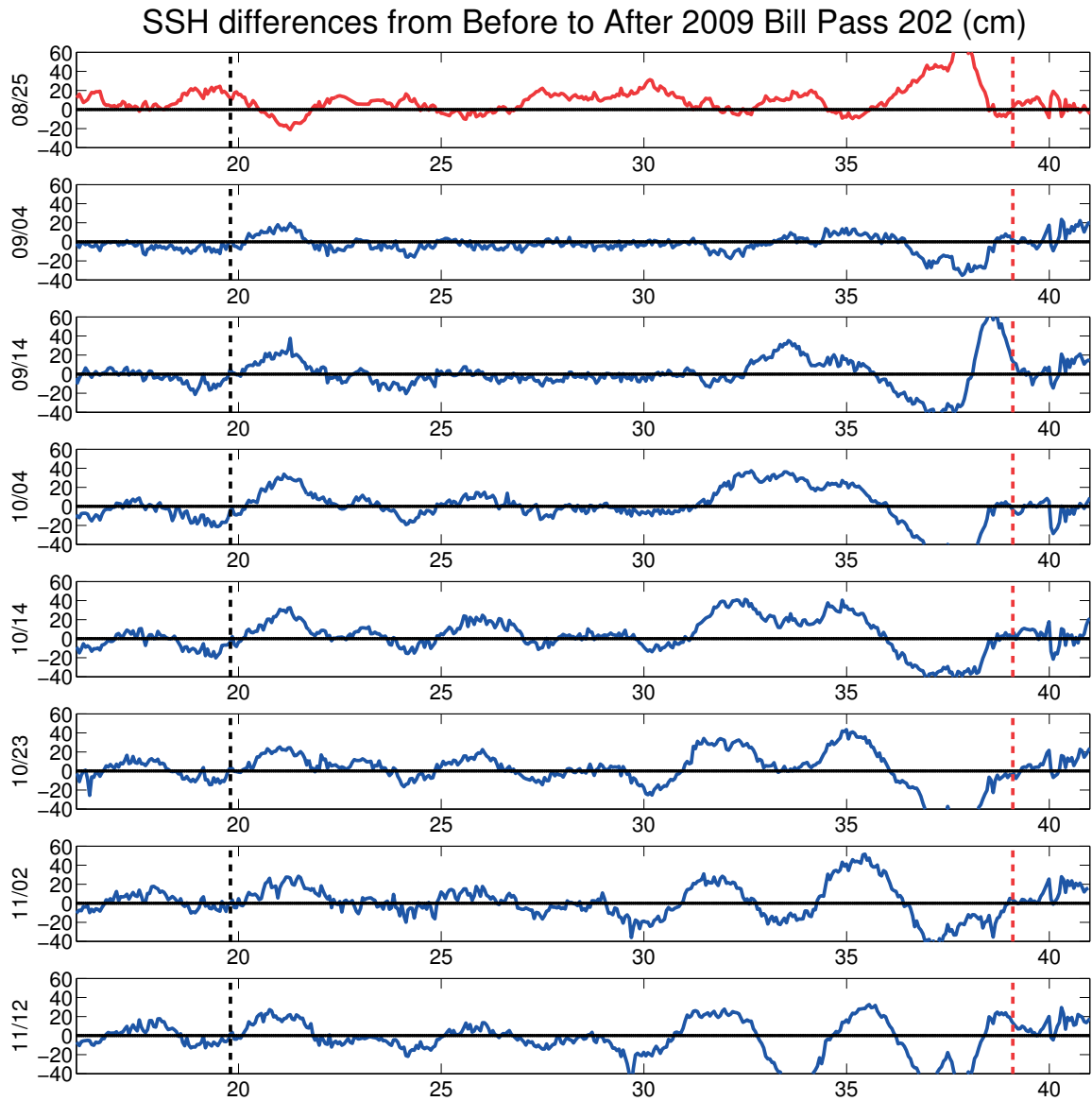
Figure 3.19: Sea surface height anomalies (cm) as calculated from the JASON-1 Altimeter for pass 202 during hurricane Bill (2009). Each time series represents the difference from the original date at the bottom to the date listed on the y-axis.
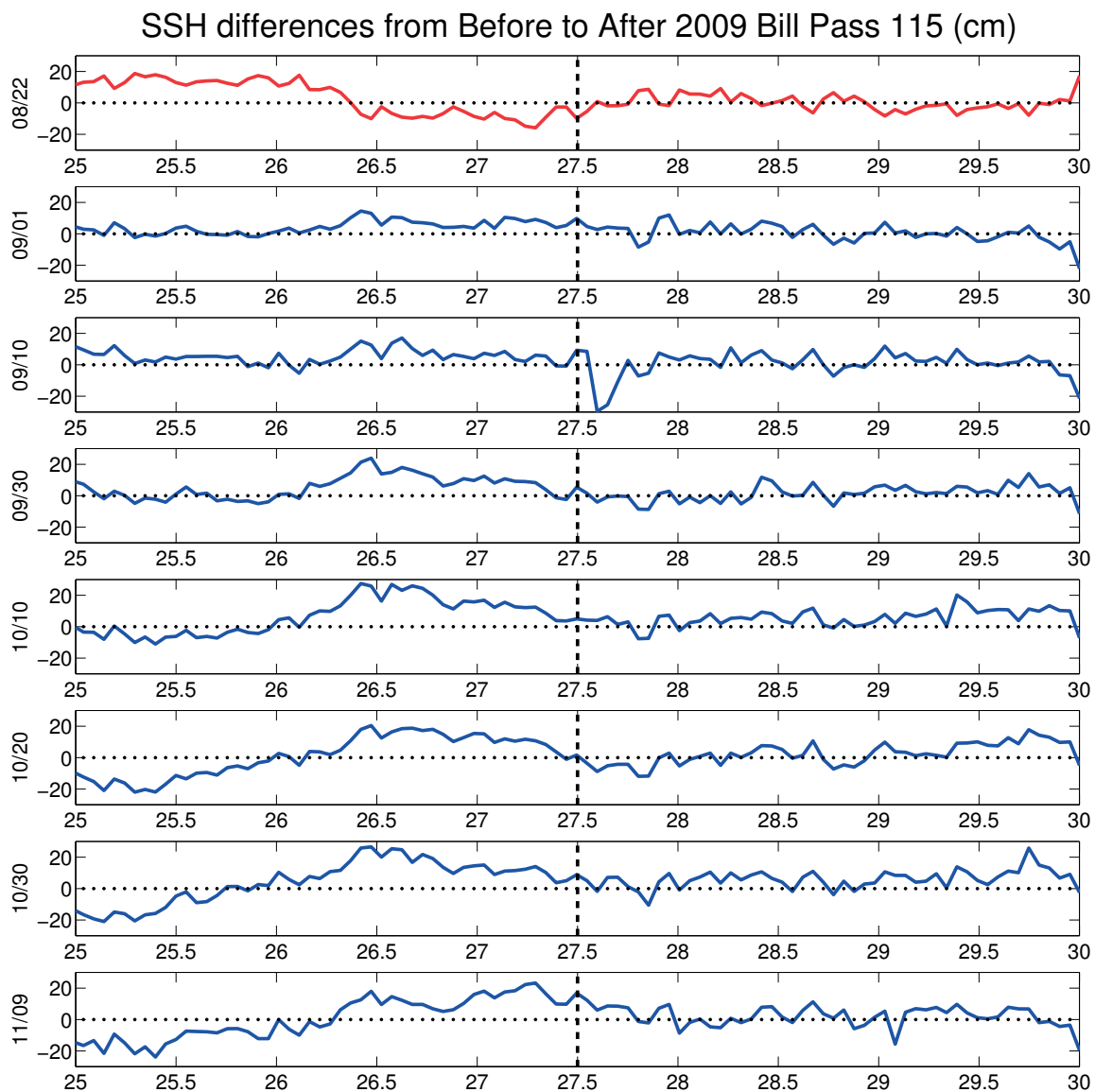
Figure 3.20: Sea surface height anomalies (cm) as calculated from the JASON-1 Altimeter for pass 115 during hurricane Bill (2009). Each time series represents the difference from the original date at the bottom to the date listed on the y-axis.
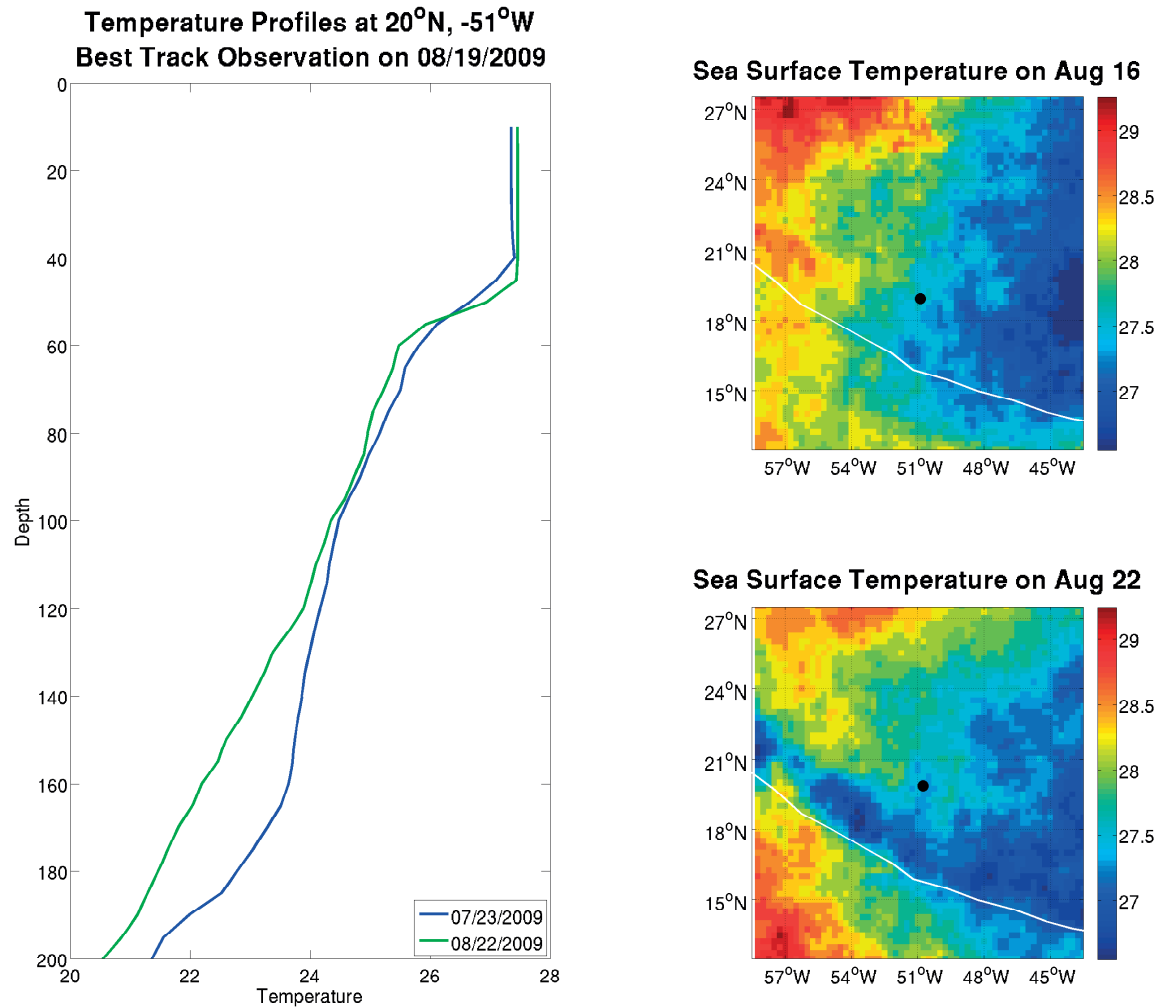
Figure 3.21: Argo profile for hurricane Bill (2009) located within a 1° x 1° box centered at 20°N 51°W. The temperature profile (^{o}C) is shown on the left and the SST (^{o}C) fields on the right represent the SST during the date of the observation of the temperature profile.

Figure 3.22: Argo profile for hurricane Bill (2009) located within a 1° x 1° box centered at 20^oN 60^oW. The temperature profile (^{o}C) is shown on the left and the SST (^{o}C) fields on the right represent the SST during the date of the observation of the temperature profile.
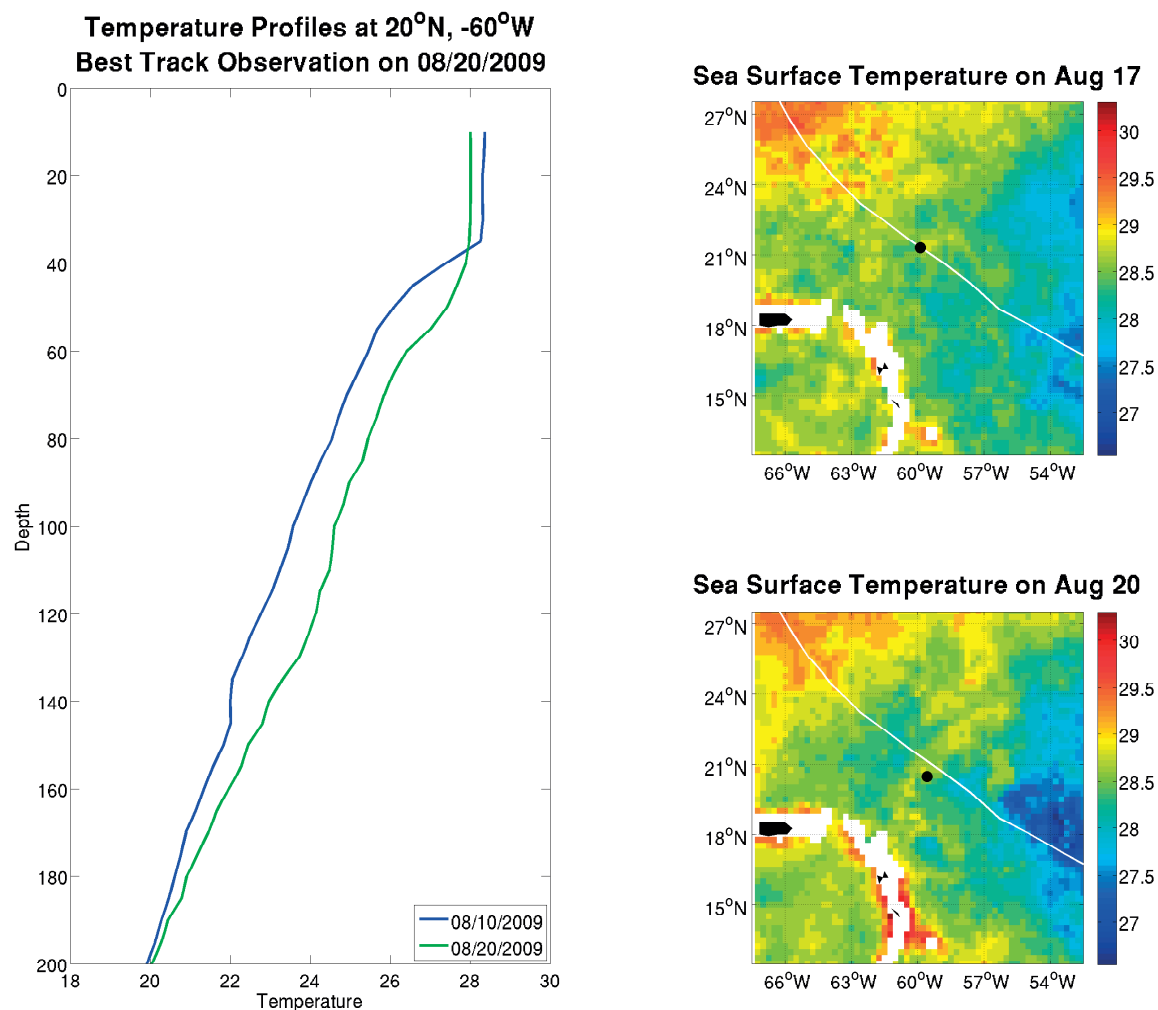
Figure 3.23: Argo profile for hurricane Bill (2009) located within a 1° x 1° box centered at 24^oN 65^oW. The temperature profile (^{o}C) is shown on the left and the SST (^{o}C) fields on the right represent the SST during the date of the observation of the temperature profile.
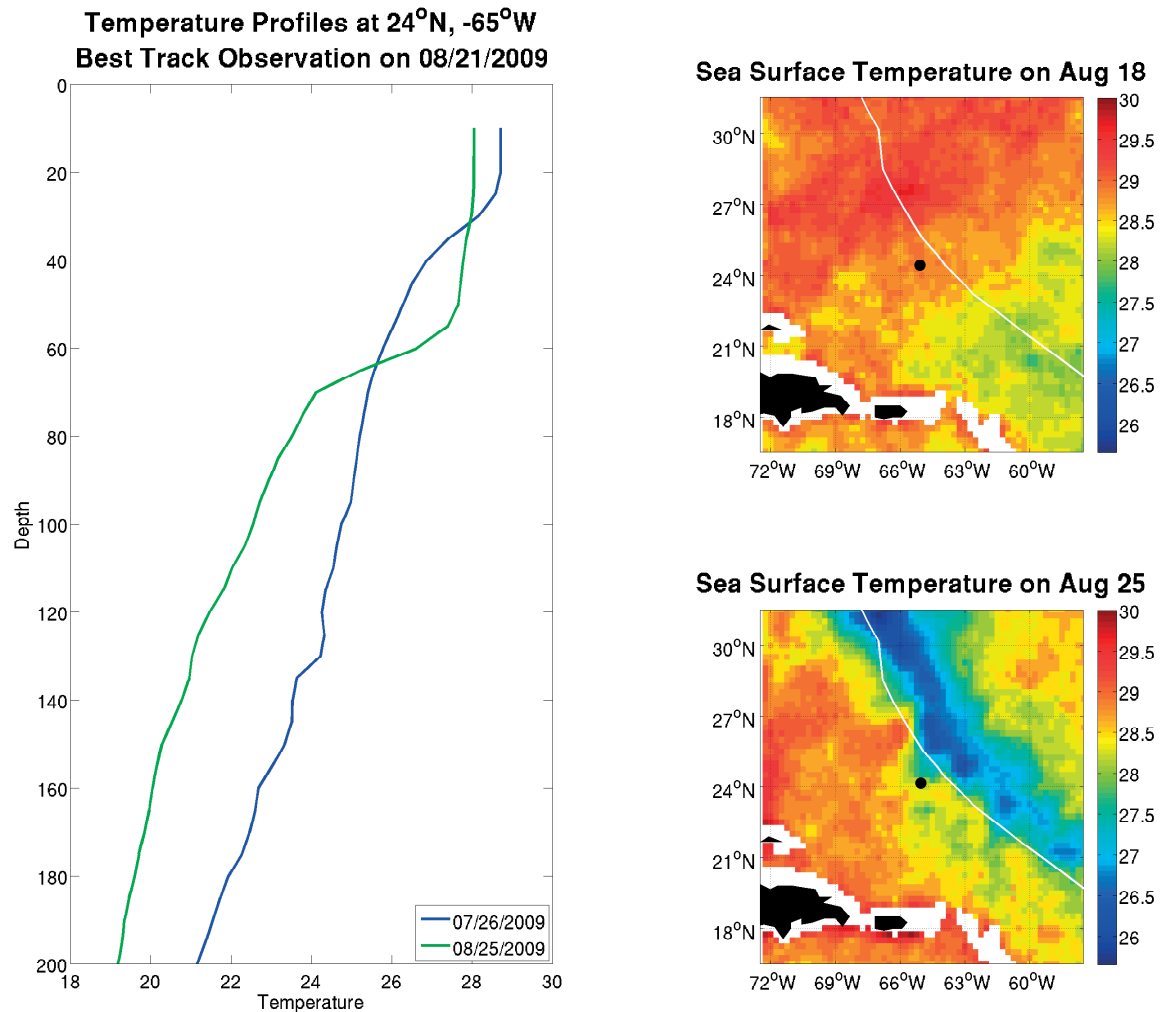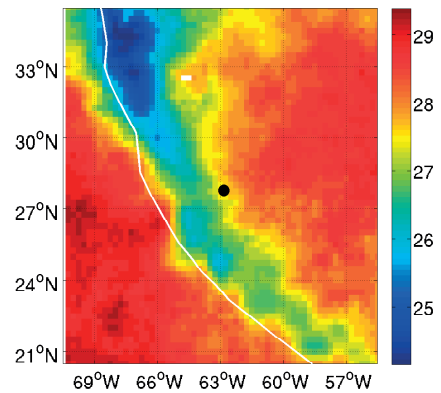
Figure 3.24: Argo profile for hurricane Bill (2009) located within a 1° x 1° box centered at 28^oN 63^oW. The temperature profile (^{o}C) is shown on the left and the SST (^{o}C) fields on the right represent the SST during the date of the observation of the temperature profile.

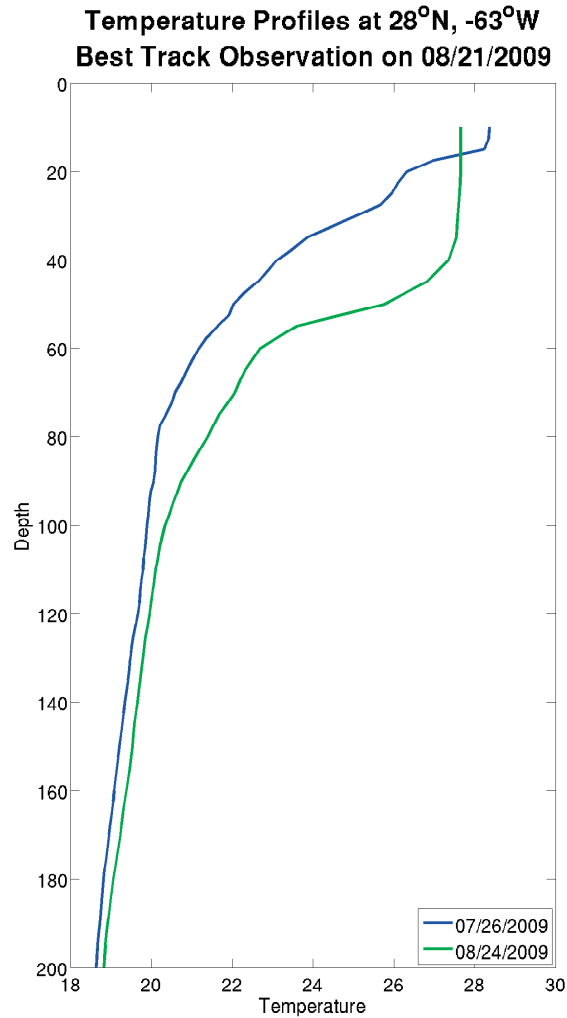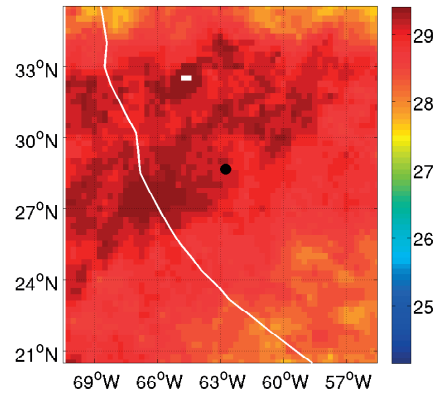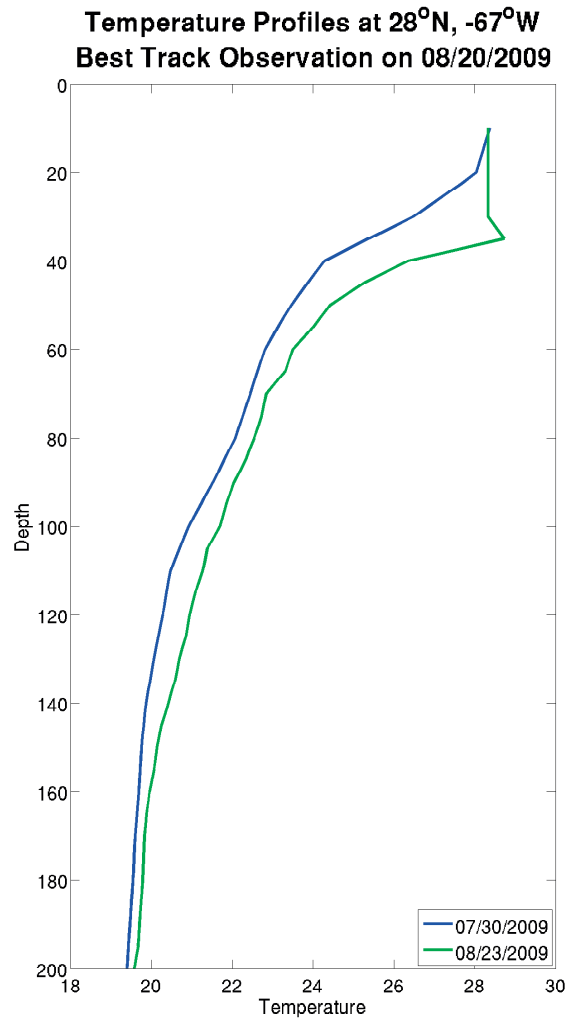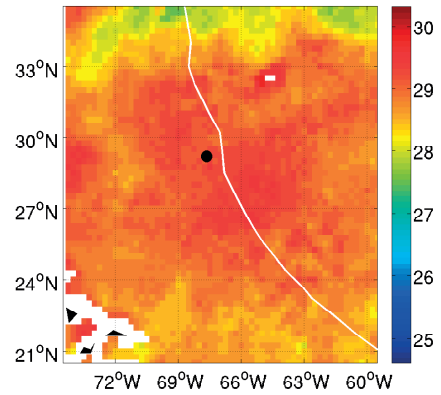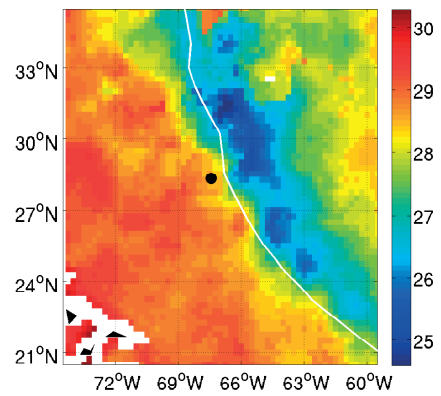Figure 3.25: Argo profile for hurricane Bill (2009) located within a 1° x 1° box centered at 28^oN 67^oW. The temperature profile (^{o}C) is shown on the left and the SST (^{o}C) fields on the right represent the SST during the date of the observation of the temperature profile.
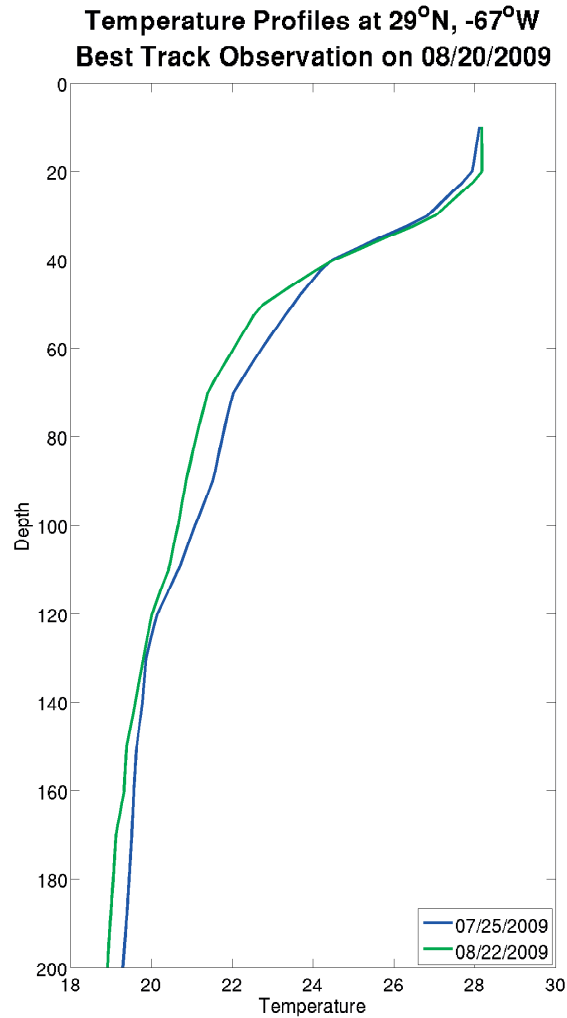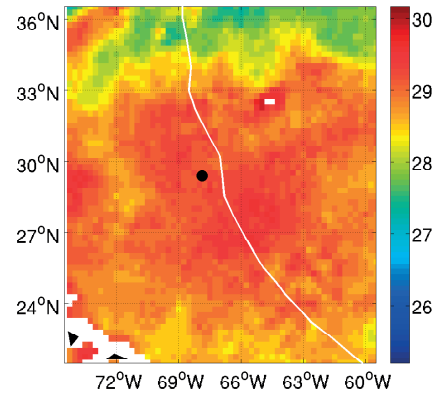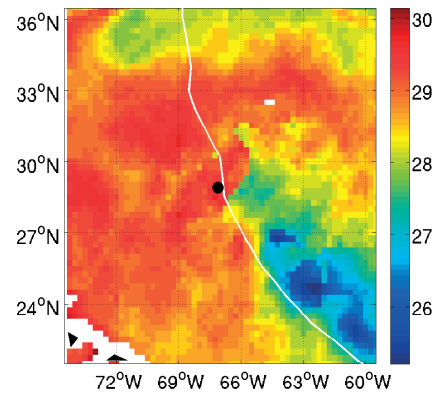
Figure 3.26: Argo profile for hurricane Bill (2009) located within a 1° x 1° box centered at 29^oN 67^oW. The temperature profile (^{o}C) is shown on the left and the SST(^{o}C) fields on the right represent the SST during the date of the observation of the temperature profile.
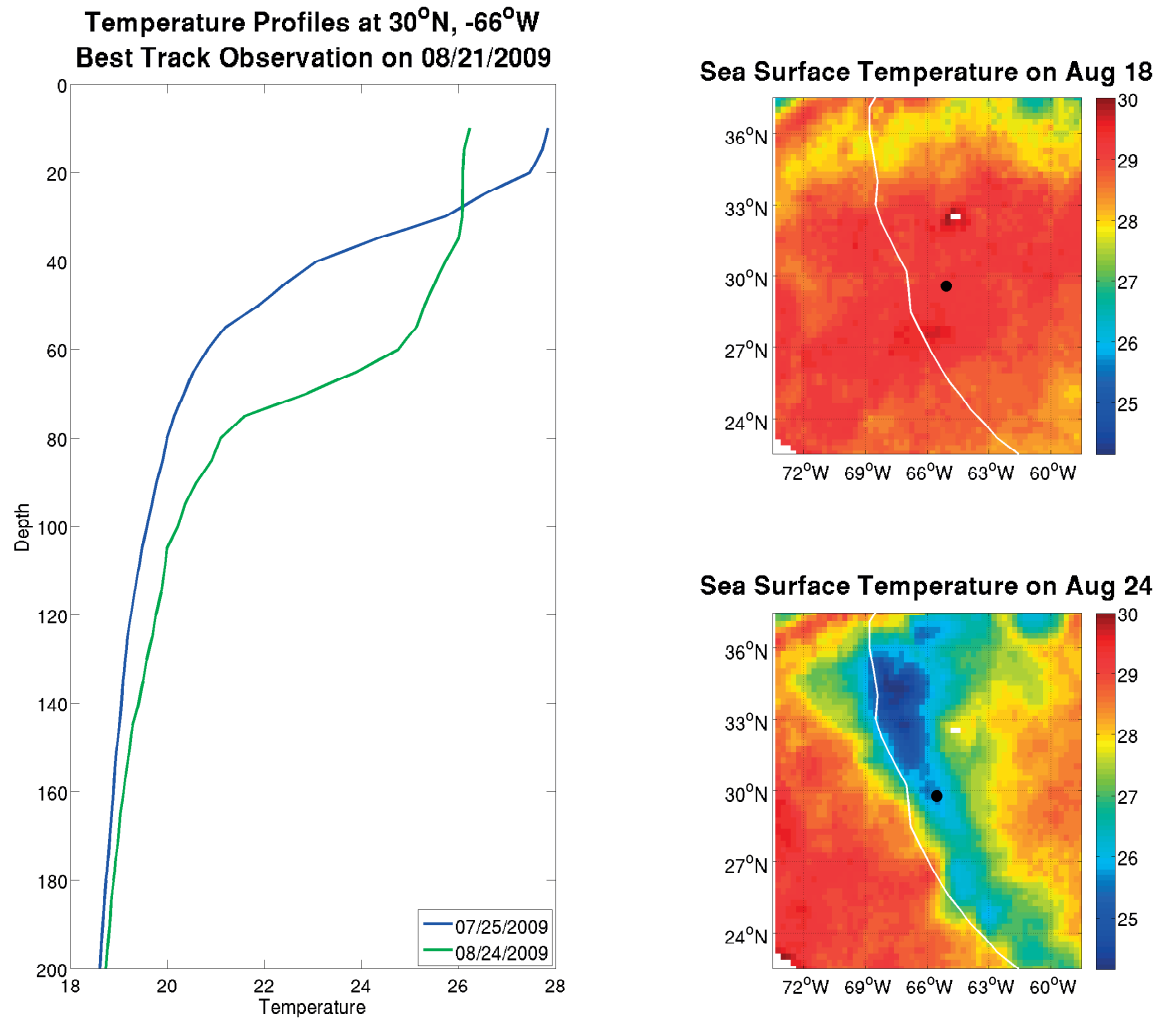
Figure 3.27: Argo profile for hurricane Bill (2009) located within a 1° x 1° box centered at 30^oN 66^oW. The temperature profile (^{o}C) is shown on the left and the SST (^{o}C) fields on the right represent the SST during the date of the observation of the temperature profile.
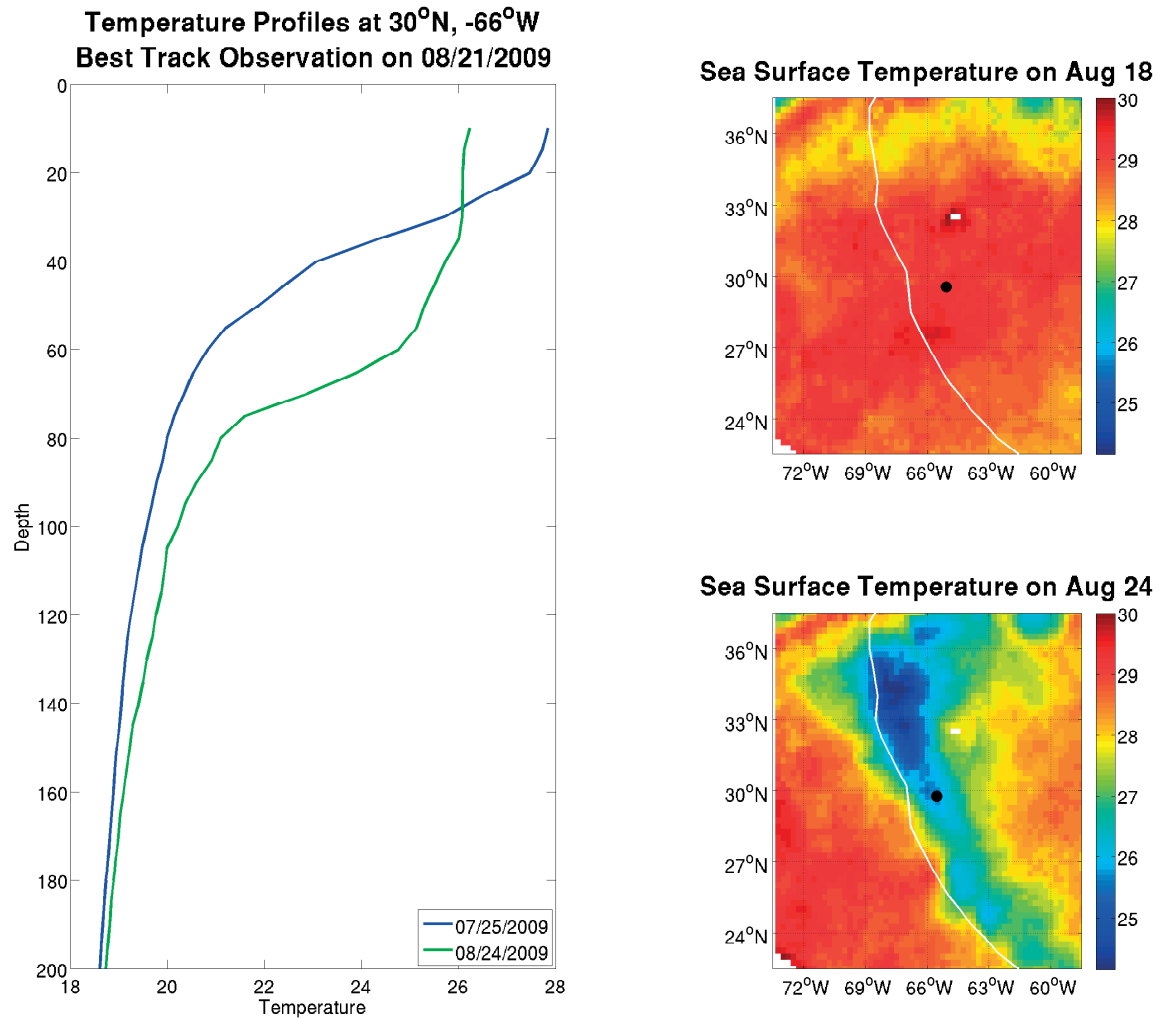
Figure 3.28: Argo profile for hurricane Bill (2009) located within a 1° x 1° box centered at 30^oN 66^oW. The temperature profile (^{o}C) is shown on the left and the SST (^{o}C) fields on the right represent the SST during the date of the observation of the temperature profile.
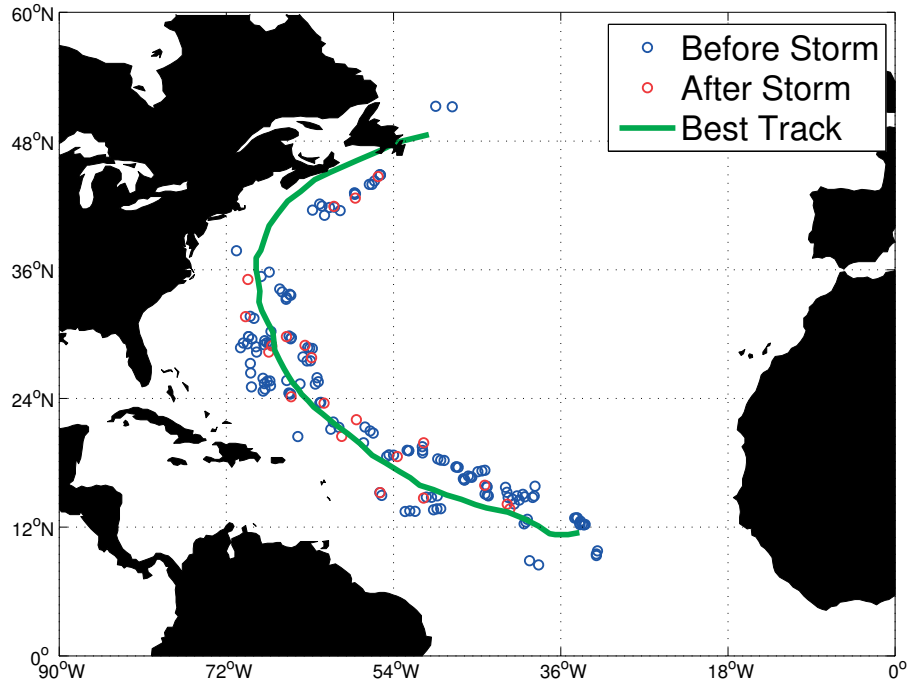
Figure 3.29: Location of Argo floats from before and after storm that met the criteria for timing with the passing of the hurricane. The blue circles represent the before storm observations and the red circles represent the after storm observations. The green line represents the best track for the storm.
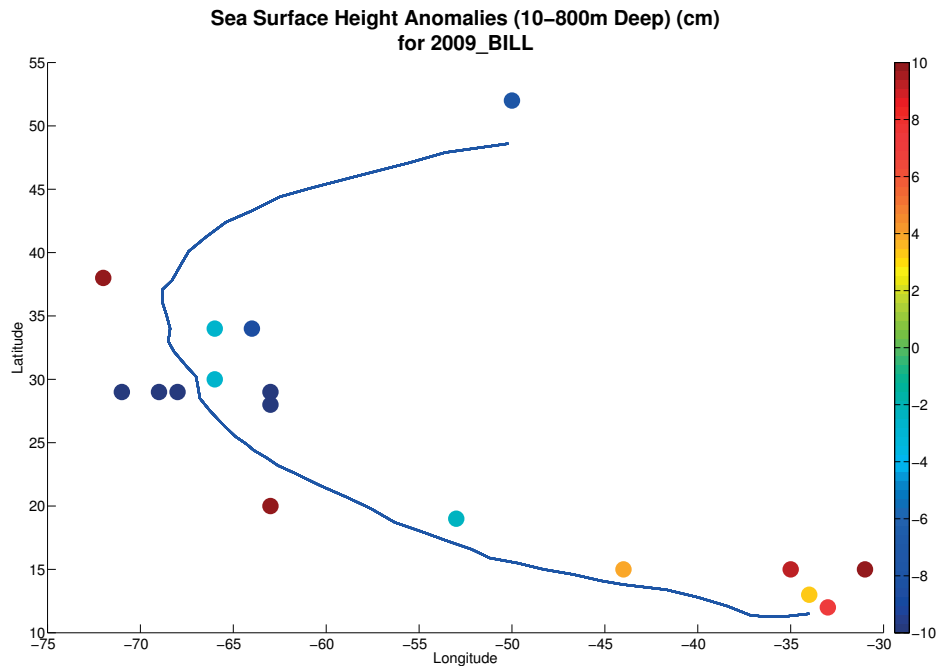
Figure 3.30: Argo calculated height anomaly via Emanuel (2001) for hurricane Bill in (2009). The blue line represents the track of the hurricane and the dot are the location where the anomaly is calculated.

CHAPTER 4

RESULTS OF CFSR MODEL

4.1   Storm Characteristics in Model

In order to augment the sparseness of the observational field, the CFSR model results were chosen as an additional analysis resource. The main reason for using this model, as opposed to other reanalyses is, that it is a coupled atmospheric and ocean model. Thus, during the re-stratification period there is some correspondence between the air-sea fluxes and the response of the upper ocean. However, unless the model includes some fairly realistic hurricane and ocean response characteristics, it would not be useful for this comparison. Therefore, the first step was to determine whether or not the model resolved the hurricane in the atmosphere and the impacts in the ocean. The wind field with speeds of greater than 20 mph for hurricane Felix (2001) are shown in Figure 4.1. The model has a realistic wind field, and the intensity is also realistic given the coarse grid of the CFSR dataset. The model does a good job of resolving the structure of the hurricane and shows a distinct minimum in wind speeds at the center consistent with eye of a hurricane. The eyewall is less defined but at 0.5^o resolution that is to be expected. The wind pattern also shows the strongest winds in the right flank of the storm.

Figure 4.2 shows the wake of the storm created by the model. Similar to Figure 3.1 the area of largest cooling occured after the storm had curved back and was moving to the east-northeast. Therefore the CFSR model does resolve the hurricane and does model cooling of temperatures due to the wind forcing from the hurricane. The maximum cooling in CFSR

63

SST was between 1.25^{o}C and 2°C and the corresponding dSST from the OI TMI/AMSRE SST were between 3 to 5°C. Therefore the modeled drop in SST is slightly less then half of the drop in SST from the TMI and AMRSE product.

Figures 4.3 and 4.4 represent the maximum wind fields for Hurricane Isabel (2003) and Bill (2009) respectively. Hurricane Isabel (2003) is a well-defined storm in the model data with wind speeds reaching category 1 strength on the Saffir-Simpson scale. Similar to Hurricane Felix, the CFSR model does a good job representing the structure and symmetry. Along with the structure of the storm, the model represents the order of intensities correctly. In both the model and the best track the storm with the strongest intensity is Isabel (2003), followed by Bill (2009), and the weakest storm was Hurricane Felix (2001). Later in this chapter some more detailed comparisons with the ARGO float data will provide some further characterization of any possible differences from the true ocean state.

The major difference between the case for Hurricane Felix (2001)and the cases for Hurricane Isabel (2003) and Bill (2009) is the timing of the storm. The model developed Hurricane Felix fairly accurately with respect to time. The maximum wind speed from the model is the same as the maximum wind speed from the best track. For Hurricane Isabel this is not true. Figure 4.5 shows the wind speed from the day when the max winds are reported in the best track. Comparing those wind speeds to Figure 4.3, the wind speeds are roughly halved. In the top right of the figure are the remnants of Hurricane Fabian (2003). At this point the best track has Hurricane Isabel as a fully developed category 5 storm however the model shows a weaker storm with a large eyewall and maximum wind speeds between 30 and 33kt. Thus initially the model underestimated the development of Hurricane Isabel and through the noted lag time associated with the CFSR model in developing tropical storms the storm to continued to increase in intensity when in fact it was actually weakening (Schenkel and Hart, Accepted).

Hurricane Bill presents an interesting case. Figure 4.4 shows the wind speed on the day, which according to the best track analysis has the maximum storm strength. The CFSR model shows this to be the peak intensity of the storm as well. However, in Figure 4.6, 3

days later, Bill (2009) has only slightly weakened to a maximum wind speed of 54kt. So in the model there is a weakening of just 3kt and in the best track over the same time there is a decrease from 100kt to 74kt. The next run of the model at 00Z on the 20 September (not shown) shows a more defined eye and has much better organized symmetry in the wind field but has weaker maximum wind speeds of only 52kt. There is general agreement in wind speeds with some disagreement between the model and observations on the timing of organization.

Figures 4.7 and 4.8 show the difference in CFSR SST over the path of the storms for hurricane Isabel (2003) and Bill (2009) respectively. In both figures, there is a clear area of colder temperatures in the wake of the storm. For hurricane Isabel (2003), the corresponding SST drops were approximately 2 to 3.75 ^{o}C in the CFSR SST as compared to nearly 6°C in the AMSRE/TMI SST product. For Bill (2009), the CFSR SST show a decrease of temperatures from between 1.25 to 2.75 ^{o}C while the AMSRE/TMI SST show drops in temperature of 3 to 5 ^{o}C. Once again, the modeled SST changes are slightly more consistent with observational results then the wind speeds but how much is that due to data assimilation versus data sampling in the wind field. In comparing the magnitude of the differences in SST for each case, the greatest change in SST was reflected in the strongest storm hurricane Isabel (2003) followed by Bill (2009) and then Felix (2001).

4.2   Comparisons of ocean characteristics of CFSR with observations

Since one of the original goals of this research was to use the SSH data from altimeter observations for calculation of the cold wake heating loss, it is helpful to compare the SSH altimeter measurements with the CFSR SSH data. It should be noted that the altimeter data is not assimilated into the CFSR model, so the results present a valid comparison of the two quantities without any overlap (Saha et al., 2010). Figure 4.9 shows the difference in SSH over the same time frame as the SST field in Figure 4.2 for hurricane Felix (2001).

While not identical, the same general pattern exists in each field. There is an SSH drop of at least 3 cm over the area where the largest drop in temperature occurred, so there is good agreement in this case. For hurricane Isabel (2003), Figure 4.10, there is a large drop in the SSH of 10 cm over a good portion of the storm track. The maximum height difference for Hurricane Isabel was 15 cm and so again for this case there is agreement between a decrease in SST and a decrease in SSH.

The final case is shown for hurricane Bill (2009) in Figure 4.11. Recalling Figures 3.18 through 3.20, there is no clear signal for all of the satellite altimetry passes. The CFSR is similar in that it does not show as distinct a pattern as Hurricane Felix(2001)and Isabel (2003). There is an area near the location of the storm track that does show a slight increase in magnitude, but is not reflected by the entire length of the track. It is also not collocated with greatest drop in SST. The lack of signal is consistent for a case in which a large fraction of the SST change is due simply to mixing/upwelling rather than heat loss to the atmosphere. If this assumption is true it is anticipated that changes at depth will highlight the differences between these three storms and will be evaluated below. In summary all three storms showed good agreement between the altimeter data and the model results or lack thereof.

The model response at depth is evaluated by comparisons with the ARGO float profiles. The CFSR model assimilates ARGO profile data so there should be relative agreement between the observations and the modeled results. Figures 4.12 and 4.13 show the comparison for the model and observation for the pre- and post-storm profiles for Felix (2001) and Isabel (2003). It is important to realize that for each of the observed profiles, they represent the average profile within a 1° x 1° box centered at a specific latitude and longitude. As a result, the profiles could be sampling different bodies of water. The profiles for Hurricane Felix show a matching change in profile structure with a deeper mixed layer, then a sharp temperature gradient, and then a normal decrease in temperatures to a depth of 200m.

Similarities between the float profiles and the modeled profiles are also seen for most of the other comparison points (see Figures 4.12 through 4.17). In only a few situations do

66

the profiles not agree between the observations and the model. The profiles for Hurricane Isabel are not similar, with differences of up to 2 degrees over almost the entire depth in Figure 4.13. The profile pattern of this float is subject to question due to the face that there is almost no change in the temperature profile for the Argo profile from before the storm to after (even with satellite SST changes of nearly 2 degrees; Figure 3.16). In contrast, the CFSR results during the pre-storm profile show a clearly defined near-surface layer that is well-mixed to about 30 meters deep. This layer extends to 60 meters after the passage of the storm along with a decrease of 2^oC at the surface. This is the expected profile structure of a profile from a time period after a hurricane passes over the area. One of the Argo floats during Bill (2009) also shows large differences from the model profiles (Figure 4.17). As in the previous example, while the model demonstrates some cooling and deepening of the mixed layer, the float observations are more ambiguous. In addition, the in-situ observations have very different temperatures between pre- and post-storm profiles even at 200 m depth. This may be an indication that the float is sampling two different water masses which the ocean model, because of its poorer horizontal resolution, cannot differentiate.

4.3   Estimation of heat needed to restore upper ocean

The next step in the process is to determine if the ocean's temperature cooled at depth, and if so, how much? The effects of the storm on the entire upper ocean profile can be seen by an analysis of potential temperature cross sections that were taken perpendicular to the path of the storm. Several examples of these cross sections are shown here. The times chosen represent the ocean before the passage of the storm, the initial impact of the storm and then a few days after the storm in order to show the lasting impact of the storm. The cross sections are potential temperatures, but given that the density is nearly constant at the near surface, the impacts of using potential temperature instead of in-situ temperature should be negligible. First in Figure 4.18, the cross section is shown meridionally across what became the track of Hurricane Felix (2001). The cross sections shown for Felix (2001)

are from 21°N to 39°N at the 33°W meridian. In the next time frame shown, Figure 4.19, the storm has just passed through the area, and shows a clear colder volume of temperatures relative to the surrounding water reaching to a depth of 40 meters. The 22°C isotherm is shallower indicating a warming beneath the mixed layer. In this particular case the surface expression of the wake in terms of visible SST is only evident for about 4 days.

The cross sections for Isabel (2003) show a much more dramatic impact on the ocean. At the first time frame, Figure 4.21, the ocean is fairly constant zonally in temperature from about 30 meters to 90 meters. The cross section for Hurricane Isabel is taken from 75°W to 65°W across the 28°N parallel. In Figure 4.22, the area where the storm affected the ocean is shown by a clear drop in temperature in the center of the figure. There is a well-mixed column of water reaching from the surface, where there is a 3° C change, to about 60m. Below the first column there is a second column of colder water caused by upwelling, but is not mixed and is zonally stratified. To the right of the colder upwelled water, there is a column of warming water. This is the result of cooling beneath the well mixed column of water. Both the upwelled colder water and the warmer column are impact the ocean to depths of greater than 105m. This shows that stronger storms can affect the ocean to depths greater than 100m.

Looking at the next time frame, Figure 4.23, the ocean has started the process of re-stratification and has warmed by 2° C over a period of 8 days. The structure of the cold wake now shows that the colder stratified water has been displaced to the left of the storm, as the forced response has caused the column of warmer water to increase spatially in the width and vertical aspect. As a result, the effects of the cold wake are now tilted over the column. At the next point of the ocean's recovery, 6 October 2003 which is shown in Figure 4.24, the surface has nearly completed its recovery as compared to the initial well mixed column of water. The initial column has deepened 20m, and the cross section still shows the tilted axis of colder water with a corresponding column of warmer waters from 40 to greater then 105m. At this point the recovery has taken 19 days to nearly recover at the surface but still shows large impacts from 40m to 105m. The next time frame shown is

more than a month later on 11 November 2003. As shown in Figure 4.25, the ocean surface no longer shows any indication of the initial column of cooler waters above 50m. Between 50 and 60m the ocean is becoming more stratified and below that there is an oscillating pattern of warmer temperature to the left of the track with cooler temperatures where the storm passed through. To the right of the track the temperatures are warmer. Nearly 40 days after the storm, there is still a body of water in the wake of the hurricane that has not yet returned to its pre-storm zonal temperature pattern. Finally, in the last time frame, 14 December 2003, shown in Figure 4.26, the area of cooler temperatures seems to have been completely wiped away. Curiously, there is now a temperature maximum where the cold wake previously existed. This phenomena began to show in the cross section on 11 November 2003. The feature grew larger with each successful day and while the magnitude is only 1° warmer, it is interesting that the model developed a temperature maximum after the storm has passed.

Hurricane Bill (2009) shows a similar pattern to Isabel (2003), but with a slightly weaker impact in Figures 4.27 and 4.28. In the pre storm cross section the ocean has a bit of an oscillating pattern towards the west. There is a bit of warming just to the left of where the storm will cross through, and an area of cooling in the deep middle in the region where the Bill intersects the cross section. The cross section for Hurricane Bill (2009) is along the 29° N parallel from 75^oW to 55^oW crossing the region with the greatest ΔT from Figure 4.8. Comparing the cross section from before the storm, to when the storm has passed through the area in Figure 4.28, and it is clear that the ocean has mixed up deeper colder waters to the surface and a wake has formed in the region where the storm crossed through. There is a 2^oC change in near surface temperature and a succinct colder volume of water extending down to 90 meters. It is interesting to note that between 50 and 100m deep, there is a pattern of warm, cold, warm oscillations. It is likely that these are just waves passing in the ocean. In the case of hurricane Bill (2009) the fluctuations in temperature are more severe then in hurricane Isabel (2003). There is a very sharp gradient along the temperature boundaries for this storm, especially at depth. Through a visible inspection, it appears that

on 19 September 2009, shown in Figure 4.29, the ocean has nearly re-stratified to the zonal condition prior to the storm, demonstrating a fairly rapid recovery.

The methodology described earlier has been employed on the CFSR data in order to objectively determine the duration of the cold wake signature. A temperature gradient product was taken across a line of constant depth at 5 different depths. To get the pre-storm value, 10 days worth of CFSR model data was averaged to create an initial field. Once the post storm temperature gradient was within two standard deviations of the initial value, it was determined that the wake was no longer being felt at that depth. Figure 4.30 shows the results of this analysis for Hurricane Felix (2001). Given the direction of the best track for hurricane Felix (2001) (see Figure 4.18), a meridional temperature gradient was used. The initial temperature gradient was already somewhat noisy due to the cooling temperatures as the cross section moved from the south to the north into colder waters. Yet even with the noisy pre storm data, the passage of the hurricane is still quite clear. The rapid increase in magnitude on day 17 represents the passage of the storm due to the change in temperatures as the storm passed. The magnitude of the value is much less important than the relative shape of the curve, and the relative magnitude of the different depths compared to the other depths. From the figure, the gradient at the closest depth to the surface, 35m, was the first to return to its pre-storm value after roughly 10 days. By comparison, at 75 m the restoration time is over 70 days. The depths with the highest peak gradients are those nearest the surface, however since the re-stratification is strongly affected by surface fluxes, the ocean re-stratifies more quickly near the surface than at depth.

A similar structure of change in gradients is shown by hurricane Isabel (Figure 4.31). It should be noted that as opposed to hurricane Felix (2001), this slice is not near the North Atlantic Drift with its baroclinic instabilities and it is zonally oriented; thus the overall initial variability is less. As before there is a period of pre-storm conditions that are relatively constant in time and then a sharp increase in gradients as the storm moves through the area. In this case, the depth with largest impact was the middle depth of 55m

and the depth affected the least is actually the depth closest to the surface. This differs from Hurricane Felix where the shallowest depth was the second most affected depth. Similar to the case with Hurricane Felix 2001, the first depth to return to its pre-storm condition is the depth closest to the surface and the last depth to recover is the deepest depth. The cold wake is objectively over after approximately 35 days at the first depth and 90 days at the deepest depth.

The return of the gradient conditions to near normal in hurricane Bill (2009) follows a slightly different pattern as compared to the other cases (Figure 4.32). For both Isabel (2003) and Felix (2001), there was a sharp spike in the gradient value followed by a roughly linear decrease to the pre-storm conditions. In the case of Hurricane Bill, the decreases appear as an exponential decay. In all three cases, the sharpest gradient occurs at mid depths (45 to 55m). In the case of Hurricane Bill, it is not the shallowest depth that returns to pre storm conditions first. Recovery actually came first at the 45m depth. This may be an indication that surface forcing is not the most important factor in the re-stratification, as this would occur from the surface downwards. The re-stratification times for the various depths varied from 12 to 35 days, which is a much shorter time period than the other two cases based on this objective thermal gradient technique.

The temperature gradients show that for each storm, each was able to modify the temperature of the ocean to at least a depth of 75 meters for at least a period of 10 days from depths ranging from 35m to 75m. In two cases, the shallowest depth had the shortest recovery time and the deepest depth had the longest, but in the third case (Bill 2009) this pattern was not followed. Thus it is possible that re-stratification from ocean dynamics is relatively important for Bill (2009). It should also be noted that Bill (2009) recovered 20 days faster then the weakest storm, Felix (2001), and more then 60 days faster then the strongest storm, Isabel (2003). The following section discusses the estimation of heat loss due to the storm and the amount of heating required to re-stratify the ocean.

4.4 Estimation of Ocean Heating Budget for a Hurricane Passage

Calculation of the heat loss across the cold wake is performed as described in Chapter 2. The first step is the calculation of the area affected by evaluating all points along the best track in which there was at least a 1^oC decrease over a 24 hour period. Once the area affected was determined, Equation 2.3 was used to calculate the ocean heat loss over a four day period, two days before and two days after the storm had passed through the area. This was calculated for each day during the life of the storm and the maximum value was kept and used as the heat loss at that grid point for the storm. Figures 4.33, 4.34, and 4.35 show the calculations for each of the three cases, Hurricane Felix (2001), Isabel (2003) and Bill (2009) respectively. For Hurricane Felix (2001), there is a apparent heat loss of greater than 1.2×10^9 Jm^{-2} in the area. Likewise for Hurricane Isabel (2003) and Bill (2009) those values are 1.0×10^{10}Jm^{-2} and 5.0×10^9Jm^{-2}. Therefore for each case the amount of heat loss was on the order of 10^9 Jm^{-2}. If the assumption that the re-stratification is solely a function of surface heating from Emanuel (2001) is correct, then the ocean needs to absorb approximately 10^9 Jm^{-2} over some amount of time in order to fully re-stratify the ocean.

The temperature gradient data provides an estimate of the length of time needed to restore the ocean. Figures 4.36, 4.37, and 4.38 show the amount of incoming heat flux at the surface of the ocean from the time of the storm until the end of the re-stratification period. In the case of Hurricane Felix, Figure 4.36, there was a positive flux into the ocean over most of the affected area and it was between 4×10^9Jm^{-2} and 1.2×10^{10} Jm^{-2}. This means that the incoming flux over the region is actually greater then the maximum required, 1.2×10^9 J/m^2, heating to re-stratify the ocean. The same is true for hurricane Isabel (2003) and hurricane Bill (2009) in figures 4.37 and 4.38 respectively. The maximum amount of positive incoming surface flux is approximately 2×10^{10} J/m^{-2} for Hurricane Isabel and between 1×10^{10}J/m^{-2} to 1.7×10^{10} J/m^{-2} for Hurricane Bill (2009). To compare to Emanuel (2001), the units must be converted to W/m^2. Multiplying the maximum incoming flux by the area of the

polygon affected by the storm and then dividing by the total time of the recovery, the values for comparison are $1.12{\times}10^{11}$ W for Felix (2001), $6.31{\times}10^{10}$ W for Isabel (2003) and $2.50{\times}10^{11}$ W for Bill (2009). The problem with making a direct comparison is that Emanuel (2001)'s values are over an entire season and not just over one particular storm. So for this estimate it was shown that the amount of required heating is actually less then the amount of incoming heat flux. It is possible that Emanuel (2001) could be correct in that all of the required heating to re-stratify the ocean is done through incoming surface heating.
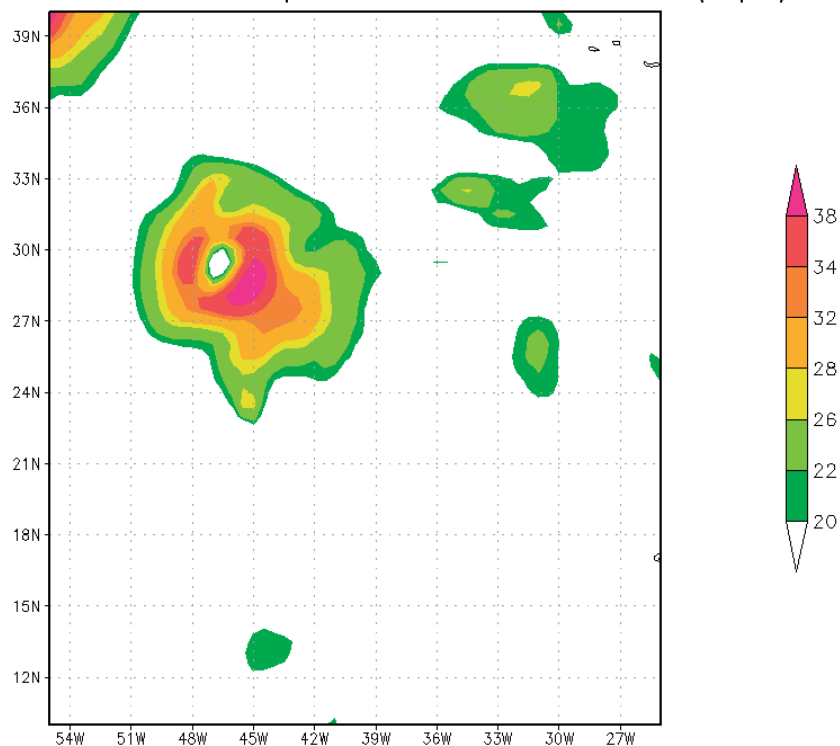
Figure 4.1: CFSR wind speeds at 1000 hPa for hurricane Felix (2001) on 14 September 2001 in miles per hour.
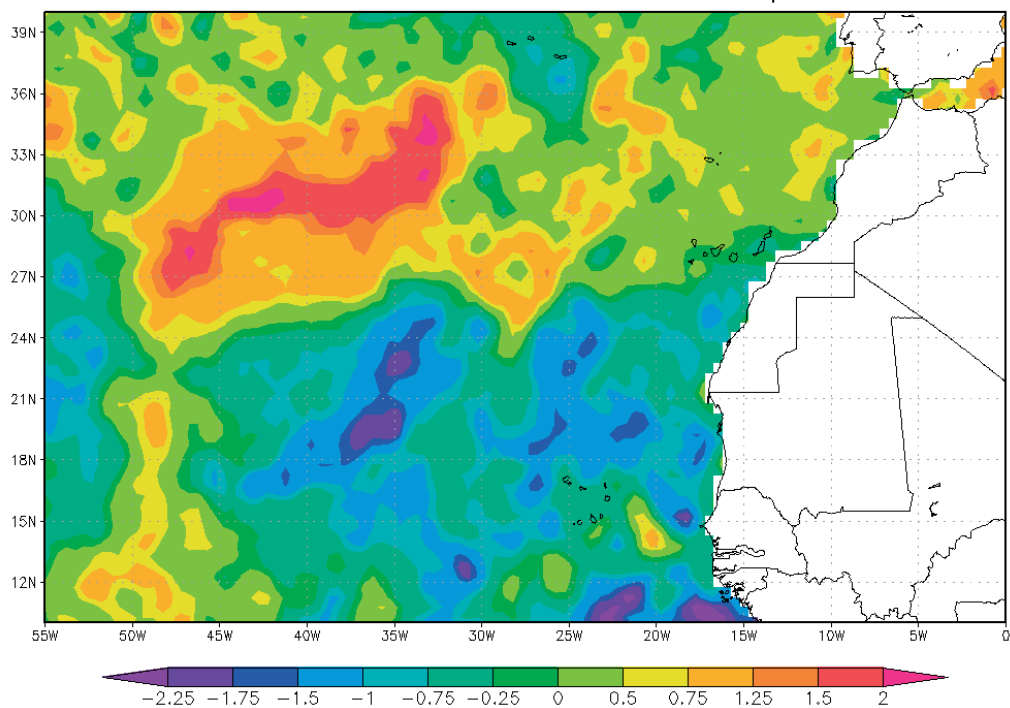
Figure 4.2: Difference in model ocean SST(^oC) from 10 September 2001 to 18 September 2001 for Hurricane Felix (2001).
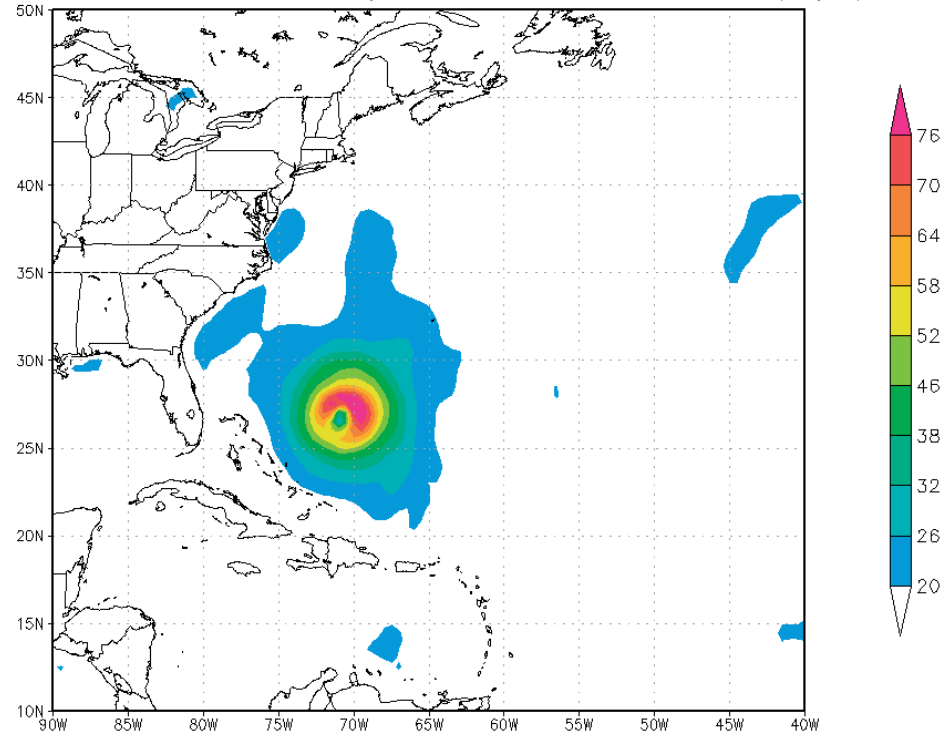
Figure 4.3: CFSR wind speeds at 1000 hPa for hurricane Isabel on 16 September 2003 in miles per hour.
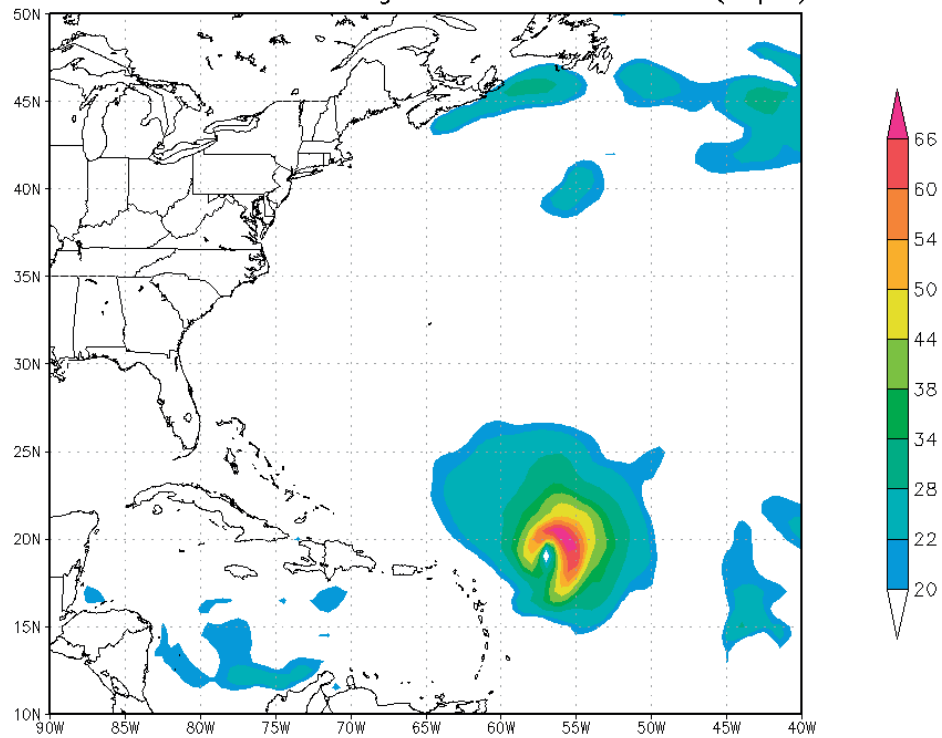
Figure 4.4: CFSR wind speeds at 1000 hPa for hurricane Bill on 19 August 2009 in miles per hour.
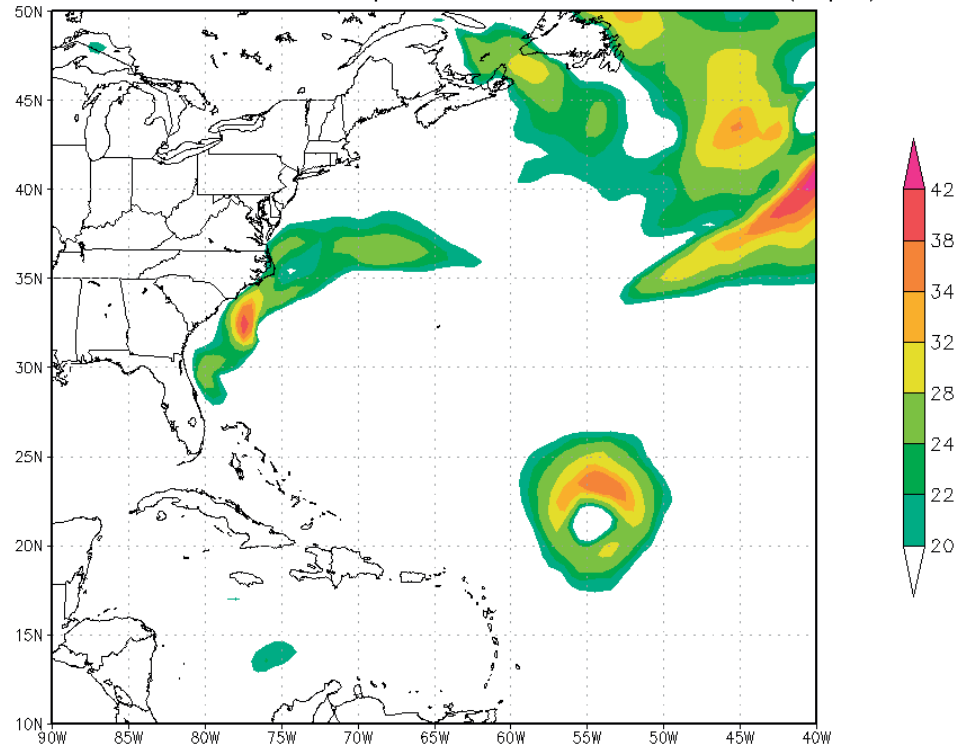
Figure 4.5: CFSR wind speeds for hurricane Isabel on 11 September 2003 in miles per hour.
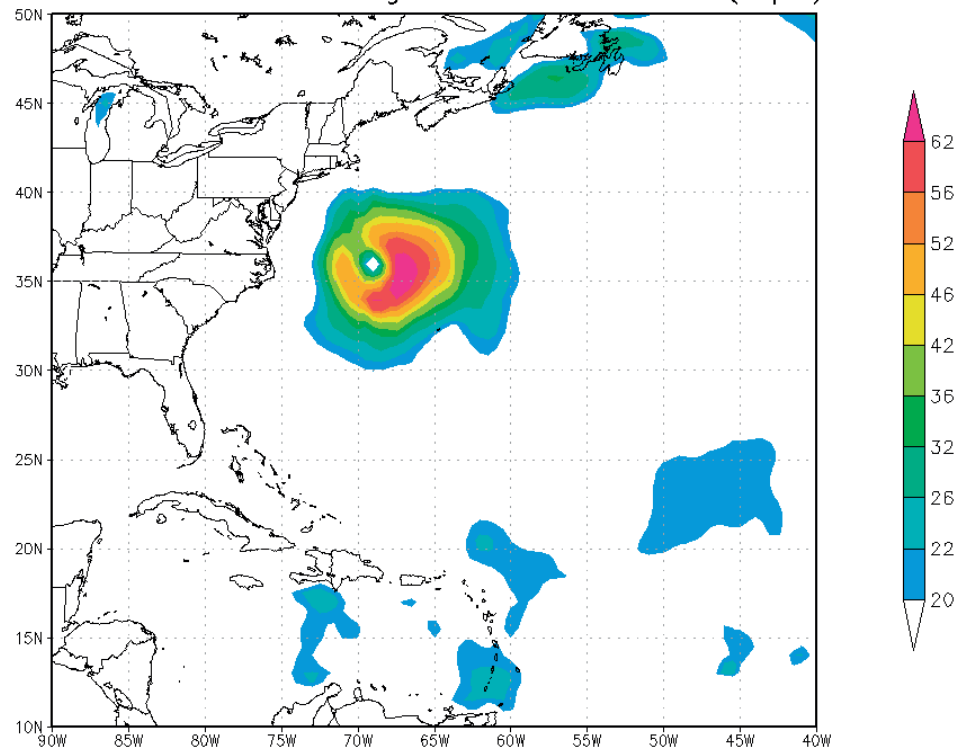
Figure 4.6: CFSR wind speeds for hurricane Bill on 22 August 2009 in miles per hour.
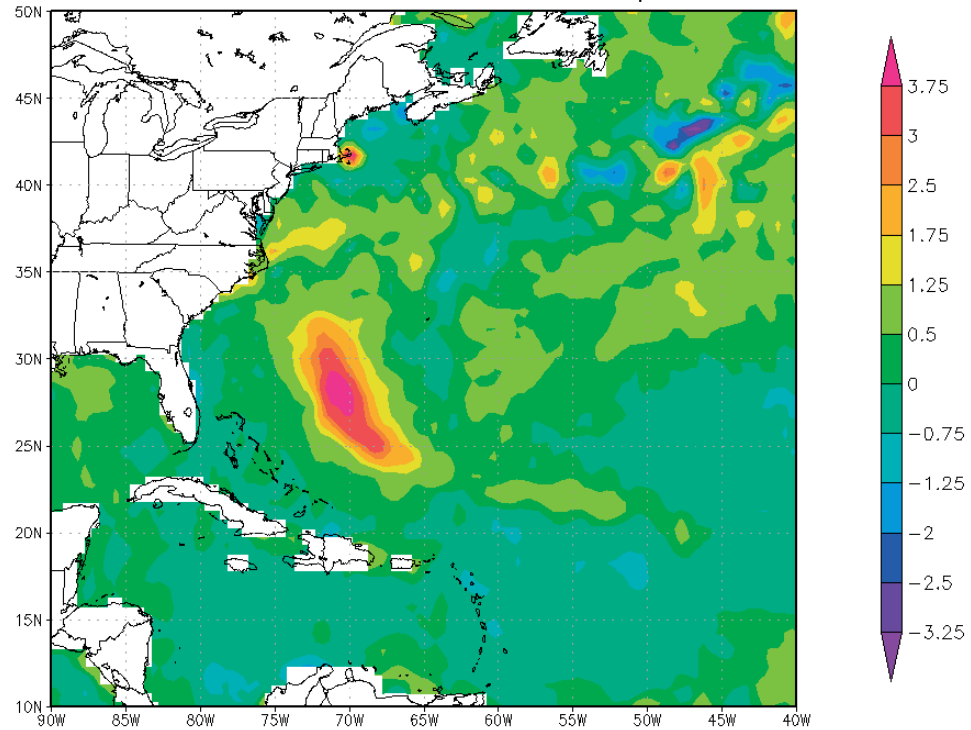
Figure 4.7: Difference in model ocean SST(^oC) from 10 September 2001 to 18 September 2001 for hurricane Isabel (2003).
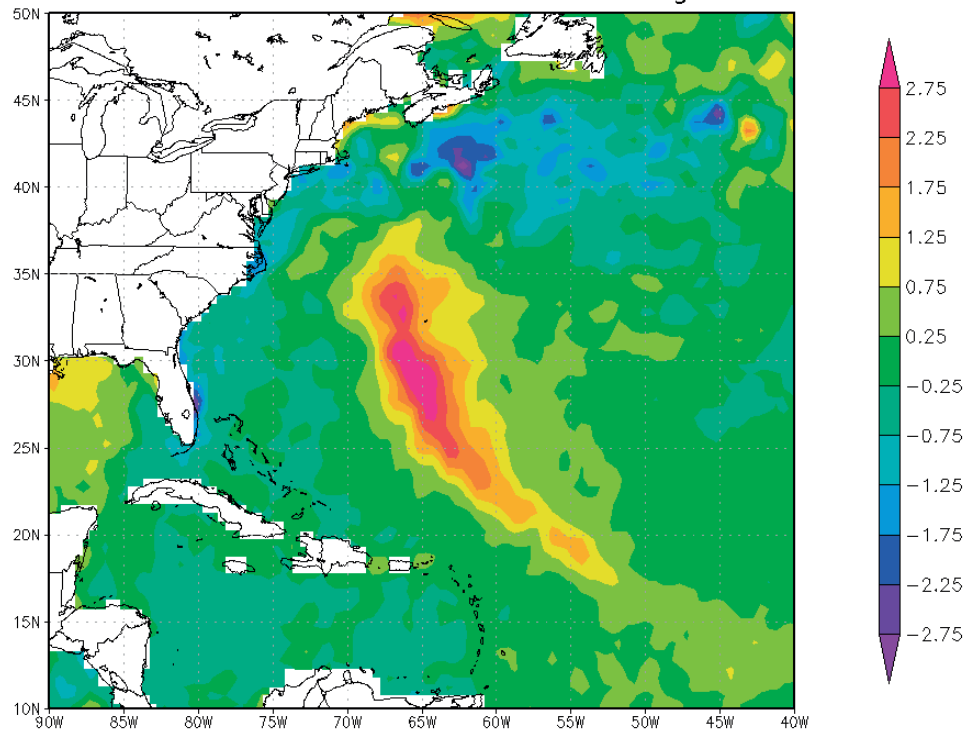
Figure 4.8: Difference in model ocean SST(^oC) from 17 August 2009 to 23 August 2009 for hurricane Bill(2009).

2001 Felix Cold Wake SSH Difference Aug 10−18
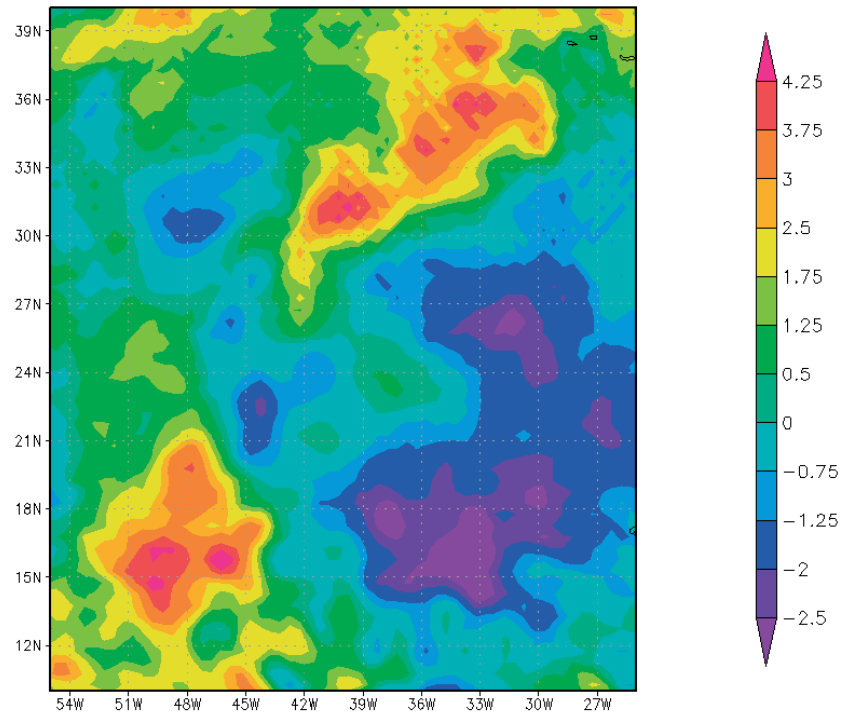
Figure 4.9: CFSR modeled difference in SSH for hurricane Felix (2001) from 10 September 2001 to 18 September 2001 in cm.

2003 Isabel Cold Wake SSH (cm) Difference Aug 10(00z)−18(00z)
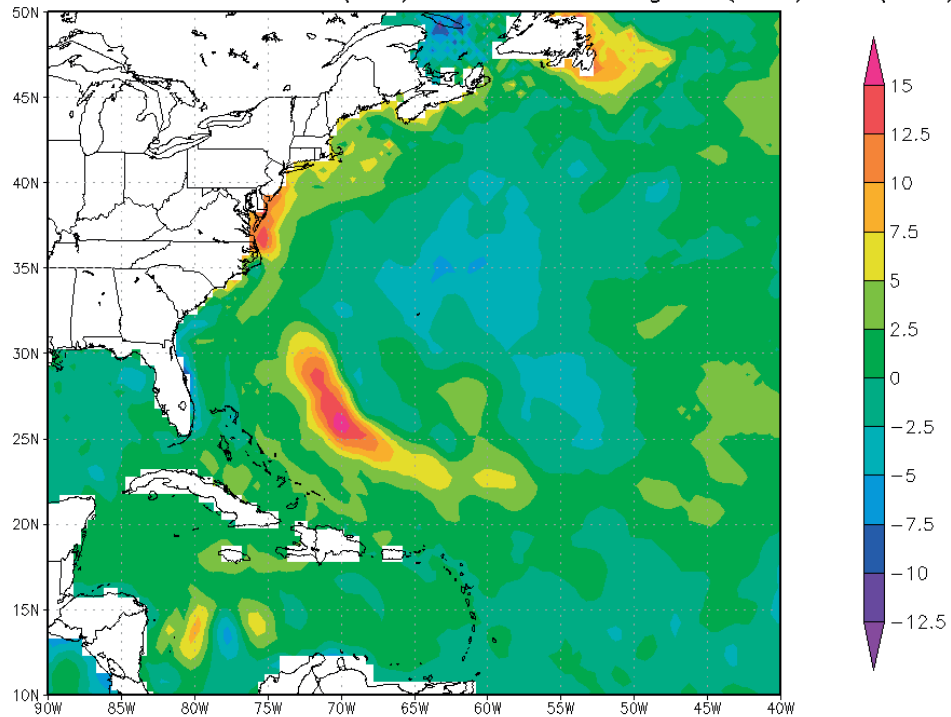
Figure 4.10: CFSR modeled difference in SSH for hurricane Isabel (2003) from 10 September 2003 to 18 September 2003 in cm.
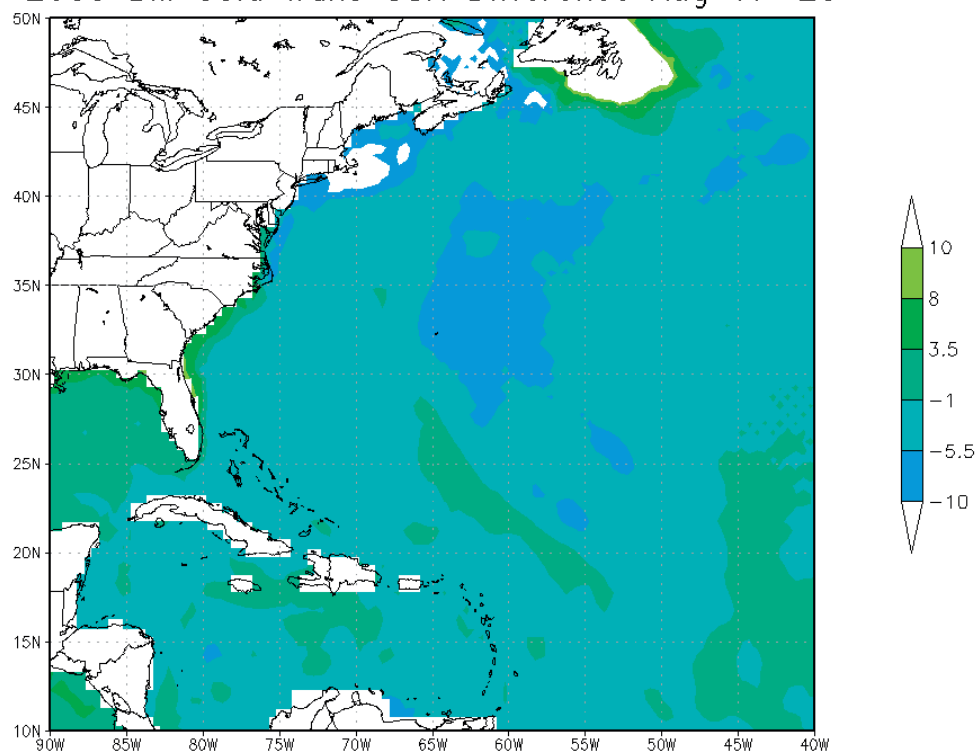
Figure 4.11: CFSR modeled difference in SSH for hurricane Bill (2009) from 14
August 2009 to 23 August 2009 in cm
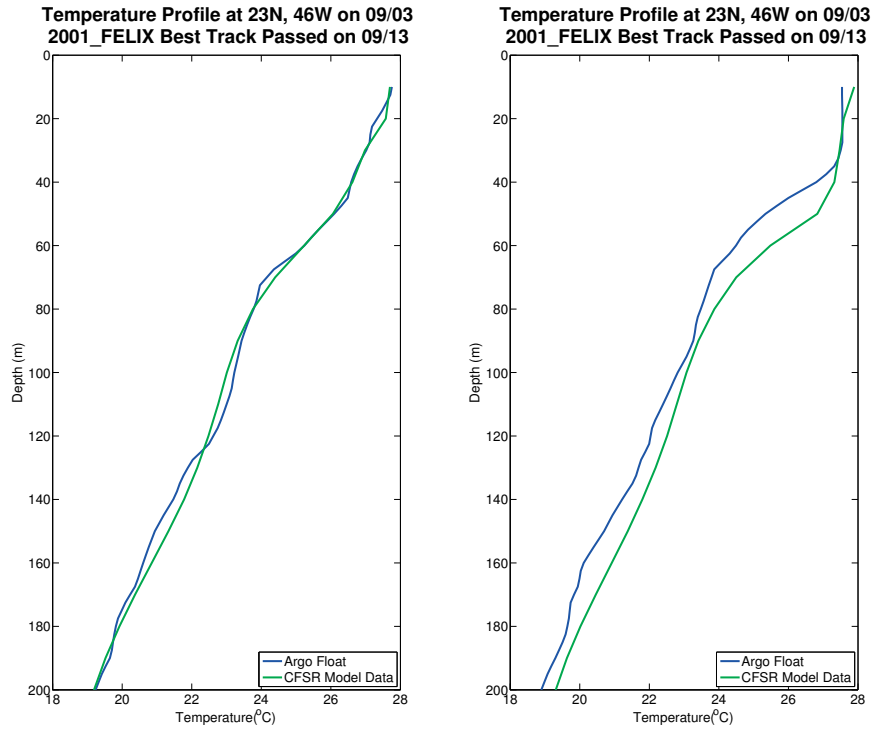
Figure 4.12: Ocean profile comparison of CFSR model and Argo float for hurricane Felix(2001)at 23° N 46^oW. The Argo float is shown in blue and the CFSR model is shown in green.
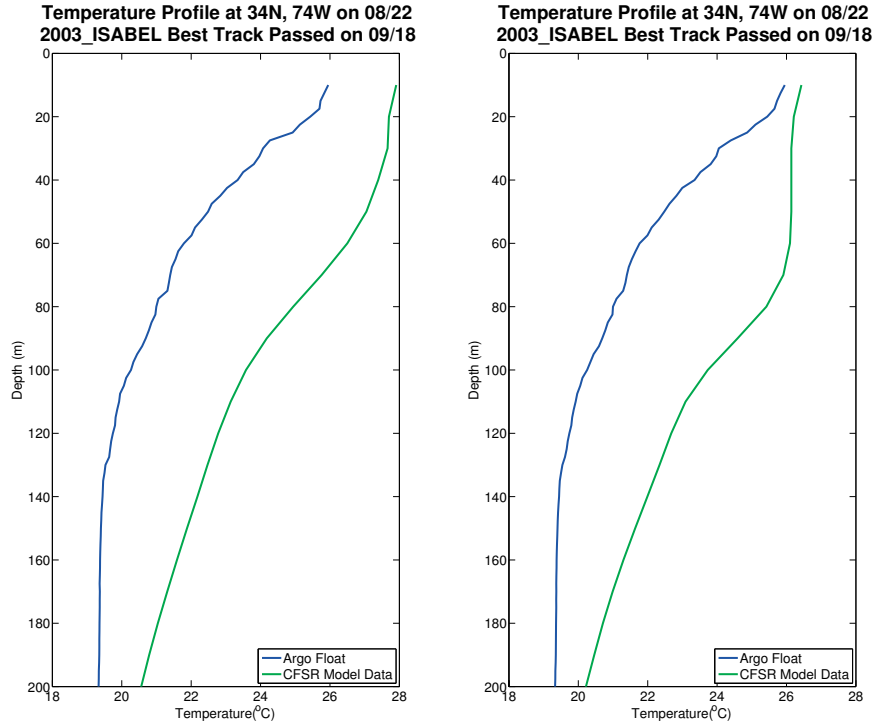

Figure 4.13: Ocean profile comparison of CFSR model and Argo float for hurricane Isabel(2003)at 34° N 76^oW. The Argo float is shown in blue and the CFSR model is shown in green.

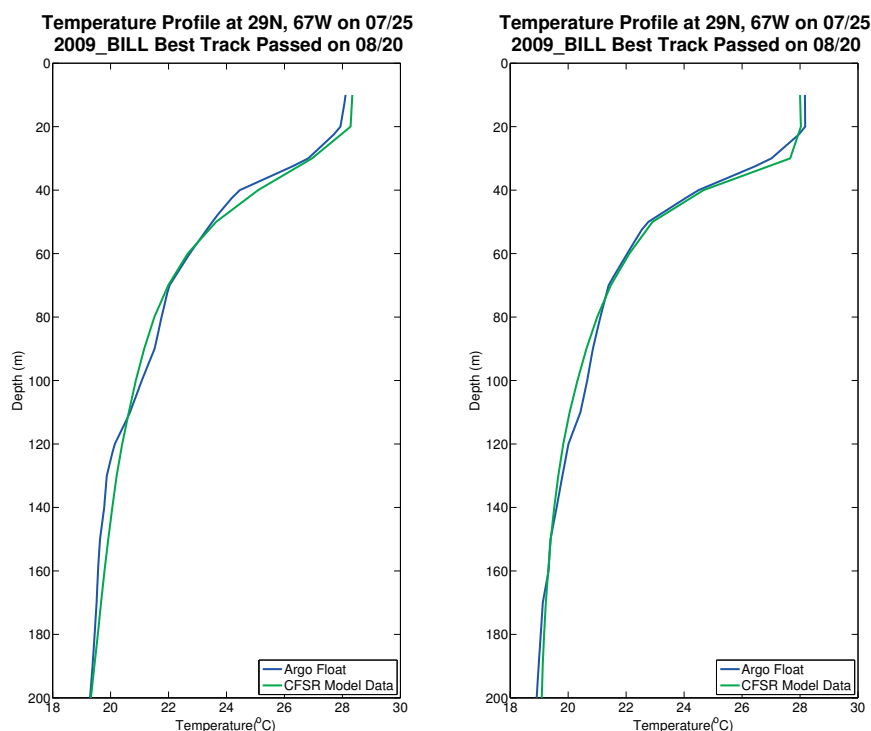Figure 4.14: Ocean profile comparison of CFSR model and Argo float for hurricane Bill (2009) at 29° N 67^oW. The Argo float is shown in blue and the CFSR model is shown in green.
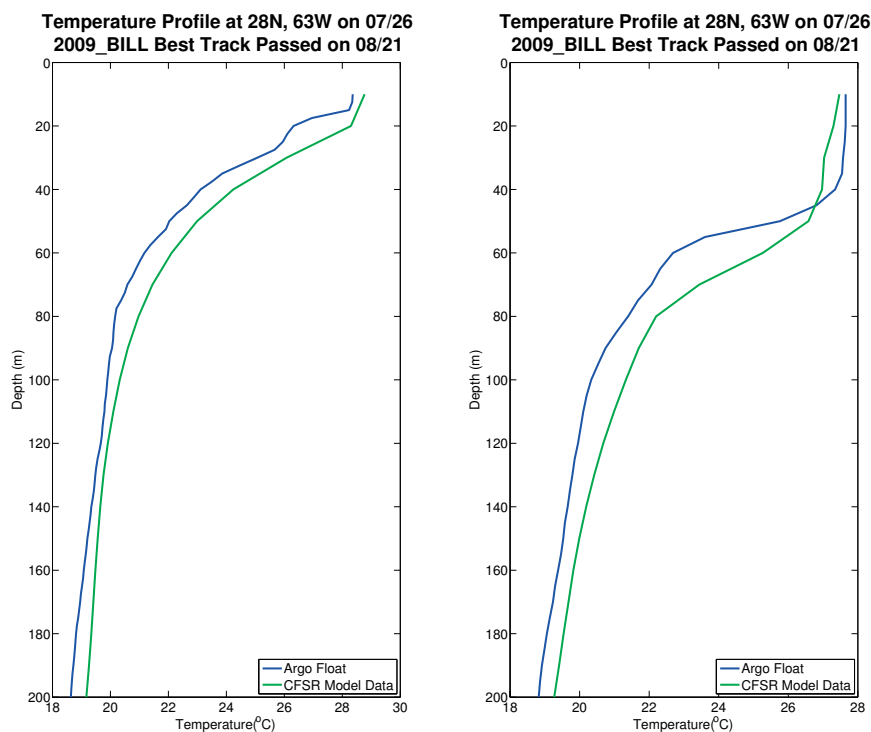

Figure 4.15: Ocean profile comparison of CFSR model and Argo float for hurricane Bill (2009) at 28° N 63^oW. The Argo float is shown in blue and the CFSR model is shown in green.

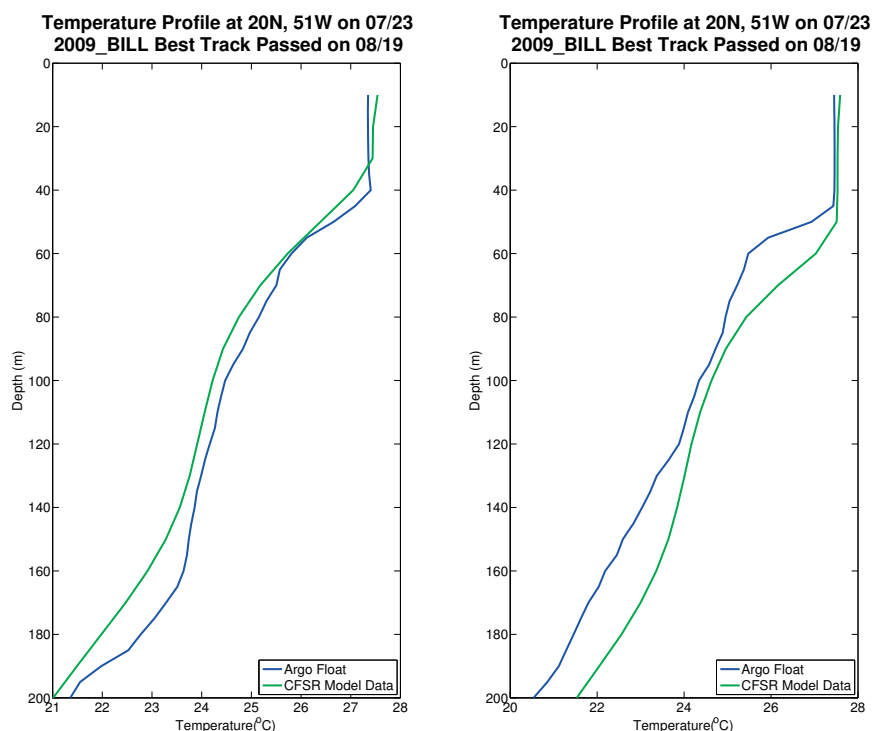Figure 4.16: Ocean profile comparison of CFSR model and Argo float for hurricane Bill (2009) at 20° N 51^oW. The Argo float is shown in blue and the CFSR model is shown in green.
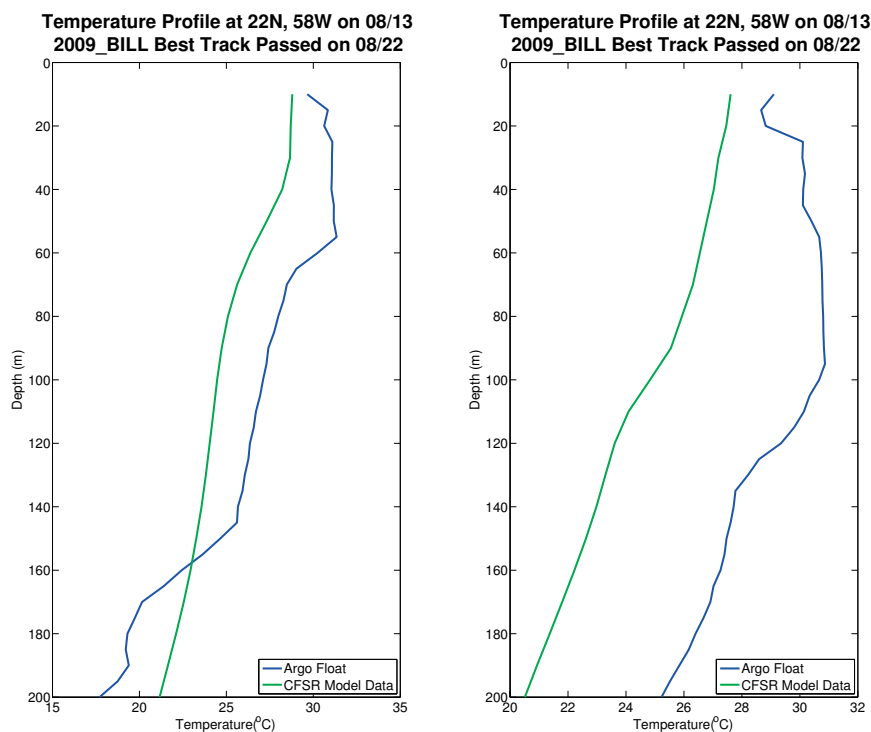

Figure 4.17: Ocean profile comparison of CFSR model and Argo float for hurricane Bill (2009) at 22° N 58^oW. The Argo float is shown in blue and the CFSR model is shown in green.
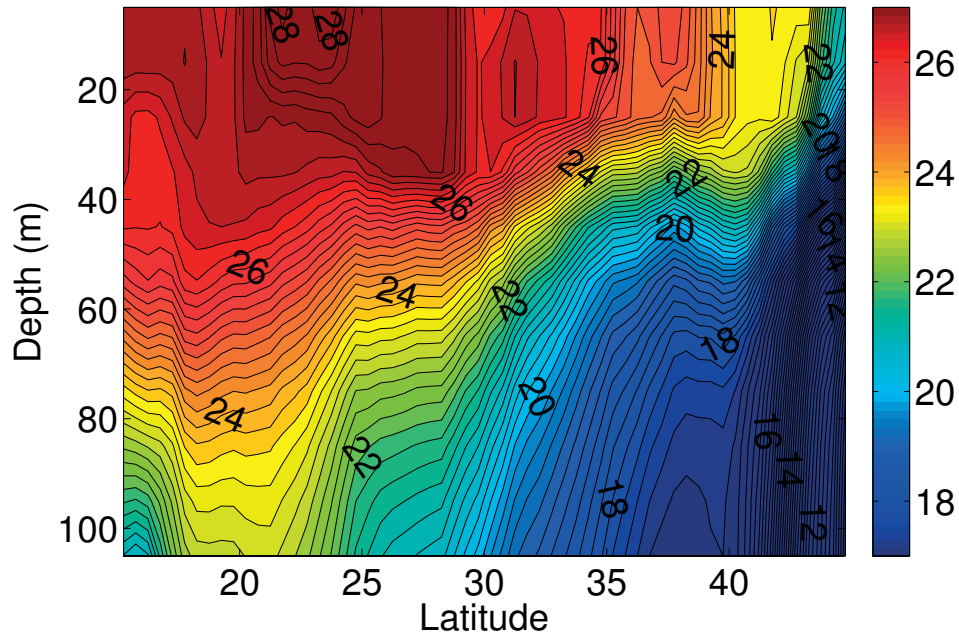
Figure 4.18: Cross section of the ocean for hurricane Felix(2001)at 33° W on 14 September 2001. The depth ranges from 5m to 105m.
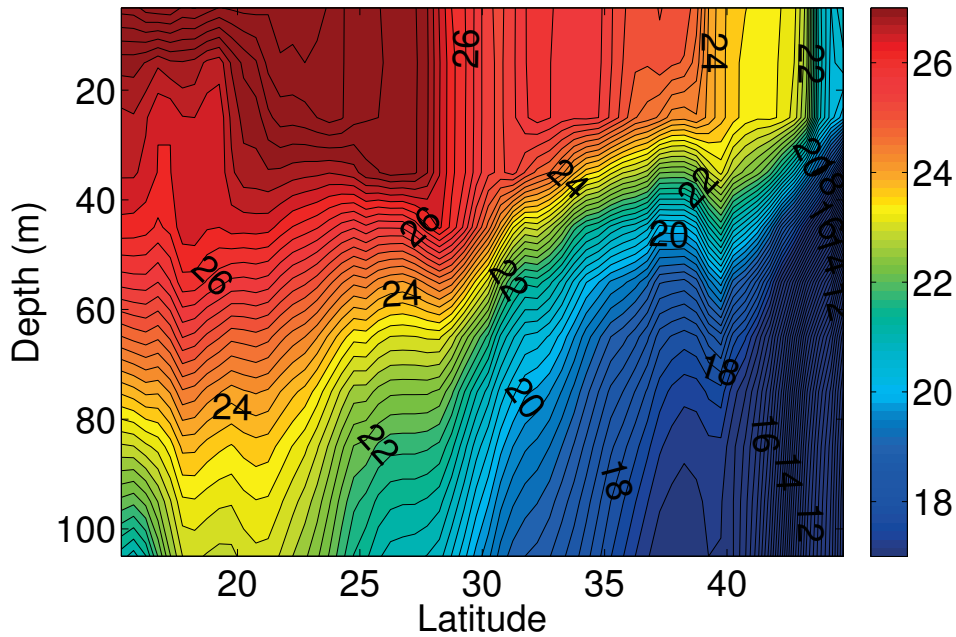

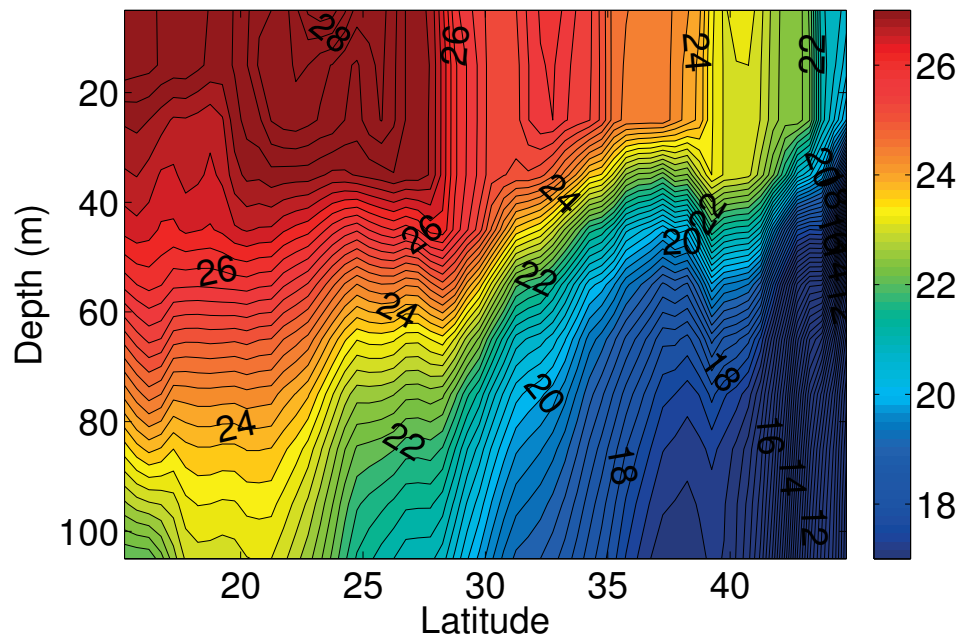Figure 4.19: Cross section of the ocean for hurricane Felix(2001)at 33° W on 19 September 2001. The depth ranges from 5m to 105m.

Figure 4.20: Cross section of the ocean for hurricane Felix(2001)at 33° W on 23 September 2001. The depth ranges from 5m to 105m.

Figure 4.21: Cross section of the ocean for hurricane Isabel (2003) at 28° N on 10 September 2003. The depth ranges from 5m to 105m.

Figure 4.22: Cross section of the ocean for hurricane Isabel (2003) at 28° N on 18 September 2003. The depth ranges from 5m to 105m.
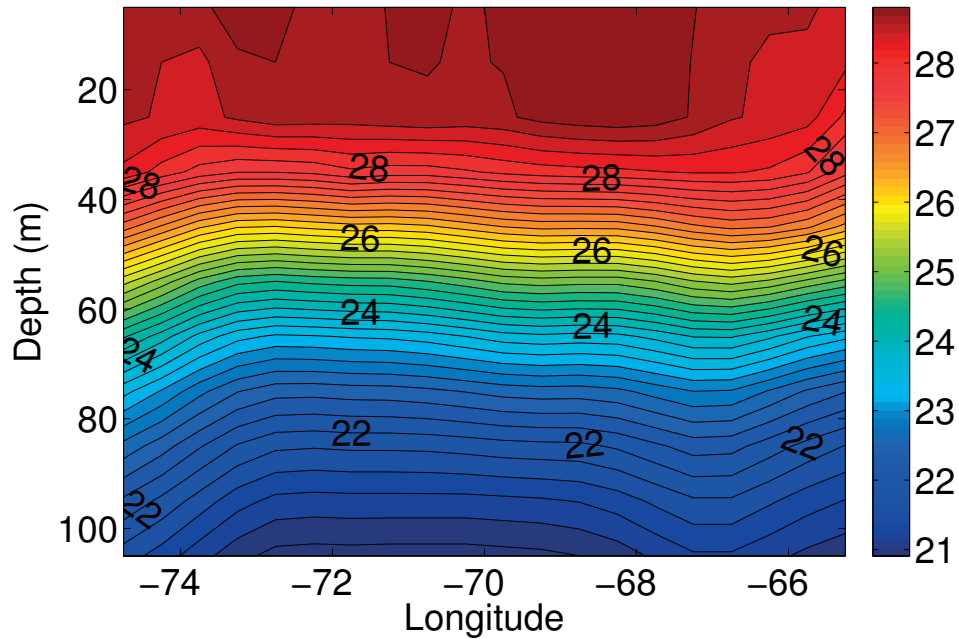
Figure 4.23: Cross section of the ocean for hurricane Isabel (2003) at 28° N on 26 September 2003. The depth ranges from 5m to 105m.
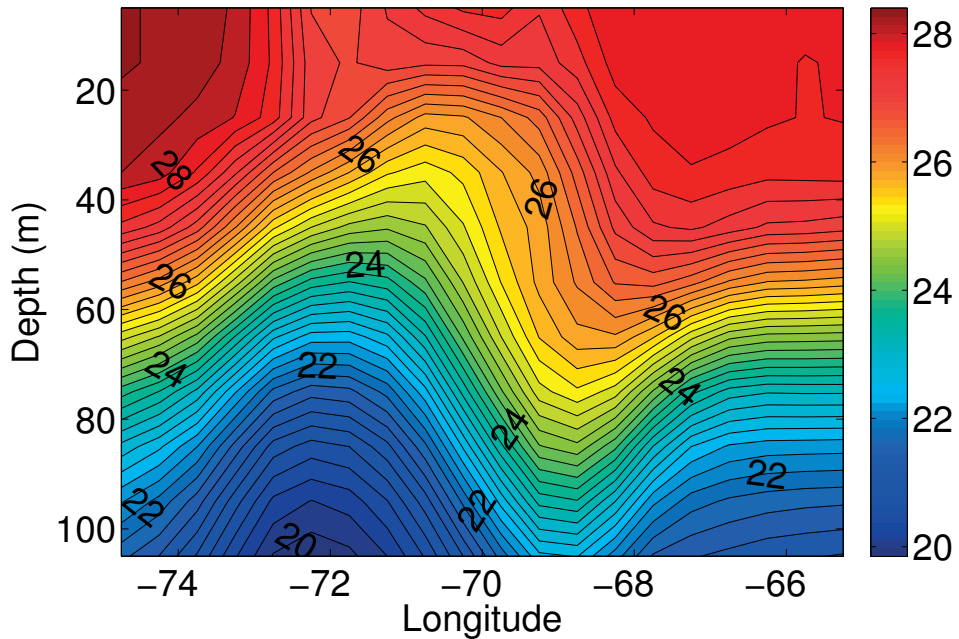
Figure 4.24: Cross section of the ocean for hurricane Isabel (2003) at 28° N on 6 October 2003. The depth ranges from 5m to 105m.
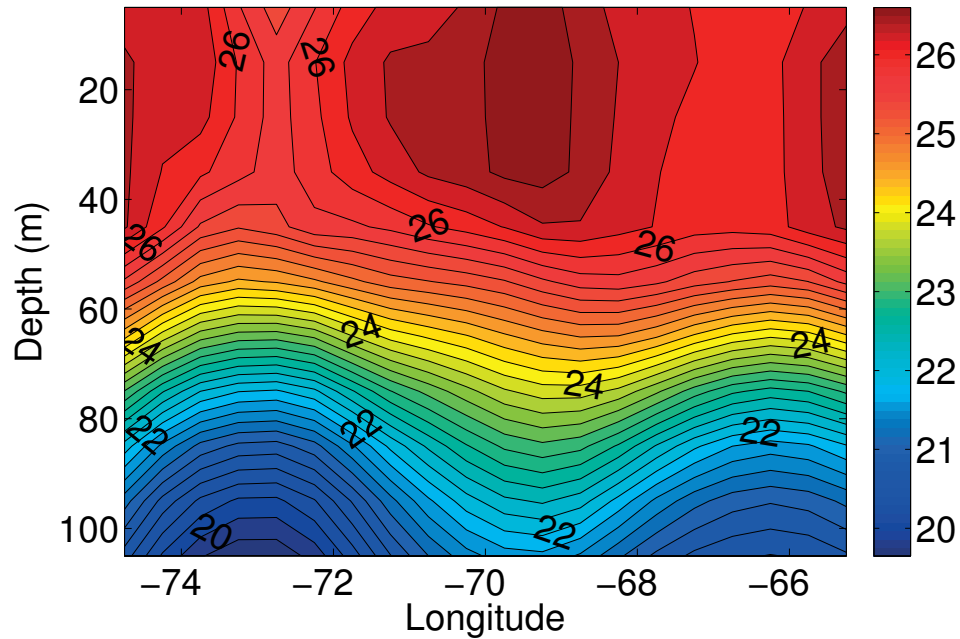
Figure 4.25: Cross section of the ocean for hurricane Isabel (2003) at 28° N on 11 November 2003. The depth ranges from 5m to 105m.
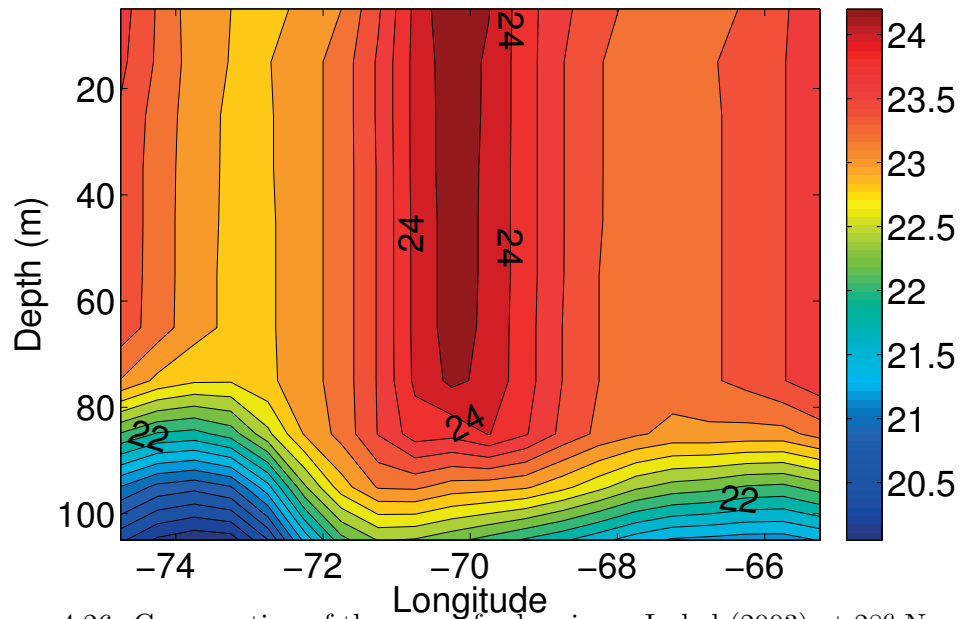
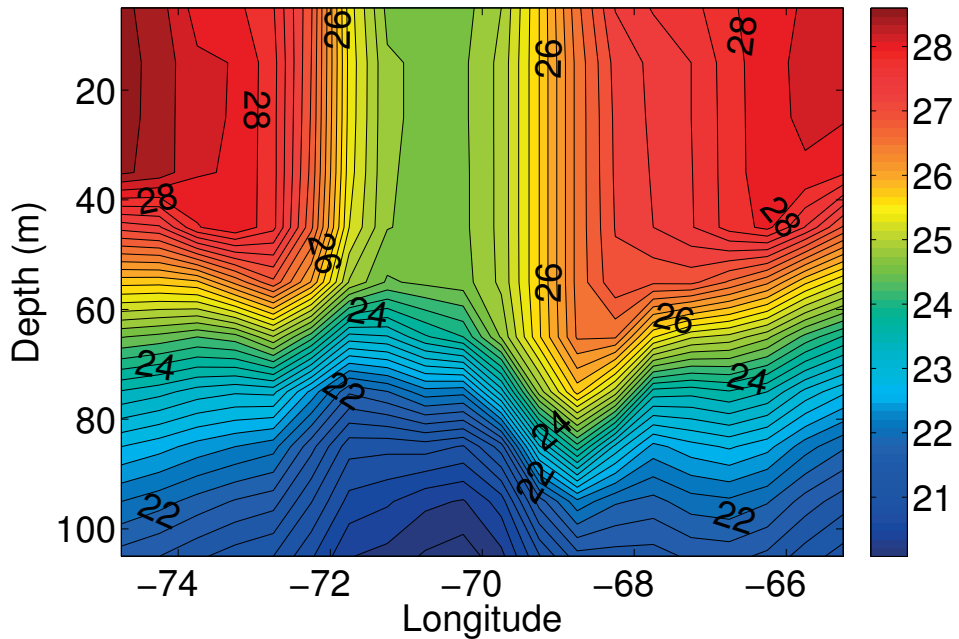**Figure 4.26:** Cross section of the ocean for hurricane Isabel (2003) at 28° N on 26 December 2003. The depth ranges from 5m to 105m.
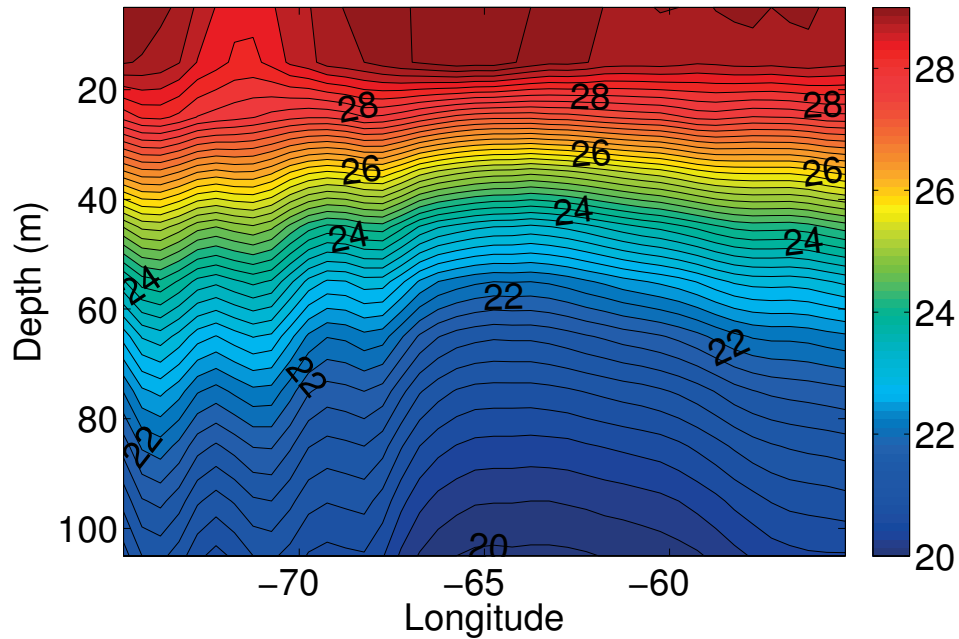
Figure 4.27: Cross section of the ocean for hurricane Bill (2009)at 29° N on 17 August 2009. The depth ranges from 5m to 105m.
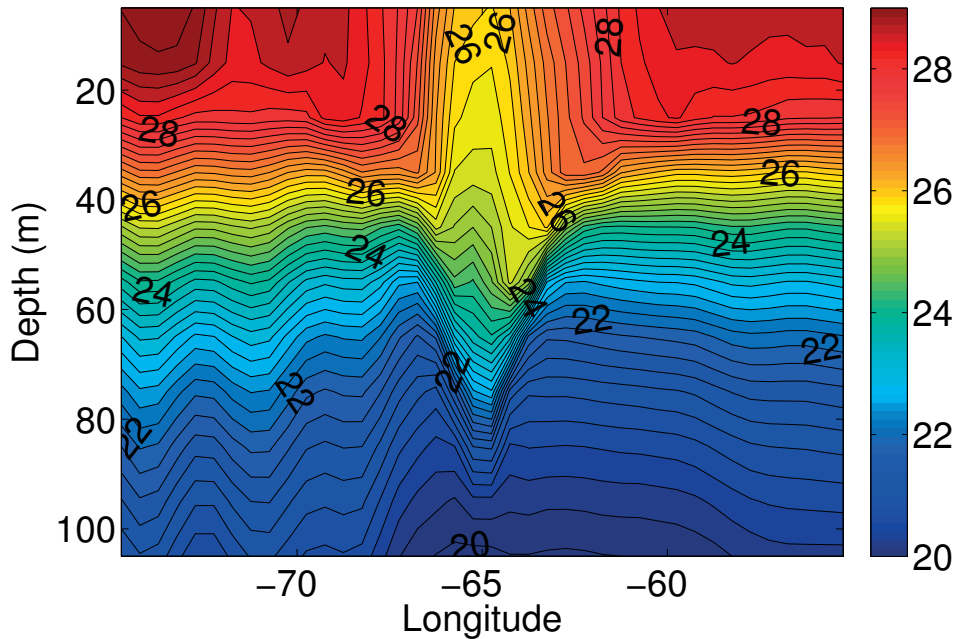
Figure 4.28: Cross section of the ocean for hurricane Bill (2009)at 29° N on 22 August 2009. The depth ranges from 5m to 105m.
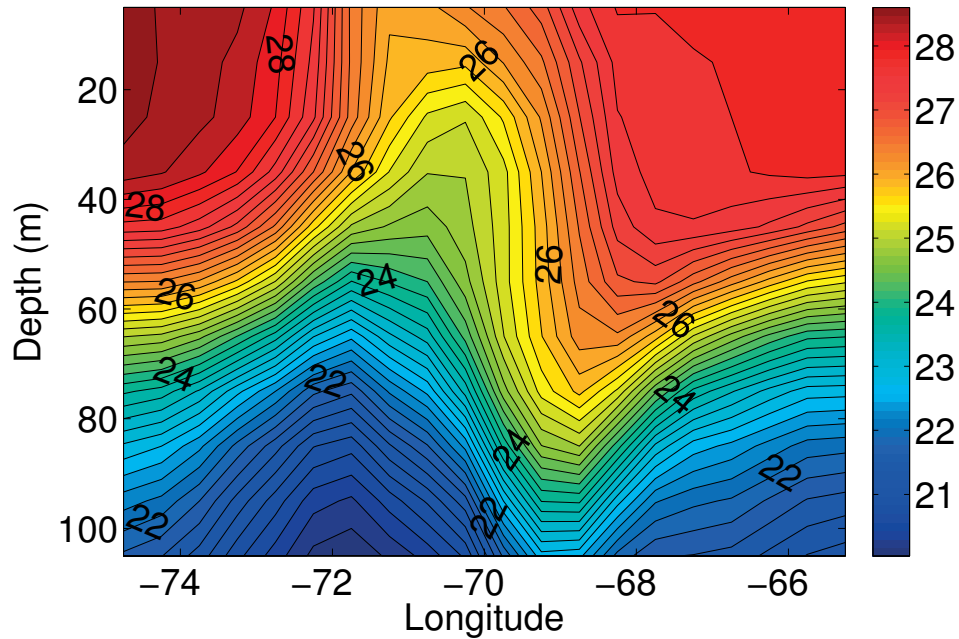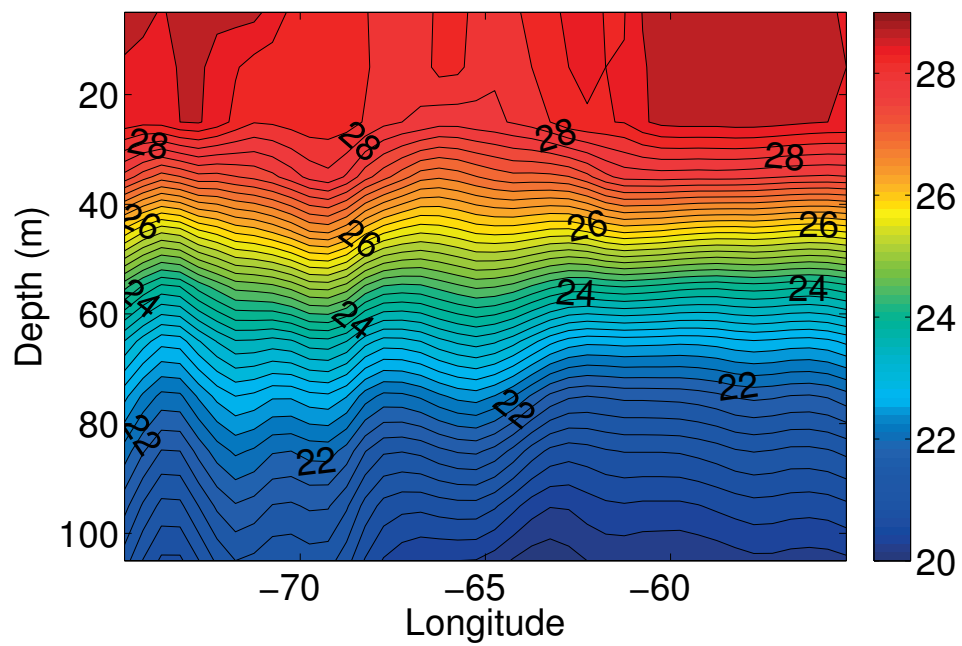
Figure 4.29: Cross section of the ocean for hurricane Bill (2009)at 29° N on 19 September 2009. The depth ranges from 5m to 105m.
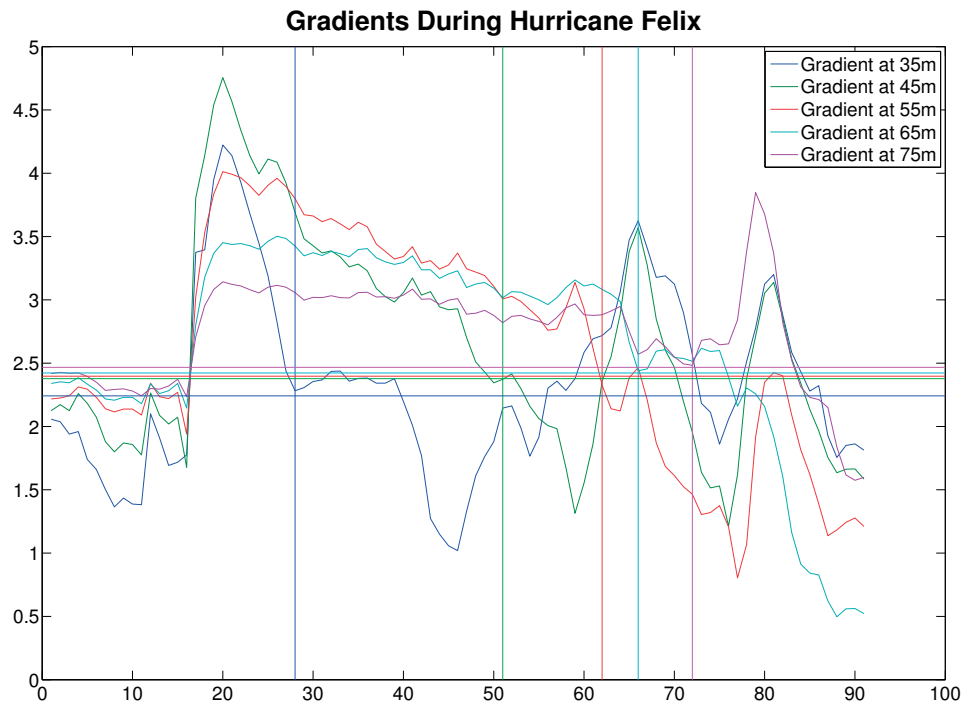
Figure 4.30: Temperature gradient perpendicular to the track of hurricane Felix (2001). The horizontal lines represent the pre-storm temperature field plus two standard deviations of that field. The vertical lines represent the point at where the gradient has returned to its pre-storm value.
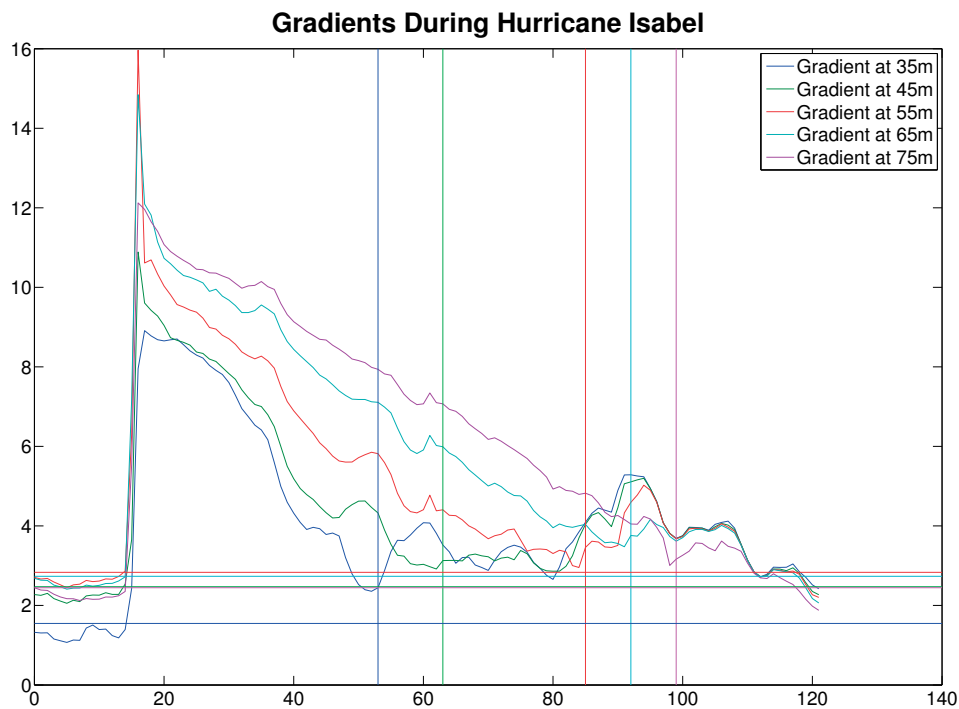
Figure 4.31: Temperature gradient perpendicular to the track of hurricane Felix (2001). The horizontal lines represent the pre-storm temperature field plus two standard deviations of that field. The vertical lines represent the point at where the gradient has returned to its pre-storm value.
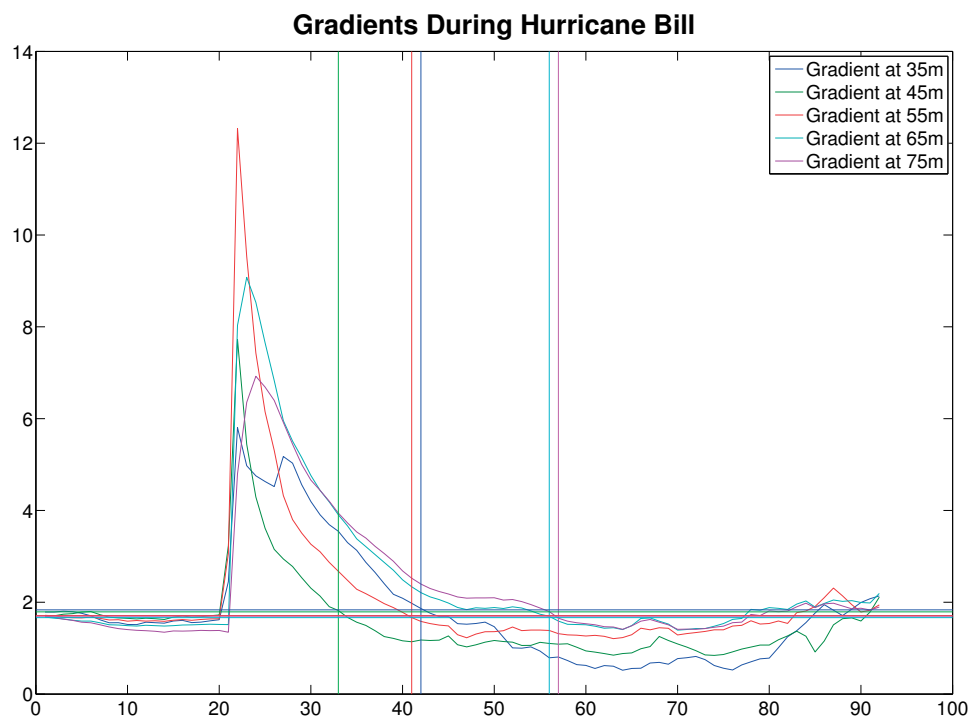
Figure 4.32: Temperature gradient perpendicular to the track of hurricane Felix (2001). The horizontal lines represent the pre-storm temperature field plus two standard deviations of that field. The vertical lines represent the point at where the gradient has returned to its pre-storm value.
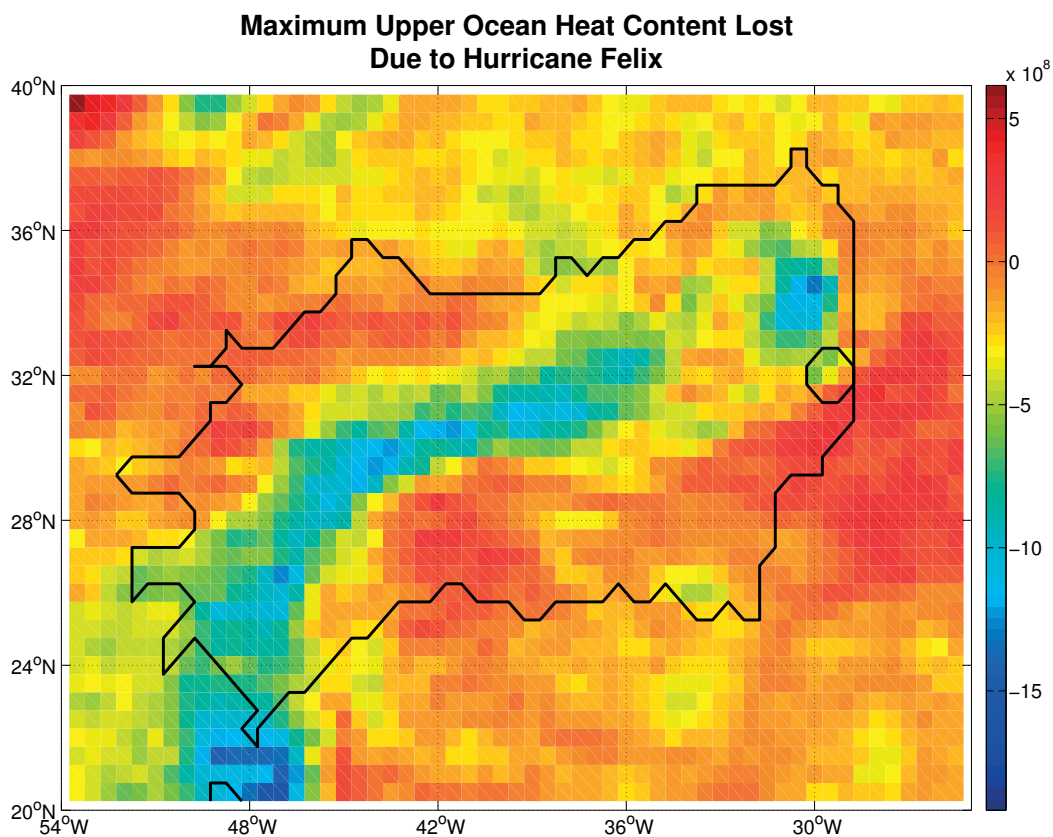
Figure 4.33: Maximum upper ocean heat content loss due to hurricane Felix (2001). The colors represent the maximum value from the integration of Equation 2.3 during which there was a best track observation for hurricane Felix (2001). The black line represents the area that was affected by the storm as calculated through the cooling of SSTs
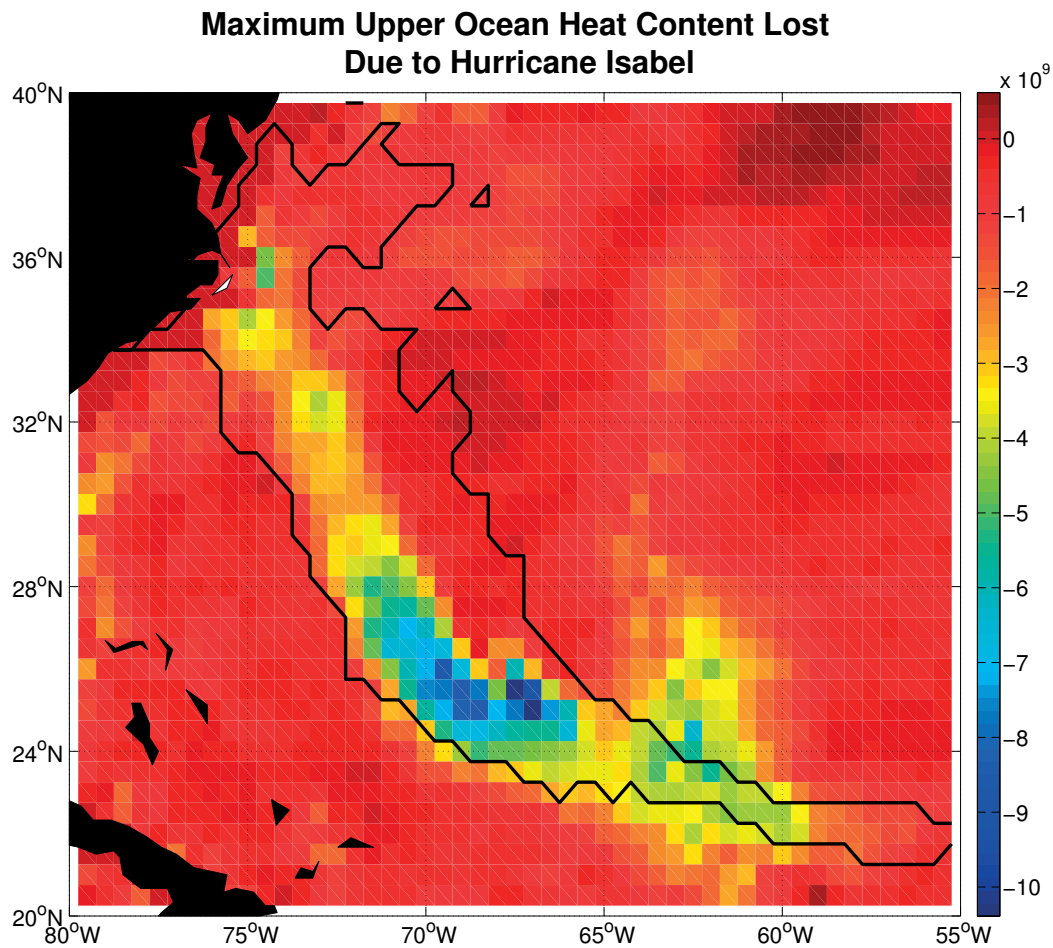
Figure 4.34: Maximum upper ocean heat content loss due to hurricane Isabel (2003). The colors represent the maximum value from the integration of Equation 2.3 during which there was a best track observation for hurricane Isabel (2003). The black line represents the area that was affected by the storm as calculated through the cooling of SSTs

Figure 4.35: Maximum upper ocean heat content loss due to hurricane Bill (2009). The colors represent the maximum value from the integration of Equation 2.3 during which there was a best track observation for hurricane Bill (2009). The black line represents the area that was affected by the storm as calculated through the cooling of SSTs
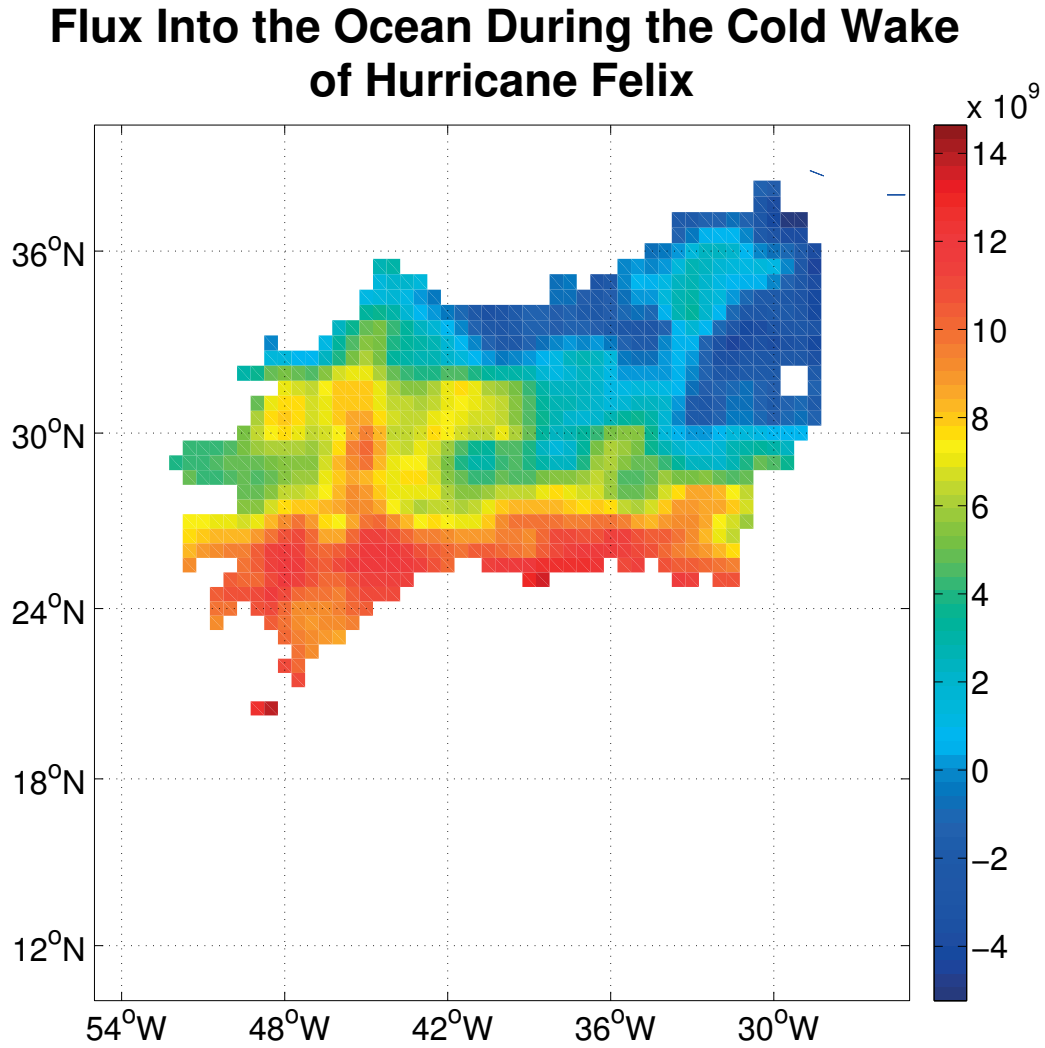
Figure 4.36: Sum of total incoming heat flux into ocean during hurricane Felix(2001)and corresponding cold wake over the same area affected by the storm calculated via the cooling of SST's. The summation is in units of W/m^2.
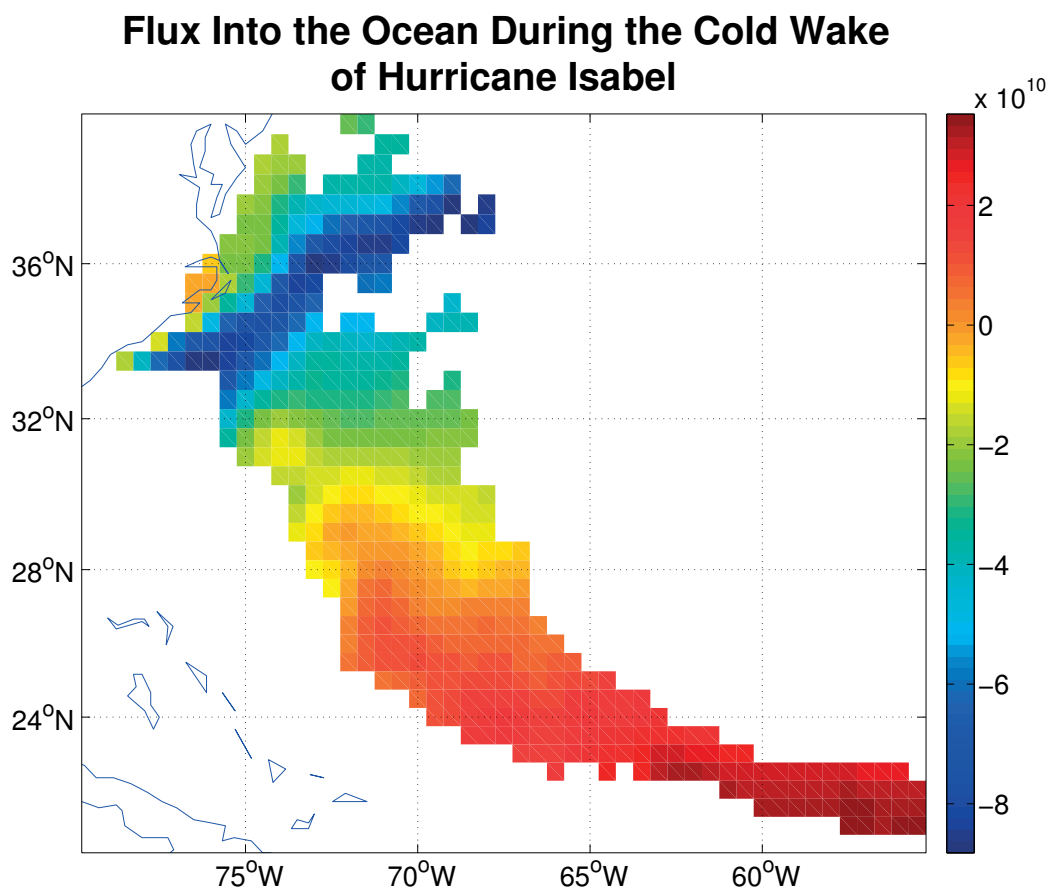
Figure 4.37: Sum of total incoming heat flux into ocean during hurricane Isabel (2003) and corresponding cold wake over the same area affected by the storm calculated via the cooling of SST's. The summation is in units of W/m^2.
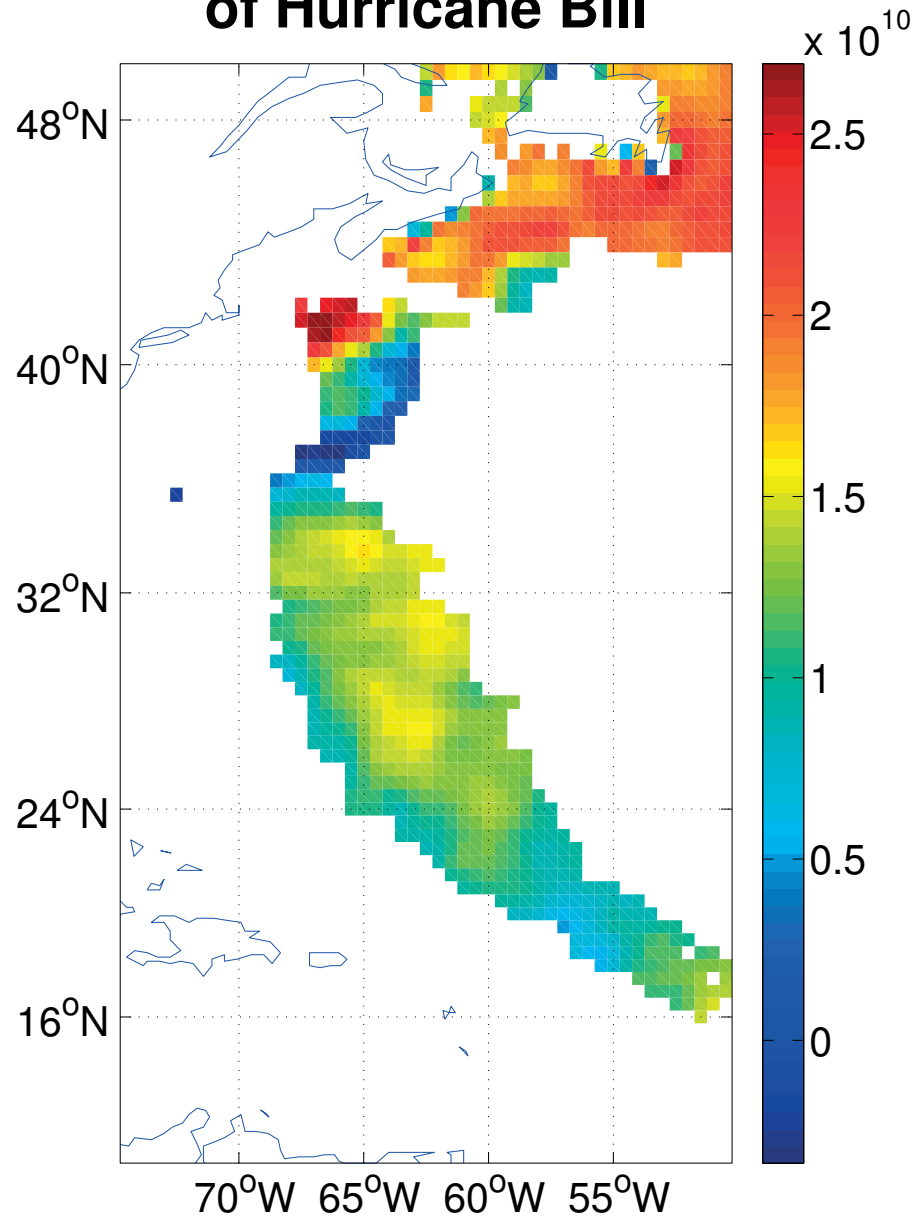
Figure 4.38: Sum of total incoming heat flux into ocean during hurricane Bill (2009) and corresponding cold wake over the same area affected by the storm calculated via the cooling of SST's. The summation is in units of W/m^2.

CHAPTER 5

CONCLUSIONS

5.1 In-situ Results

The motivating factor in this research was to evaluate the hypothesis of Emanuel (2001), which stated that the net ocean heating induced by tropical cyclone activity was a large factor in the total observed poleward heat flux. However, the initial estimates of Emanuel (2001) assumed that the all of the change in heat towards re-stratification of the cold wake is from surface heating, whereas some of the re-stratification may occur due to horizontal ocean dynamics and eddy mixing. This study used three cases to look at the feasibility of using satellite altimeter data to estimate the amount of heating required to re-stratify the ocean following the passage of the tropical cyclone. In the first case, Hurricane Felix, there was an area of increased SSH in each of the two passes shown and the largest estimated Q' using Equation 2.2 resulting from the SSH anomaly was on the order of approximately 1.5439×10^{14} J/m. For Hurricane Isabel (2003), the SSH anomalies show an increase of between 15cm and 20cm over a width over approximately 225km. This h' resulted in an estimation of 1.029×10^{15} J/m. In the final case, Hurricane Bill (2009), while two of the passes show no apparent increase in SSH over the hurricane's path, one of the passes shows a very clear increase in SSH at it crosses the path of a cold wake. Using the pass that does show a signal the required heating can be estimated to be 6.59×10^{14} J/m. All of the estimations for each storm are consistent with the results from Emanuel (2001). The estimated Q' for Hurricane Isabel is actually an order of magnitude larger than the estimated

heating for Hurricane Edouard (1996) in Emanuel (2001)

To validate the estimates in the SSH, the Argo floats were chosen next for the ability to have direct profile measurements in the wake of the storm and in the recover time period. As the Argo project became more robust in data coverage there were and increasing number of initial floats per storm; however, the requirements of this study were pairs of floats sampling the same water masses with profiles both before and after the passing of the storm. The number of pairs meeting the criteria were few. Even when there were observations, as in the case with Hurricane Bill (2009), there was not a clear signal in the height anomalies. These results suggest that the use of the ARGO floats to study this issue will not be feasible.

5.2 CFSR heating estimations

In the CFSR model the first step was to determine if the model resolved the hurricanes and, if so, did it also resolve a cold wake? In each case the model did resolve both a storm and an impact of the storm on the ocean. The wind field was weaker then the actual observed maximum wind speeds, but that is to be expected due to the coarse resolution of the model as compared to the very fine scale at which the strongest wind speeds occur. In two of the cases, the model showed a lag in maximum wind speed compared to the corresponding time of the observations. The modeled SST response was quite realistic, and was more accurate with respect to timing then the atmosphere, perhaps due to the data assimilation constraints used. The CFSR model assimilates both radiances and ARGO profiles. Thus it is unsurprising that our comparisons of the model and observations show good agreement from these sources. However, the CFSR model also shows a similar signal in the SSH for all cases as compared to the satellite altimetry. In the case of both Felix (2001) and Isabel (2003), the model showed a distinct signal in the area where the cold wake was and in the case of Bill (2009), the model was similar to the SSH from satellite showing no distinct signal of a cold wake.

Based on the estimated duration of the cold wake through the temperature gradient

calculations, the model showed that the cold wake lasted between 35 and 90 days. This time scale is certainly long enough for baroclinic instabilities to play a role in re-stratification, as described by Pasquero and Emanuel (2008). This compares favorably to Hart et al. (2007) in which the authors show that the estimated local memory of the storm was between 30 and 35 days for a tropical storm and 50-60 days for major hurricanes. With a sample size of only three, it is difficult to make any definitive statements regarding the strength of the storm and the re-stratification time. It should be noted that while the strongest storm did leave the longest cold wake, Bill and Felix where opposite with regards to strength and lifetime of the cold wake.

Using the change in temperature over the upper ocean as an estimate of the amount of heating required to re-warm the ocean the resulting values ranged from 6.31×10^{10} W to 2.5×10^{11} W. These numbers differ greatly from the modeled heating required by Emanuel (2001) of $1.4 \pm 0.7 \times 10^{15}$W, a difference of 6 orders of magnitude. The large difference is primarily due to the fact that in this study the amount of energy was per storm and in Emanuel (2001) the values were calculated for an entire global season of tropical cyclones. Emanuel (2001) also proposed that all of the heating required to rewarm the ocean was done through surface heating. This study showed the amount of incoming heat flux was larger than the amount of required heating for the storm. It is hypothesized that all of the required heating was performed through incoming surface heating. This study shows that this is possible because the amount of required heating is less than in the incoming flux over the duration of the cold wake.

5.3   Future Research

The initial approach to this research question was to use observations, such as altimeter and ARGO float profiles to look at the impacts on the ocean caused by a hurricane. However, it is clear that current observation systems are not capable of providing the coverage needed to be used as the sole method for determining the upper ocean heat content changes. If

the numbers of ARGO floats were to increase, there would be a greater likelihood of useful pairs of profiles (as was evident in comparisons between these case studies over time).

An obvious next step is to provide a more robust comparison by using a larger sample size of storms in order to determine seasonal, global heating. In addition, from the results of these three storms, the satellite-derived SSH anomaly does not always determine of the upper ocean heat content anomaly. This was also shown using SSH from CFSR. Therefore SSH can not be used as a conclusive metric for the upper ocean heat anomaly. The inclusion of more cases would help constrain the error budgets on our estimates. Another option that would be useful would be to compare the results of the CFSR model to another coupled model for another approach at error estimation.

Further research would demonstrate the robustness of the gradient method proposed here as a metric for determining the time scale of the cold wake re-stratification. Given that the case for Hurricane Bill 2009 showed an apparent exponential decay, perhaps an e-folding technique would be an adequate estimator. The increased proposed sample size would give further indication as to the best metric for objectively determining the lifetime of the cold wake. With a larger sample size and a more robust gradient method for determining the lifetime of a cold wake, it would be possible to have more conclusive results about the actual amount of heat loss and surface heat flux on a global scale.

BIBLIOGRAPHY

Arakawa, A. and W. H. Schubert, 1974: Interaction of cumulus cloud ensemble with the large-scale environment. part 1. *J. Atmos. Sci.*, **31**, 671–701.

Avila, L. A., 2009: Tropical cyclone report hurricane bill. URL `http://www.nhc.noaa.gov/2009atlan.shtml`, URL `http://www.nhc.noaa.gov/2009atlan.shtml`.

Beven, J. and H. Cobb, 2004: Tropical cyclone report hurricane isabel. URL `http://www.nhc.noaa.gov/2003isabel.shtml?`, URL `http://www.nhc.noaa.gov/2003isabel.shtml?`

Chang, S. W. and R. A. Anthes, 1978: Numerical simulations of the ocean's nonlinear, baroclinic response to translating hurricanes. *J. Phys. Oceanogr.*, **8**, 468–480.

D'Asaro, E. A., 2003: The ocean boundary layer below hurricane dennis. *J. Phys. Oceanogr.*, **33**, 561–579.

D'Asaro, E. A., T. B. Sanford, P. P. Niiler, and E. J. Terrill, 2007: Cold wake of hurricane frances. *Amer. Geophys. Union*, **34**.

Dickey, T. D., et al., 1998: Upper-ocean temperature response to hurricane felix as measured by the bermuda testbed mooring. *Mon. Wea. Rev.*, **126**, 1195–1201.

Emanuel, K. A., 2001: The contribution of tropical cyclones to the oceans' meridional heat transport. *J. Geophys. Res.*, **106 (14)**, 14 771–14 782.

Ferrari, R. and D. Ferreira, 2011: What processes drive the oean heat transport. *Ocean Modeling*, **Submitted**.

Gould, J., et al., 2004: Argo profiling floats bring new era of in situ ocean observations. *Eos, Trans. Amer. Geophys. Union*, **85 (19)**, 179, 190–191.

Griffies, S. M., M. J. Harrison, R. C. Pacanowski, and A. Rosati, 2004: Technical guide to mom4. gfdl ocean technical report. Tech. Rep. 5, GFDL, www.gfdl.noaa.gov/ fms.

Hart, R. E., R. N. Maue, and M. C. Watson, 2007: Estimating local memory of tropical cyclones through mpi anomaly evolution. *Mon. Wea. Rev.*, **135**, 3990–4005.

Jordan, C. L., 1964: On the influence of tropical cyclones on the sea surface temperature field. *Proc. Symp. Trop. Meteor.*, 614–622.

Landsea, C. W., S. Feuer, A. Hagen, D. A. Glenn, N. T. Anderson, J. Sims, R. Perez, and M. Chenoweth, 2004: The atlantic hurricane database re-analysis project: Documentation for the 1851-1910 alterations and additions to the hurdat database. hurricanes and typhoons: Past, present and future. *Columbia University Press*, 177–221.

Leipper, D. F., 1966: Observed ocean conditions and hurricane hilda. *J. Atmos. Sci.*, **24**, 182–196.

Monaldo, F. M., T. D. Sikora, S. M. Babin, and R. E. Sterner, 1997: Satellite imagery of sea surface temperature cooling in the wake of hurricane edouard (1996). *Mon. Wea. Rev.*, **125**, 2716–2721.

Murray, R. J., 1996: Explicit generation of orthogonal grids for ocean models. *J. Comput. Phys.*, **126**, 251–273.

Pasquero, C. and K. A. Emanuel, 2008: Tropical cyclones and transient upper-ocean warming. *J. Climate*, **21**, 149–162.

Price, J. F., 1981: Upper ocean response to a hurricane. *J. Phys. Oceanogr.*, **11**, 153–175.

Price, J. F., T. B. Sanford, and G. Z. Forristall, 1994: Forced stage response to a moving hurricane. *J. Phys. Oceanogr.*, **24**, 233–260.

Reynolds, R. W., N. A. Rayner, T. M. Smith, D. C. Stokes, and W. Wang, 2002: An improved in situ and satellite sst analysis for climate. *J. Climate*, **15**, 1609–1625.

Saha, S., et al., 2010: The ncep climate forecast system reanalysis. *Bull. Amer. Meteor. Soc.*, 1015–1057.

Schenkel, B. and R. E. Hart, Accepted: An examination of tropical cyclone position and intensity differences within reanalysis datasets. *J. Climate*.

Shay, L. K., G. J. Goni, and P. G. Black, 2000: Effects of a warm oceanic feature of hurricane opal. *Mon. Wea. Rev.*, **128**, 1366–1383.

Stewart, S. R., 2001: Tropical cyclone report hurricane felix. URL http://www.nhc.noaa.gov/2001felix.html, URL http://www.nhc.noaa.gov/2001felix.html.

Stramma, L., P. Cornillon, and J. F. Price, 1986: Satellite observations of sea surface cooling by hurricanes. *J. Geophys. Res.*, **91**, 5031–5035.

Tiedtke, M., 1983: The sensitivity of the time-mean large-scale flow to cumulus convection in the ecmwf model. *ECMWF Workshop on Convection in Large Scale Models*, 297–316.

Walsh, K. J. E., M. Fiorino, C. W. Landsea, and K. L. McInnes, 2007: Objectively determined resolution-dependent threshold criteria for the detection of tropical cyclones in climate models and reanalyses. *J. Climate*, **20**, 2307–2314.

Wentz, F. J., C. Gentemann, D. Smith, and D. Chelton, 2000: Satellite measurements of sea surface temperature through clouds. *Science*, **288**, 847–850.

Wentz, F. J., D. K. Smith, C. A. Mears, and C. L. Gentemann, 2001: Advanced algorithms for quickscat and seawinds/amsr. *IGARSS '01.*

BIOGRAPHICAL SKETCH

Robert Deal grew up in Hampton, VA the older son of Peter and Elizabeth Deal. Always having a fond interest in weather and excelling in math and physical science he enrolled as a freshman at Florida State University in 2005. While in school as an undergraduate he took a position as a student researcher working for Shawn Smith at the Center for Ocean Atmosphere Prediction Studies in the summer of 2007 in the field of Air-Sea Interaction. Specifically the work involved quality control of data in the Pacific Ocean. He also performed some research in the variability of fluxes in the Indian Ocean. He also completed an Honors in the Major Research Project under the direction of Dr Robert Hart comparing the two hurricane datasets in the Spring of 2008. Due to prior AP coursework he was able to complete his Bachelor's Degree in Meteorology in 3 years and graduated in Spring of 2008 with honors. In the Fall of 2008, he began working under the direction of Dr Carol Anne Clayson in the field of Air-Sea Interaction. In the Spring of 2009, his interests peaked at the idea of working on the effects of hurricanes on the ocean and began work researching the impact of hurricanes on the ocean. In the Spring of 2010, he began a volunteer program with the National Weather Service in Tallahassee and recognized his true interests, researching while also working in the field of operational meteorology.

Robert's research interests include tropical meteorology, and physical oceanography. His non professional interests include cycling, backpacking, kayaking and all things at the beach. He was lucky enough to take a job working for the National Weather Service in December of 2010 and now lives in Lake Charles, Louisiana with Claire Forbes and is enjoying life.